MASTER OF SCIENCE

IN

ELECTRICAL AND ELECTRONIC ENGINEERING

DEVELOPMENT OF AN ANALYTICAL METHODOLOGY FOR THE LOSS CALCULATION OF THE MODULAR MULTILEVEL CASCADED INVERTER WITH THIRD HARMONIC INJECTED (THI) PWM.

by

Tania Annur

Department of Electrical and Electronic Engineering

Islamic University of Technology (IUT)

Organization of Islamic Cooperation (OIC)

Board Bazar, Gazipur-1704, Bangladesh.

February, 2021

MASTER OF SCIENCE

IN

ELECTRICAL AND ELECTRONIC ENGINEERING

DEVELOPMENT OF AN ANALYTICAL METHODOLOGY FOR THE LOSS CALCULATION OF THE MODULAR MULTILEVEL CASCADED INVERTER WITH THIRD HARMONIC INJECTED (THI) PWM.

by

Tania Annur

Department of Electrical and Electronic Engineering

Islamic University of Technology (IUT)

Organization of Islamic Cooperation (OIC)

Board Bazar, Gazipur-1704, Bangladesh.

February, 2021

CERTIFICATE OF APPROVAL

The thesis entitled " Development of an Analytical Methodology for the Loss Calculation of the Modular Multilevel Cascaded Inverter with Third Harmonic Injected (THI) PWM." submitted by Tania Annur, Student No. 132629 of Academic Year 2013-2014 has been found as satisfactory and accepted as partial fulfillment of the requirement for the Degree of MASTER OF SCIENCE IN ELECTRICAL AND ELECTRONIC ENGINEERING.

BOARD OF EXAMINERS:

1. ----------
Dr. Md. Ashraful Hoque (Chairman)
Professor and Dean (Supervisor)
Department of Electrical and Electronic Engineering
Islamic University of Technology, Board Bazar, Gazipur-1704

2. ----------
Dr. Md. Ruhul Amin (Member)
Professor and Head (Ex-Officio)
Department of Electrical and Electronic Engineering
Islamic University of Technology, Board Bazar, Gazipur-1704

3. ----------
Dr. Golam Sarowar (Member)
Professor
Department of Electrical and Electronic Engineering
Islamic University of Technology, Board Bazar, Gazipur-1704

4. ----------
Dr. Ashik Ahmed (Member)
Professor
Department of Electrical and Electronic Engineering
Islamic University of Technology, Board Bazar, Gazipur-1704

5. ----------
Dr. Md. Monirul Kabir Member (External)
Professor
Department of Electrical and Electronic Engineering
Dhaka University of Engineering & Technology (DUET), Gazipur-1700, Bangladesh

DECLARATION

It is hereby declared that this thesis or any part of it has not been submitted elsewhere for the award of any Degree or Diploma.

Dr. Md. Ashraful Hoque
Professor & Dean
Department of Electrical and Electronic Engineering
Islamic University of Technology (IUT)
Date: / /2021

Tania Annur
Student No. – 132629
Academic Year: 2013-2014
Date: / /2021

Dedicated to my beloved mother, **Monowara Huq**, whose patience, mental strength and good will for everyone inspires me all the time.

TABLE OF CONTENTS

List of Tables

List of Figures

List of Abbreviations

A	Ampere
kV	kilo Volt
V	Volt
AC	Alternating current
DC	Direct current
DVUF	Device voltage utilization factor
NPC	Neutral Point Capacitor
FC	Flying capacitor
MMC	Modular Multilevel Cascaded
Hz	Hertz
I/O	Input and (or) output
IGBTs	Insulated gate bipolar transistors
I-V	Current versus voltage
MW	Mega Watt
kW	kilo Watt
W	Watt
SPWM	Sine pulse width modulation
THIPWM	Third harmonic injected pulse width modulation
THD	Total harmonic distortion

Acknowledgment

First of all, I would like to express my heartiest gratitude to the Almighty Allah for providing me the strength to complete this thesis work. After the Almighty, it is my great pleasure to express gratitude to the people who made this thesis possible. Foremost, I would like to express my deepest gratitude to my supervisor, Prof. Dr. Md. Ashraful Hoque, PhD, Dept. of EEE, IUT, whom I have found very helpful in my academic and administrative work and whose expertise, understanding and patience added significantly to my Master's degree experience. I would also like to thank Dr. Golam Sarowar and Dr. Ashik Ahmed, Professor, Dept. of EEE, IUT, who sacrificed their valuable time for continuously guiding and motivating me for completing the thesis. This study could have never been done without all of my teachers' (IUT) motivation, guidance and inspiration.

My special gratitude to my entire family especially my mother-in-law Laila Parvin, my husband Imtiaz Shafiq and my only son Yasin Huq Shafiq without whose continuous support and patience I would not be the person I am today.

Abstract

Three main foundations such as hydro, wind and solar belong to renewable resources, nevertheless, solar energy is considered as the most reliable and continuous source of energy consumed by photovoltaic array. For the profusion, omnipresent and easy existence of solar energy, it becomes the strong competitor against fossil fuel. To generate continuous electric power using renewable energy resources, Multilevel power converters has been receiving attention in the past few years by gaining synthesized waveforms with lower THD for Medium or high power high voltage applications. Multilevel power converters are various types. Among them Modular Multilevel Cascaded (MMC) converter is being widely used in order to achieve more efficiency than obtained from the Conventional converter system.The losses that exist in the Multilevel converter are much more complicated to evaluate compared to the Conventional converters. Loss evaluation in this type of converter needs special attention because current always varies in different switches of the converter depending on PWM techniques, also a few percentage of loss in MW system represents kW range power loss which has a large effect in the system. Moreover, the losses are represented as switch loss and conduction loss in the Multilevel converters/Inverters. The overall losses depend on three different parameters, such as modulation technique, Inverter level and inherent manners of respective IGBTs. In this thesis work, Third harmonic injected (THI) Pulse width modulation with level shifted scheme is used as switching technique and Insulated Gate Bipolar Transistors (IGBTs) are used as switching devices in the converter/Inverter. The Proposed research is aimed for developing an Analytical Methodology for the loss calculation of the Modular Multilevel Cascaded (MMC) Inverter. In this book the above concept is presented through modeling and simulating the 15 level Modular Multilevel Cascaded (MMC) converter/Inverter by MATLAB. After simulation, it is found that, when comparing with the Reference paper with Proposed Loss Calculation Method using SPWM modulation technique, the switching losses come higher which is about 79% than conduction loss which is 21% . On the other hand, using Third Harmonic Injected (THI) PWM, switching loss is lower than conduction loss. All the results have been evaluated and compared for the MMC converter/Inverter.

CHAPTER 1

INTRODUCTION AND BACKGROUND

Energy is a basic and essential ingredient for all living entities. The sun is no doubt the cause of all of the earth's energy, directly or indirectly. As the demand for energy is increasing globally gradually, energy reserves are not increasing in that way. Hence, world researchers are constantly focusing on the process of energy in the most efficient way to make it affordable, reliable and efficient for people. Having all these challenges, the application of modern electronic circuits and systems is essential to be considered. This is a strategic framework of power electronics. It is an orderliness defined in terms of the conversion of electrical energy, applications, and electronic devices.

1.1 Introduction to Power Electronics

From 1900 to 1950, electronics were primarily based on the vacuum tubes, such as gas discharge tubes, ignitrons, thyratrons, and mercury arc rectifiers. As the vacuum tube had a set of disadvantages, mercury equipment took the place of the vacuum tube in the 1930^{th}. In the year 1948, the first electronics revolution began with the transistor's invention, and approximately all of today's advanced electronic technologies are traceable from it [1].

"General Electric" developed the first germanium diodes in 1952. In 1954, G. Teal developed a silicon transistor at “Texas Instruments,” which achieved tremendous market acceptance due to the improved quality and durability of the temperature. From the mid-1950s to the early 1960s, electronic circuit designs started to move from vacuum tubes to transistors, thereby opening up numerous new possibilities and growth in research [1].

The invention of a consumer thyristor was the second electronics revolution that started in 1956, but it is possible to classify the period of 1956-1975 as the age of first-generation control devices. General Electric invented the silicon-based thyristors. After that, several generations of power semiconductor devices and conversion Methods were carried out based on thyristors' discovery. Semiconductor engineering was considered as part of electrical engineering of medium and low

voltage, such as below one amp and just a few tens of volts up to 1959, respectively. Several other devices like gate turn-off thyristors, MOSFETs, BJTs, microprocessors, and power integral circuits were developed during and after the years of second-generation power devices.

The IGBT was created in the 1990s as the third generation power switch, considered a modern trend in electronics, introducing intelligent power devices and modules. The golden era of power electronics was steered by the incremental developments of many advanced power semiconductor devices such as microprocessor/DSPs, FPGAs, ASIC chips, advanced converter topologies, PWM techniques, and advanced control techniques. The decrease in costs and scale, along with increase in performance, began the proliferation of power electronics applications in automotive, commercial, domestic, transport, aerospace and armed forces systems [2].

1.1.1 Modern Power Electronics

In order to minimize reliance on oil and gas, most developed countries use renewable energy options such as solar energy, wind power, geothermal energy, and biomass. It has thus gained a high degree of demand in recent times [3]. In real life, the value of power electronics is now a requirement. Examples include High Voltage DC(HVDC), Static VAR Compensator (SVC), Flexible Ac Transmission System (FACTS) for active and reactive power flow management, Uninterruptible Power Supply (UPS), and variable frequency drive industrial process control to increase product efficiency and quality in modern factories [2]. It is also used for high-frequency drives used in pumps and compressor drives, drives for paper and cloth mills, rolling metal and textile mills, electric and hybrid cars, elevators, propulsion for subways and locomotives, air conditioners for variable speeds, machine tools and robots, home appliances, wind energy systems and propulsion for ships. In power electronic systems such as domestic, commercial, transport, industrial pumps, utility systems, aerospace, telecommunications, etc., enormous applications can be made [4-5]. With the aid of power electronics, saving electricity offers financial gain immediately where the cost of energy is huge. A preliminary calculation by the Electric Power Research Institute (EPRI) is that 15-20 percent of utility electricity can be saved by using power electronics extensively [2].

Power electronics play a significant part in addressing global warming, which is now a huge global concern. The primary cause for the global warming issue is the human-made greenhouse gas produced. Renewable energy can satisfy a large portion of the energy demand. So it can be concluded that due to the vast expansion of the power electronics applications concerning the size, cost reduction of the implementation and improved performance, it will undoubtedly flourish everywhere soon.

1.1.2 Power Electronic Systems

The mixture of electronics, power, and control is power electronics. The steady-state and dynamic aspects of closed-loop systems are represented by control systems. Power is the static and moving power equipment used to generate, transfer and convey electrical power. Solid-state instruments and signal processing circuits reflect circuitry that achieve the desired control objectives are represented by electronics. It is then applied to the devices and goods used in the transfer and management of electrical energy flow, ensuring that electricity is provided in a tiny thin package with optimum efficiency.

The conversion process is achieved with two functional modules called the power processor and controller in most power electronic systems. The block diagram of the power electronics system for a single source and single load converter is shown in figure 1.1. In the Method for transforming and regulating the flow of electrical energy, this procedure is introduced, ensuring that power is provided with optimum efficiency. It consists of power semiconductor devices and passive devices. The controller deals with the operation of the switches by controlling the voltages and currents calculated at the input and/or output of the device according to particular algorithms [4].

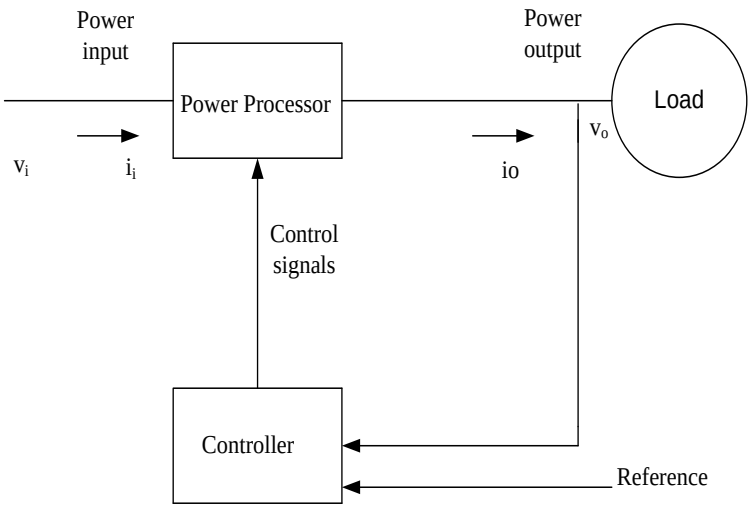

Figure 1.1 Block diagram of a power electronic system

1.2 Switch Mode Converter

The switched-mode power supply (SMPS) is an electronic power supply that integrates a switching regulator for effective transfer of electrical power. The SMPS transmits DC or AC power to DC or AC loads. Switch mode converters, transform DC source to AC, are used to drive ac motors and uninterrupted ac power supplies to achieve an ac output- the magnitude and frequency of which can be controlled [5]. The switch-mode Inverter is a converter by which the transfer of electricity is reversible. The input dc voltage of the Inverter is accomplished by rectifying and filtering the line voltage, considered an ac motor drive, and the voltage across the output terminals is needed to be sinusoidal with modified magnitude and frequency. The switch-mode dc-to-ac Inverter performs this operation. Generally, electricity passes from the side of dc to the side of ac, which is referred to as the mode of operation of the Inverter. On the other hand, the kinetic energy associated with the motor's inertia and its load is restored, and the ac-engine serves as a generator. Alternative regenerative braking is applied to avoid this rectifier mode of operation, if the braking occurs regularly, to have the energy extracted from the inertia of the motor load and fed back to the utility grid.

The power of electrical and electronic devices can be converted and controlled with the help of power electronics, and the system can run efficiently as per human requirements. The main element

of power electronics is the switching converter [6]. Converters are classified into the following types, depending on the mode of conversion for single-phase and three-phase ac outputs.

- AC-AC converters
- DC-DC converter
- AC-DC converters
- DC-AC converters

1.2.1 AC to AC converters

The AC to AC cycloconversion converters are also known as ac voltage controllers. They can control load voltage without changing the frequency; applied in industrial heating, on-load transformer tap changing, light controls, poly-phase induction motor's speed control, and ac magnet controls.

1.2.2 DC to DC converters

DC to DC converters, referred to as choppers, transform a dc source of fixed voltage into a dc source of variable voltage that has recently been commonly used in green energy systems. As it may be used to step-up or step-down a dc source, it can be viewed as dc equivalent to an ac transformer with a continuously variable turn ratio. Portable computing devices such as cellular phones, notebook computers and even space crafts are the other applications. The output voltage level of the Spacecraft Fuel Cell is very low. To raise the voltage level to the desired dc voltage level, step-up converters are used.

1.2.3 AC to DC converters

The AC to DC converters are commonly known as rectifiers. Rectifiers are used in a variety of commercial, residential, rural, and other applications to transform ac voltage or current into dc, carrying a greater or smaller magnitude. Thanks to its nearly infinite output energy and fine controllability, it is used as a stand-alone unit feeding single and multiple dc loads. In order to tackle electromechanical transients occurring in motor drives and power supplies, the speed of reaction is usually adequate.

1.2.4 DC to AC converters

The DC to AC converters are commonly referred to as Inverters. This transforms a dc input voltage of the desired magnitude and frequency to a symmetrical ac output voltage. The output voltage could be constant or variable. A traditional power Inverter needs a reasonably reliable DC power source capable of producing adequate current for the system's estimated power requirements. The input voltage has been planned in compliance with market demand.

In automotive applications such as variable-speed ac motor drives, induction heating, standby power supplies and uninterruptible power supplies, Inverters are widely used. A battery, fuel cell, solar cell or other DC sources may be the input. One of the booming applications nowadays is the Multilevel converters/Inverters in grid-tied PV energy conversion systems.

1.3 Literature review and problem identification

1.3.1 Literature review

The thesis work concentrates on the development of an Analytical Methodology for the Loss Calculation of the Modular Multilevel Cascaded Inverter with Third Harmonic Injected (THI) PWM. However, different circuit topologies of DC-AC Multilevel Inverters have been studied from the beginning of the thesis work. It has been found that various isolated and non-isolated Inverter topologies have been developed to provide a medium or high voltage high power conversion.

There exist some losses in the Multilevel Inverters in the form of switch loss and conduction loss. Loss evaluation in this type of Inverter needs special attention because currents always vary in different switches of the Inverter depending on PWM techniques. In [7], average power loss was calculated using device threshold voltage. Diode conduction loss has not been considered. Also, total device numbers were not considered in loss calculation. The average switching loss for IGBT and diode are obtained by multiplying switching energy with instantaneous current and switching frequency Evaluating the losses in Multilevel Inverters are very important because power loss is considered a very important indicator of the system's expense, performance and reliability. Diode losses include losses or conduction of the on-state, losses of the diode turn-on and losses of the

diode reverse recovery. The diode turn-on losses in the calculation are so minimal that they can be overlooked [8]. In some experiments, the instantaneous switching current of IGBT has been taken for calculation [9-12]. A specific IGBT manufacture Company's datasheet has been required as a reference to get an exact value for loss calculation [13]. For IGBT and diode, the most reliable way of switching loss measurement is the determination of current and voltage waveforms during the transition, where switching energy at turn-on or turn-off transitions is the field under the power waveform [14]. The failure calculation also allows the manufacturer to maximize the overall efficiency of the system, pick the system's heat sinking equipment, and cooling Method [15]. The individual current/voltage and the service cycle of semiconductors are the key variables influencing switching and conduction losses of Inverters. At each switching event, the energy dissipation is proportional to the current level and the junction temperature at that moment.

SMPS (Switched Mode Power Supply) converters are very important in this aspect due to ease of application and scope of improvement. To operate the switch-mode power Inverters, the Inverters must be connected with a dc voltage source. Renewable energies such as photovoltaic system is a great aspect for the dc source. Due to solar radiation, temperature and load, the PV modules are affected, and the output characteristics of the PV array become nonlinear. High cost and low efficiency these two vital factors are the reason to limit the implementation of PV systems in energy conversion. In recent times, grid-connected photovoltaic systems are the higher developing solar energy applications. Certainly, the efficient use to harvest solar energy requires the implementation of maximum power point tracking (MPPT) unit [20]. The possible power Inverters of a PV system are of two types such as - Inverters in Small-Scale Solar PV Systems (Output voltage obtained below 6 kV) and Inverters in Medium and Large-Scale Solar PV Systems (Output voltage obtained between 6-36 kV). The Small-scale PV systems are then subdivided into three categories such as - Two-Stage Solar PV Inverters Systems [23], Multiple-Stages Solar PV Inverters Systems [32] and Single-Stage Solar PV Inverter Systems [33]. On the other hand, Multilevel Inverters, as the topologies of the Multilevel Inverters, are discussed in the following chapter, used for Medium and Large-Scale Solar PV Systems [48-49,55-57].

In [32], Multiple-Stages Solar PV System is categorized under Small-scale PV Systems; it has been described that galvanic isolation is mandatory to reduce the ground leakage currents. Via a power frequency transformer on the grid side of the PV Inverter, which can also operate for voltage

step-up operation, the insulation can thus be accomplished. This transformers of power frequency are heavy, increase the cost of installation of the PV Inverter and require daily maintenance. Instead, several high-frequency transformer-based Solar PV Inverter topologies have been developed for Small-Scale Systems. The PV-based high-frequency transformer can decrease performance and increase system costs, but it can greatly reduce the power conversion system's weight and volume and mitigate the problems of grid isolation. Among all the Multilevel Inverters used for Medium and Large-scale PV systems, the diodes and the capacitors are eliminated, and multiple isolated and balanced DC sources are connected across each H-Bridge in the Modular Multilevel Cascaded (MMC) Inverter. To balance the voltage of the DC sources with (MPPT) operation – a common high-frequency magnetic link is used [52-53]. Electrical separation between the PV array and the grid is also provided by the high-frequency magnetic connection. For this thesis work, the output obtained from the Conventional 15-level Inverter has been studied and analyzed for implementing the Proposed loss calculation Methodology [55-57].

In the Conventional 15-level Multilevel Inverter's input side, a control signal as a continuous triangular frequency is required in order to compare with the 3-phase sinusoidal signal, which is called a reference signal. As this Multilevel Inverter is working with a 15-level control signal, so the 3-phase sinusoidal reference signals are comparing with 15 levels, and as a result, gate pulses are generated for the switch (IGBT).

The Inverters which are operated with Pulse Width Modulation (PWM) are called PWM Inverters. There are various schemes for pulse width modulation applied in the Inverter switches to achieve the desired ac output voltages. Many varieties of reference signals are used in both traditional converters as well as Multilevel converters. The Sinusoidal, Third Harmonic Injected Sinusoidal, 60^{o} Modulated Sinusoidal and Trapezoidal are the vital reference signals or control signals (constant or slowly varying in time) used in both the Conventional Inverter system and the Multilevel Inverter system [58-59]. All are of various characteristics having unique advantages and disadvantages. By decreasing the amount of switching occurrences in a period, the switching losses can be decreased. When these four individual reference signals with level-shifted carrier signals used in a 3-phase system, four different modulation schemes are generated, such as The level-shifted carriers with sinusoidal references known as the Sin Pulse Width Modulation (SPWM) scheme, the level-shifted carriers with Third Harmonic Injected Pulse Width Modulation

(THIPWM) scheme, The level-shifted carrier with 60^o Modulated Sinusoidal references known as the 60^o Pulse Width Modulation (SDPWM) scheme, The level-shifted carrier with Trapezoidal type references known as the Trapezoidal Pulse Width Modulation (TRPWM) scheme. In [58] and [59], the output of the 120° shifted sinusoidal three reference signals and output of the THIPWM reference signals obtained by the MATLAB/Simulink model from the 3-phase Modular Multilevel Cascaded Inverter Circuit have been illustrated, respectively.

As per the concern of the carrier signal, PWM techniques for gate signal generation generally has two Methods in Multilevel Inverters such as Level shifted Carrier Pulse Width Modulation (LSCPWM) and Phase shifted Carrier Pulse Width Modulation (PSCPWM). Also various schemes as In Phase disposition (IPD), Phase Opposition disposition (POD) and Alternate Phase Opposition Disposition (APOD). Level shifted carriers are arranged vertically, exists between two voltage levels. Thus it is named as level-shifted. By Comparing with phase-shifted carrier-based modulation scheme, level-shifted carrier-based modulation scheme provides less distorted ac outputs. In level-shifted scheme on a particular phase leg, the following parameters are calculated as (1) Carriers are level shifted by, $\theta_{ls} = \pm A_m/(m-1)$, (2) Peak to peak amplitude of carrier signal, $A_{cl} = A_m/(m-1)$ [where, A_m = peak to peak amplitude of the reference signal] and (3) Amplitude modulation index, $m_{al} = A_m/(m-1)A_{cl}$. The literature [60] defines the switching patterns produced by the PWM technique of Level Shifted in Phase Disposition (LS-IPD) where four triangular waveforms are compared to a sinusoidal relation for the generation of switching signals in each case.

By comparing with the 3-phase THIPWM sinusoidal reference signals, level-shifted 15-level carriers generate 15 signals for the H-bridge cells in this thesis work. Those 15 pulses fire the 1^{st} cross pair IGBTs of a single H-bridge cell while the other 2^{nd} cross pair is off and vice-versa. Each pair of IGBTs has 3 output voltages. There are 7 H-bridge cells for a 15-level MMC Inverter; each consists of 4 switches (IGBTs). The gate pulses generated by Level shifted In Phase disposition (LSIPD) Method by MATLAB where every carrier signal is in phase but in distinct levels [61]. In this thesis work loss calculation has been Proposed for the 3-phase 15-level Modular Multilevel Cascaded (MMC) circuit.

The total losses of the concerned Inverter vary on the modulation, level number, and the IGBTs' inherent behavior. Different switching Methods are introduced for loss evaluation of MMC with

different switching strategies [64]. Loss calculation was done by only fixed modulation index and fixed power factor for 7-level MMC circuit controlled by SPWM as well as 2^{nd} order polynomial equations were calculated for switching loss and conduction loss [72]. Moreover, IGBT type FZ250R65KE3, 6.5 kV, 250 A rated IGBT module is used for 11 kV Low to Medium Voltage System. THIPWM is used as a switching technique in the Proposed Method with a level-shifted scheme, which is aimed to obtain a better spectra property. The Proposed research is aimed for developing an Analytical Methodology for loss calculation using Modular Multilevel Cascaded (MMC) or H-bridge Inverter circuit.

1.4 Problem Identification

In previous Methods to analyze the loss, instant current and threshold voltage of the device were taken for developing the equations for the average conduction loss calculation. The average switching loss for IGBT and diode are obtained by multiplying switching energy with instantaneous current and switching frequency. In the Proposed Method, an Analytical Methodology has been developed for the loss calculation with the help of rms and average current instead of taking instant current. Instant current is avoided in this Proposed Method because at continuous and different gate pulses, currents enter into the IGBT and its antiparallel diodes continuously. The amount of current is not the same in all cases because gate pulses are not the same all the time. So current varies. Therefore, rms and average current have been calculated to develop the Proposed Analytical Methodology. 5th order polynomial equation was used for calculating conduction loss and switching loss. The loss calculation Method is applied in THIPWM-controlled MMC Inverter to get lower THD. IGBT 5SNA 1500E250300 (ABB), 2.5 kV 1500 A rated IGBT module is used in the MMC Inverter for 11 kV Medium Voltage System. Real data sheet data is used for calculation.

Hence, the aim of this research is to develop an Analytical Methodology for calculating the loss for Modular Multilevel Cascaded Inverter (MMC) and to design circuits as per the developed equations.

1.5 Thesis Objectives

The principal goal of this thesis is to develop a new Analytical Methodology for the loss calculation of the Modular Multilevel Cascaded Inverter. However, more particularly, the objectives include:

1. To analyze a loss calculation Method for computing the losses for Modular Multilevel Cascaded Inverter (MMC) with Third Harmonic Injected (THI) PWM.
2. To develop some theoretical equations as per the analysis of the loss calculation Method in terms of conduction loss and switching loss for both IGBTs and their antiparallel diodes.
3. To design some circuits applied inside the IGBTs of the Inverters as per the developed equations of the conduction loss and the switching loss.
4. To incorporate an xl sheet in order to read the loss during different switching time.
5. To justify the efficacy of the Proposed Methodology by simulation results.

1.6 Thesis Organization

This thesis focuses on the study - a new Analytical Methodology for loss calculation of the Modular Multilevel Cascaded Inverter with Third Harmonic Injected (THI) PWM.

- In **Chapter 2**, different Inverter topologies including Conventional and Multilevel Inverters are discussed. The working principle of the Conventional Inverter is explained.
- In **Chapter 3**, the different losses of IGBT and diode are identified and the Proposed Methodology for loss calculation are introduced.
- In **Chapter 4**, the performance of the Proposed Method is analyzed. Performance comparison is shown using Proposed loss calculation Method with an Inverter circuit from another published IEEE paper to measure the efficacy of the Proposed Method.
- **Chapter 5** includes the conclusion of the thesis, where a brief summary of the results is illustrated with some recommendations for future work.
- References are added at the end of the report.

CHAPTER 2

DC-AC CONVERTERS

The switch-mode dc-to-ac converters, known as Inverters, are used to provide ac power in ac motor devices and uninterruptable ac power supplies. The Inverters are designed with a particular arrangement of certain power semiconductor components, work with the technique of pulse width modulation (PWM) and switch between various circuits, which ensures that the Inverter is a nonlinear but smooth mechanism. Furthermore, the regulation strategies of the Inverter are similar to those of DC-DC converters. Different kinds of Inverters are available on the market according to the intent. The Inverter aims to adjust the input DC voltage to the desired magnitude and frequency of a symmetric AC output voltage. The output voltage and the frequency may be variable or fixed. By varying the dc input voltage and by keeping the Inverter gain constant, the variable output voltage can be obtained. On the other hand, if the DC input voltage is constant and not controllable, it is possible to achieve a variable output voltage by varying the Inverter's gain, which is regulated by the pulse width variation. The gain of the Inverter is determined by the AC output voltage ratio to the DC input voltage. Square-wave or quasi-square-wave voltages are ideal for low and medium-power applications, whereas slight twisted sinusoidal waveforms are suitable for high-power applications. The input dc is acquired from a diode-bridge rectifier and LC or C filter from a single-phase or three-phase utility power supply. There are many PWM technique and of all the control technique, the THIPWM modulation will reduce the switching losses of the Inverter. By flatting the top of the waveform of the sinusoidal reference signal decreases the number of switching occurrences in each cycle of the THIPWM.

2.1 Inverter Circuit Topologies

If the input of the switch mode Inverters are dc voltage source, they are called voltage source Inverters (VSIs) and if the input of the switch mode Inverters are dc current source, they are called current source Inverters (CSIs) though CSIs has limited applications. VSIs can also be classified

into two categories, High Power 2-level Voltage Source Inverter and Multilevel Inverters. Multilevel Inverters are further classified into Single DC source and Multiple DC source. Flying Capacitor (FC) and Neutral Point Clamped (NPC) Inverters are classified under Single DC source and Cascaded H-Bridge is classified under Multiple DC source. The Inverter Circuit topologies is shown in figure 2.1.

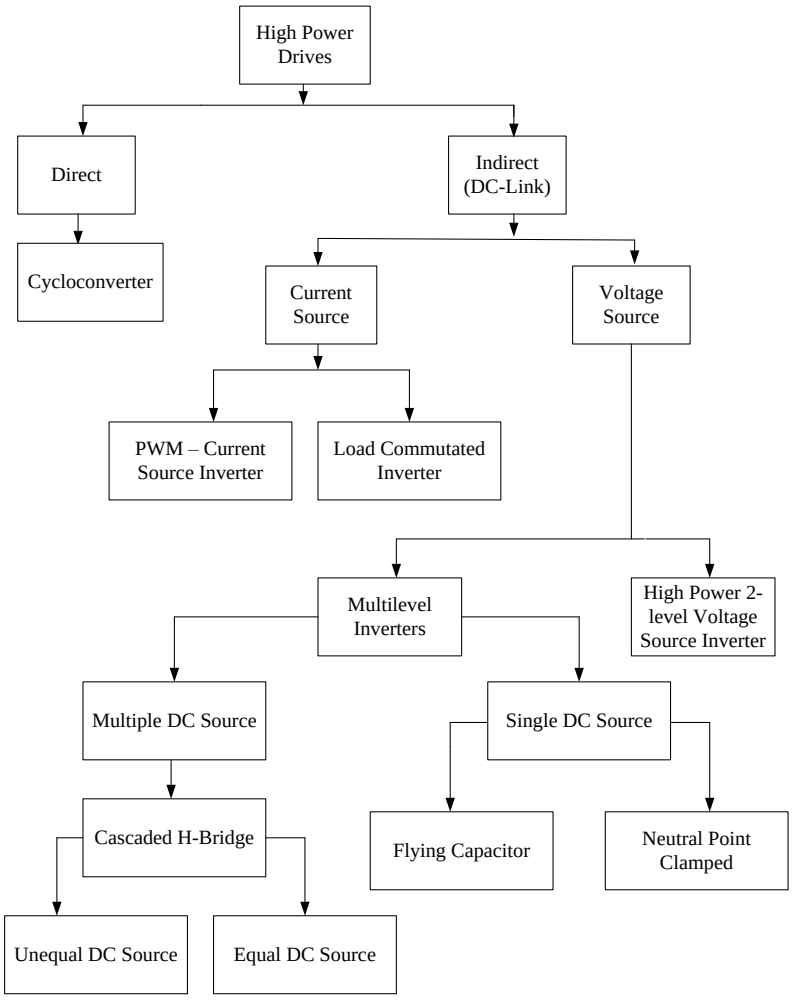

Figure 2.1 Inverter Circuit topologies

2.1.1 High Power 2-level Voltage Source Inverter/Conventional Inverter

Two level Inverter is known as Conventional Inverter which is primarily used to achieve a controllable voltage [4-6]. The two-level Inverter is a circuit which comprises of voltage sources with a certain amount of voltage and several voltage or current control switches. The traditional two-level Inverters, however, have some pitfalls in high-power and high-voltage applications, primarily due to switching losses and power system rating restrictions. Power loss is very high due to the existence of multiple switches and sources. In traditional two-level Inverters, with the help of semiconductor power switches, consists of similar three legs. Therefore, each phase's output ($V_{AN}/V_{BN}/V_{CN}$) depends only on dc bus voltage and the switching status. Since any switch of each phase can be ON at any moment, the output voltage does not change with the change of load current. In traditional two-level Inverters, with semiconductor modules' help, the input DC is converted into the output as an AC supply of the desired frequency and voltage. A switch group is operated to provide the positive half-cycle output, called positive group switches, and the negative group switches are the other group that is operated to provide the negative half-cycle. The traditional three-phase Inverter load is divided by 120^0 with each other's fundamental frequency by three different single-phase Inverters. In such situations, such as having a three-phase output transformer or independent access to each phase on the load side, this configuration is preferred. Such access is, however, not available in operation. An Inverter constructed with at least 12 switches is required to make this arrangement feasible to provide an uninterruptible ac supply referred to as a 3-level Inverter called a Multilevel Inverter. Started from 3-level or above is known as Multilevel Inverters. A Conventional/2-level 3-phase voltage source Inverter (VSI) is shown in figure 2.2.

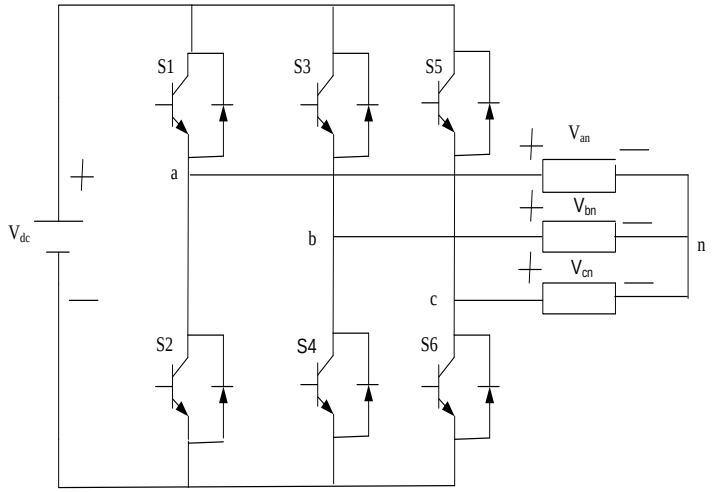

Figure 2.2 The Conventional Three Phase Inverter [4-6]

To receive three-phase balanced voltages, the above three single-phase Inverters are split into each other by 120 °. Depending on the application, traditional 3-phase VSIs contain six semiconductor switches, using IGBT, MOSFET, etc. The feedback diodes, which are located anti-parallel to the semiconductor switches, are worked to return the stored energy from the inductive load to the DC supply. The DC power is set as an input, and by providing the right gate pulses to the switches, the VSI transforms DC power into AC power. A capacitor with large capacitance is connected at the Inverter's input terminals to make the input dc voltage constant and remove the harmonics which fed back to the dc source.

The modulation scheme applied at the input side of the Conventional Inverter is shown in figure 2.3 and the output line voltage of the Conventional Inverter is shown in figure 2.4 respectively.

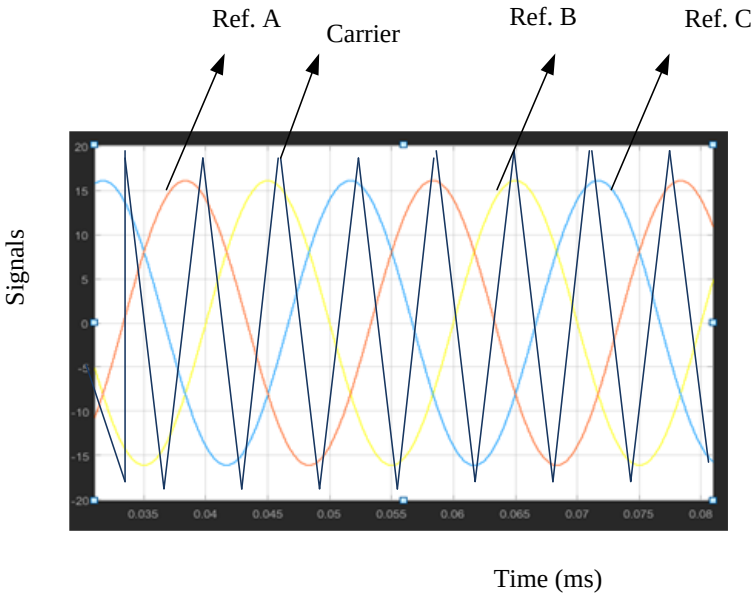

Figure 2.3 Modulation Scheme of the Conventional/2-level Three Phase Inverter

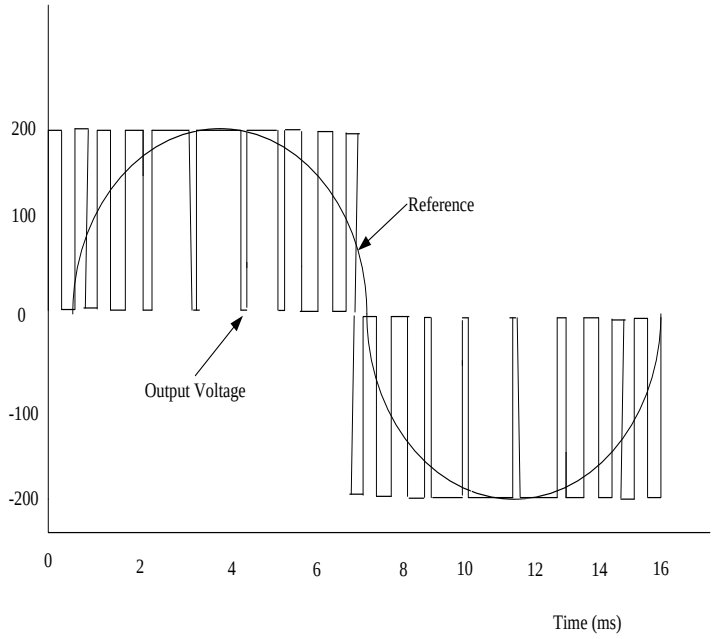

Figure 2.4 Line voltage of the Conventional/2-level (Three Phase) Inverter

2.1.1.1 Working principle of a Conventional/2-level Inverter

A three-phase Inverter consists of three single-phase Inverter where each switch of each phase can be attached to the load terminal. For the basic control system, the operation of three switches may be coordinated such that a single switch operates at every 60 degrees to create a line-to-line o/p waveform. This waveform requires a zero voltage stage between the two parts of the square-wave, positive and negative. If PWM-based Methods are applied, it is possible to take the waveform's basic shape such that the third harmonic, and its multiples, is canceled.

Usually, with a 120-degree angle, this Inverter's three arms would be delayed to produce a 3-phase AC supply. After any 60-degree angle, the switching can be performed. The switches will supplement each other, such as S_1, S_2, S_3, S_4, S_5, and S_6. In this, three single-phase Inverters are located over a similar DC source.

By contrasting a reference wave and a triangular carrier, ordinary PWM modulation for two-level Inverters is done. For the output voltage signal, the reference wave has the frequency and amplitude necessary, and in a simple ordinary case, the triangular carrier wave has an amplitude of half the DC input voltage, and its frequency depends on the application but must be higher than the reference wave frequency.

In order to obtain balanced and regulated three-phase output voltages with an approximately constant input dc voltage, pulse width modulation is used. To produce gate pulses that control the switching operations (On/Off) of the Inverter circuit for the IGBTs, a pulse width modulation technique is necessary. For regulating the conduction of IGBTs in the Inverter, there are various PWM Methods. The approach is to compare three sinusoidal control voltages, which have 120^o phase difference, with the same triangular waveform. A three-phase Inverter is mainly concerned with the harmonics of line-to-line voltages. In the output voltage, harmonics which have lower order can be removed or reduced and harmonics which have higher order can be conveniently filtered by controlling PWM. Certain variables have been taken care of, such as

- For low values of modulation ratio, a synchronized PWM should be used to eliminate the even harmonics and the ratio should be an odd integer.

- For modulation ratio which have large values, the amplitudes of sub-harmonics are small due to asynchronous PWM but results large currents which is undesirable. Therefore, the asynchronous PWM is avoided.
- The output voltage produces several more harmonics in the sidebands during over modulation (where the amplitude modulation ratio is >1), regardless of the frequency modulation ratio value.

There are basically two conduction modes of operation for 3-phase VSI such as 180^o conduction mode and 120^o conduction mode. They are described as follows.

2.1.1.2 180° Conduction Mode

The 180^o conduction mode specified that three switches conduct at a time and each of the three switches conducts for a duration of π- radians. Each switch among the three conduct for 180^0 time period and after every 60°, one of them is opened and a new one will be start conducting. Consider the pair of switches denoted by S1 and S2, S3 and S4, S5 and S6 belonging to three different legs of the three phase Inverter respectively (Figure 2.2). Both the switches which are in the similar leg should not be closed at any instant of time as it has the possibility of DC short circuiting. Therefore, it has to be kept in mind that such scenario can be prevented.

Switching sequence is started by closing the S1 switch and naming it as 0^o. S1 switch will conduct from 0^0 to 180^o for the positive half-cycle as the selected length of conduction is 180^o. To make the positive half cycle complete, after S1, S3 start conducting for second positive half cycle by 180^0 duration and after that S5 start conducting for 3^{rd} positive half-cycle by 180^0 of time period. Thus repeating the sequence a complete positive half-cycle is accomplished.

To make the negative half-cycle complete, switch S2, S4 and S6 start conducting for 180^0 of time period. When any of the positive half cycles completes, the respective switches corresponding to the negative half-cycle start conducting for the next 180^0 of the time period. In this sequence, each of the switches corresponding to positive half-cycle and negative half-cycle conducts respectively. The ideal three-phase voltage waveform is obtained as illustrated in figure 2.5 by adopting this symmetrical switching. The flipping sequences for the 180^o conduction mode are seen in Table 2.1.

Table 2.1 Switching sequences for 180^0 Conduction Mode

Interval	Duration	Conducting Switches							
1	180°	S1	S2	S3					
2	180°		S2	S3	S4				
3	180°			S3	S4	S5			
4	180°				S4	S5	S6		
5	180°					S5	S6	S1	
6	180°						S6	S1	S2

2.1.1.3 120° Conduction Mode

In all ways, the 120^o conduction mode is identical to 180^o, except that each switch's conduction time length is 120^o. The conduction mode of 120^0 stated that two switch at a time conduct and each of the two switches conducts for 120° time period. After every 60°, each switch among the two is opened and a new one will be start conducting. Consider the pair of switches denoted by S1 and S2, S3 and S4 and S5 and S6 belonging to three different legs of the three phase Inverter respectively. One of the switches of each leg must be closed and another one be opened at any instant of time or else it has the possibility of DC short circuiting.

All over again, switching sequence is started by closing the S1 switch at first and naming it as 0^o. The switch S1 will be conducted from 0^0 to 120^o of the first positive half-cycle as the selected length of conduction is 120^o. The remaining time of the positive half-cycle counting from120^0 to 180^o of the sinusoidal signal, S1 will be open and S3 will be close started from another 120^0 to 240^0. Moreover, switch S5 will be closed from 240^o to 360^o. In this sequence, S1, S3 and S5 start conducting for 120^0 of the time period to make a positive half-cycle of the sinusoidal wave. To make the negative half cycle of the sinusoidal wave, switch S2, S4 and S6 will be closed for 120^0 time period. In this sequence, the ideal three-phase voltage is obtained as depicted in figure 2.6 by following this symmetrical switching. The flipping sequences for the 120^o conduction mode are seen in Table 2.2.

Table 2.2 Switching sequences for 120^0 Conduction Mode

Interval	Duration	Conducting Switches						
1	120°	S1	S2					
2	120°		S2	S3				
3	120°			S3	S4			
4	120°				S4	S5		
5	120°					S5	S6	
6	120°						S6	S1

In conclusion, it can be seen that an alternating three-phase voltage output can be obtained from both the 180 ° and 120 ° mode of switching conduction and the output is not a pure sinusoidal wave but resembles the three-phase sinusoidal voltage waveform. For a simple or traditional VSI circuit, the above research has been completed. Nevertheless, for obtaining a better sinusoidal performance, a realistic model based on this principle can be acquired using various types of accessible semiconductor devices or using some PWM scheme or using more semiconductor switches needed for a Multilevel Inverter.

2.1.1.4 Analysis of converter waveform

The analysis of converter waveforms for both 180^0 and 120^0 conduction mode have been discussed in this section. The Inverter operates in eight switching states. All the switches which are at the same leg should not be switched ON at a time because it can short the input voltage and this is a clear violation of the KVL. Therefore, the nature of the two swithes in the same leg is paired. According to the figure 2.2,

$$S1 + S2 = 1 \qquad (1)$$

$$S3 + S4 = 1 \qquad (2)$$

$$S5 + S6 = 1 \qquad (3)$$

The switching operation is accomplished by the modulation technique that ensures only the valid states.

2.1.1.5 Output voltage calculated for 180^0 Conduction Mode

By following the mentioned symmetrical switching (table 2.1) for 180^0 Conduction mode, the phase voltages and the line voltages have been derived in the figure 2.5 sequentially. Line-to- line voltages are calculated by the equations described from the three phase output voltage waveform for 180^0 conduction mode.

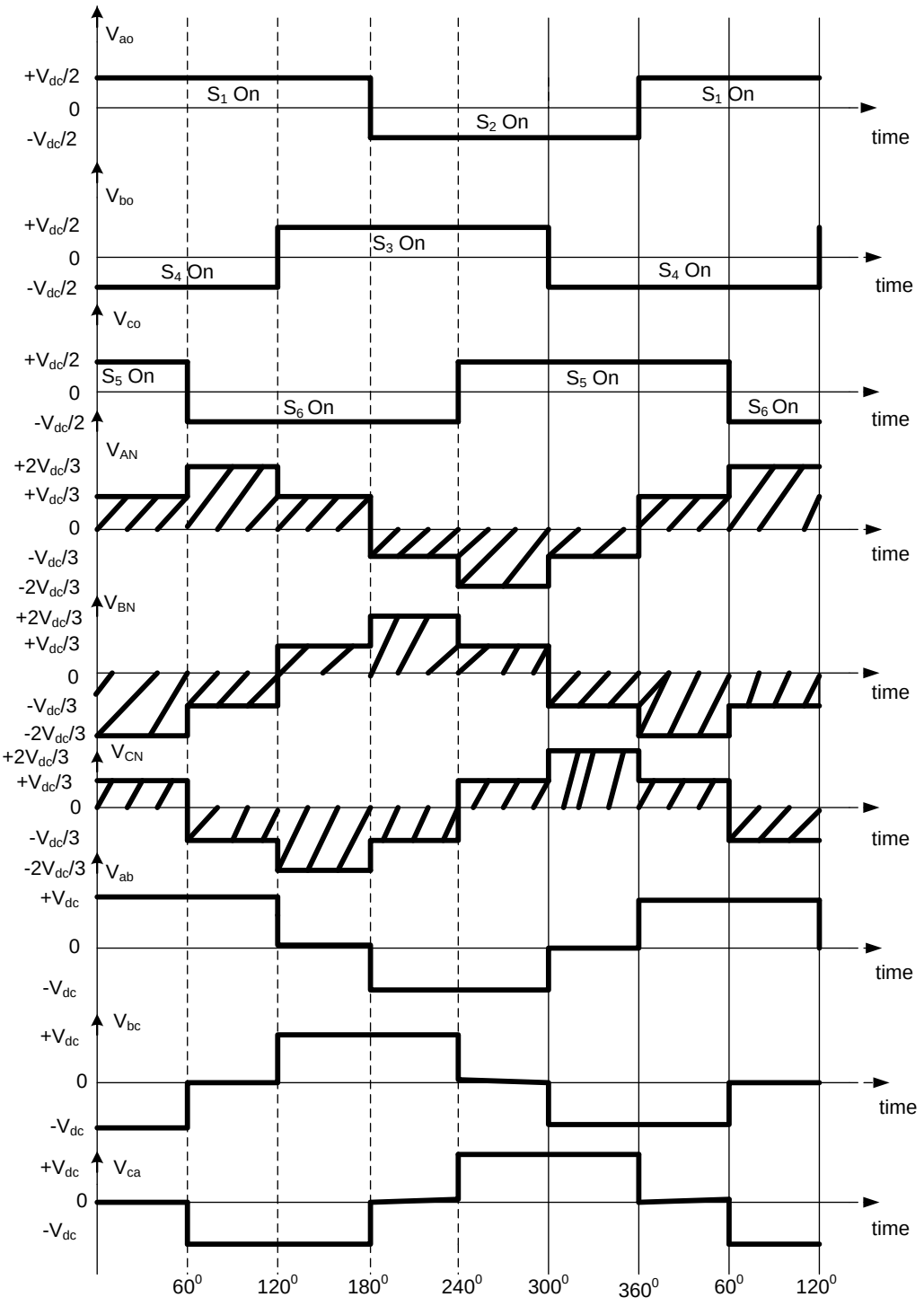

Figure 2.5 Output voltage waveform for180^0 Conduction Mode of the three phase Inverter

For 0^0 to 60^0 time period

Only S1, S4, and S5 are closed and the rest of the switches are open. Therefore, the following voltages are obtained.

Phase voltage, $\mathrm{VAN} = \mathrm{VCN} = \frac{\mathrm{Vdc}}{3}, \mathrm{VBN} = -\frac{2\mathrm{Vdc}}{3}$

By using these equations, the line voltages can be derived as below -

$\mathrm{Vab} = \mathrm{VAN} - \mathrm{VBN} = \mathrm{Vdc}$

$V\mathrm{bc} = \mathrm{VBN} - \mathrm{VCN} = -\mathrm{Vdc}$

$\mathrm{Vca} = \mathrm{VCN} - \mathrm{VAN} = 0$

For 60^0 to 120^0 time period

Only S1, S4 & S6 are close and other three switches are open. Therefore, the following voltages are obtained.

Phase voltage, $\mathrm{VBN} = \mathrm{VCN} = -\frac{\mathrm{Vdc}}{3}, \mathrm{VAN} = \frac{2\mathrm{Vdc}}{3}$

From these equations, the line voltages can be derived as below -

$\mathrm{Vab} = \mathrm{VAN} - \mathrm{VBN} = \mathrm{Vdc}$

$\mathrm{Vbc} = \mathrm{VBN} - \mathrm{VCN} = 0$

$\mathrm{Vca} = \mathrm{VCN} - \mathrm{VAN} = -\mathrm{Vdc}$

For 120^0 to 180^0 time period

Only S1, S3, and S6 are close and other three switches are open. Therefore, the following voltages are obtained.

Phase voltage, $\mathrm{VAN} = \mathrm{VBN} = \frac{\mathrm{Vdc}}{3}, \mathrm{VCN} = -\frac{2\mathrm{Vdc}}{3}$

From these equations, the line voltages can be derived as below -

$\mathrm{Vab} = \mathrm{VAN} - \mathrm{VBN} = 0$

$\mathrm{Vbc} = \mathrm{VBN} - \mathrm{VCN} = \mathrm{Vdc}$

$\mathrm{Vca} = \mathrm{VCN} - \mathrm{VAN} = -\mathrm{Vdc}$

For 180^0 to 240^0 time period

Only S2, S3, and S6 are close and other three switches are open. Therefore, the following voltages are obtained.

Phase voltage, $\mathrm{VAN} = \mathrm{VCN} = -\frac{\mathrm{Vdc}}{3}, \mathrm{VBN} = \frac{2\mathrm{Vdc}}{3}$

From these equations, the line voltages can be derived as below -

$\mathrm{Vab} = \mathrm{VAN} - \mathrm{VBN} = -\mathrm{Vdc}$

$\mathrm{Vbc} = \mathrm{VBN} - \mathrm{VCN} = \mathrm{Vdc}$

$\mathrm{Vca} = \mathrm{VCN} - \mathrm{VAN} = 0$

For 240^0 to 300^0 time period

Only S2, S3, and S5 are close and other three switches are open. Therefore, the following voltages are obtained.

Phase voltage, $\mathrm{VAN} = -\frac{2\mathrm{Vdc}}{3}, \mathrm{VBN} = \mathrm{VCN} = \frac{\mathrm{Vdc}}{3}$

From these equations, the line voltages can be derived as below -

$\mathrm{Vab} = \mathrm{VAN} - \mathrm{VBN} = -\mathrm{Vdc}$

$\mathrm{Vbc} = \mathrm{VBN} - \mathrm{VCN} = 0$

$\mathrm{Vca} = \mathrm{VCN} - \mathrm{VAN} = \mathrm{Vdc}$

For 300^0 to 360^0 time period

Only S2, S4, and S5 are close and the rest of the three switches are open. Therefore, the following voltages are obtained.

Phase voltage, $\mathrm{VAN} = \mathrm{VBN} = -\frac{\mathrm{Vdc}}{3}, \mathrm{VCN} = \frac{2\mathrm{Vdc}}{3}$

From these equations, the line voltages can be derived as below -

$\mathrm{Vab} = \mathrm{VAN} - \mathrm{VBN} = 0$

$\mathrm{Vbc} = \mathrm{VBN} - \mathrm{VCN} = -\mathrm{Vdc}$

$\mathrm{Vca} = \mathrm{VCN} - \mathrm{VAN} = \mathrm{Vdc}$

2.1.1.6 Output voltage calculated for 120^0 Conduction Mode

By following the mentioned symmetrical switching (table 2.2) for 120^0 Conduction mode, the phase voltages and the line voltages have been derived in figure 2.6 sequentially. Line-to- line voltages are calculated by the equations described from the three phase output voltage waveform for 120^0 conduction mode.

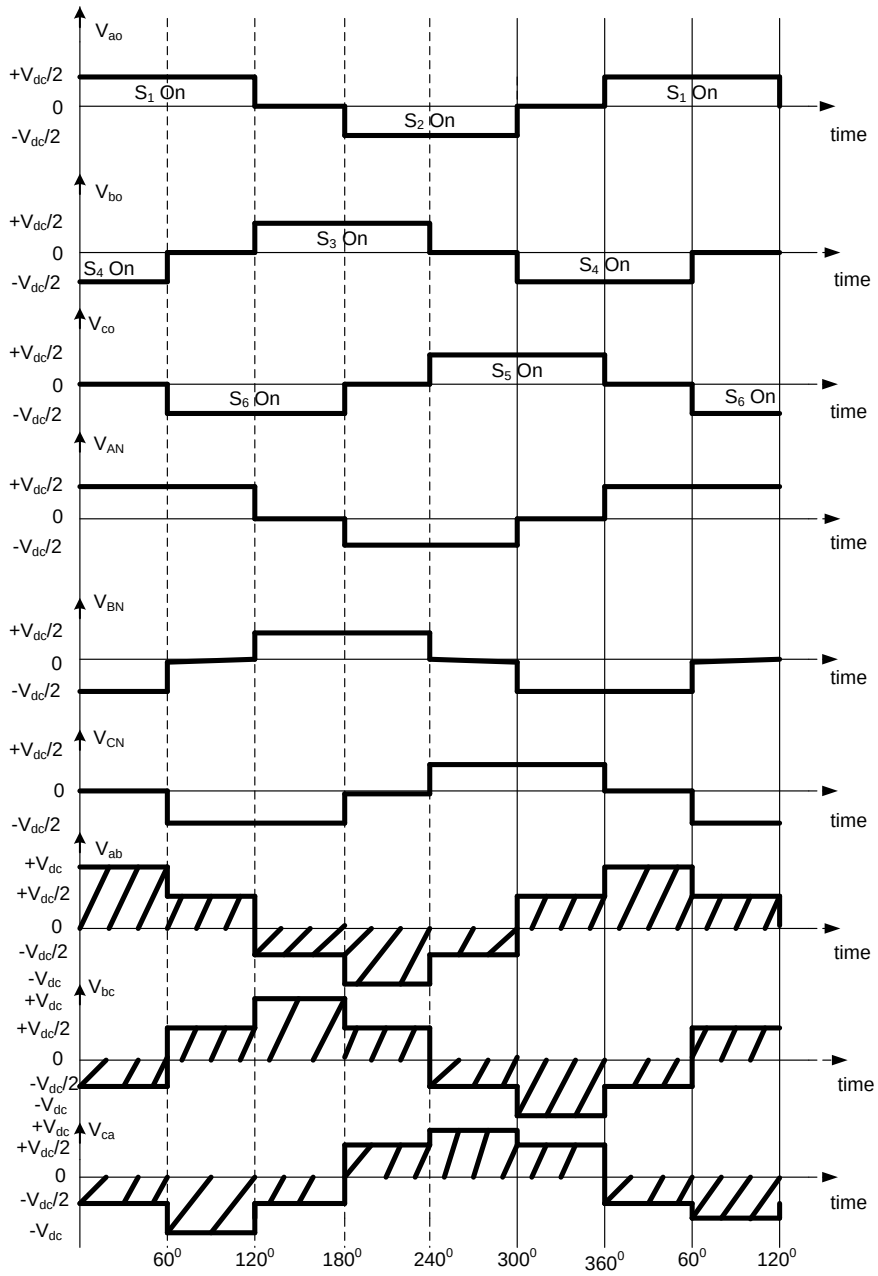

Figure 2.6 Output voltage waveform for 120^0 Conduction Mode of the three phase Inverter

For 0^0 to 60^0 time period

Only S1, S4 are close and the other three switches are open. Therefore, the following voltages are obtained.

Phase voltage, $\mathrm{VAN} = \frac{\mathrm{Vdc}}{2}, \mathrm{VCN} = 0, \mathrm{VBN} = -\frac{\mathrm{Vdc}}{2}$

From these equations, the line voltages can be derived as below -

$$\mathrm{Vab} = \mathrm{VAN} - \mathrm{VBN} = \mathrm{Vdc}$$

$$\mathrm{Vbc} = \mathrm{VBN} - \mathrm{VCN} = -\frac{\mathrm{Vdc}}{2}$$

$$\mathrm{Vca} = \mathrm{VCN} - \mathrm{VAN} = -\frac{\mathrm{Vdc}}{2}$$

For 60^0 to 120^0 time period

Only S1 and S6 are close and other three switches are open. Therefore, the following voltages are obtained.

Phase voltage, $\mathrm{VBN} = 0, \mathrm{VCN} = -\frac{\mathrm{Vdc}}{2}, \mathrm{VAN} = \frac{\mathrm{Vdc}}{2}$

From these equations, the line voltages can be derived as below -

$$\mathrm{Vab} = \mathrm{VAN} - \mathrm{VBN} = \frac{\mathrm{Vdc}}{2}$$

$$\mathrm{Vbc} = \mathrm{VBN} - \mathrm{VCN} = \mathrm{Vdc}/2$$

$$\mathrm{Vca} = \mathrm{VCN} - \mathrm{VAN} = -\mathrm{Vdc}$$

For 120^0 to 180^0 time period

Only S3 and S6 are close and other three switches are open. Therefore, the following voltages are obtained.

Phase voltage, $\mathrm{VAN} = 0, \mathrm{VBN} = \frac{\mathrm{Vdc}}{2}, \mathrm{VCN} = -\frac{\mathrm{Vdc}}{2}$

From these equations, the line voltages can be derived as below -

$$\mathrm{Vab} = \mathrm{VAN} - \mathrm{VBN} = -\frac{\mathrm{Vdc}}{2}$$

$$\mathrm{Vbc} = \mathrm{VBN} - \mathrm{VCN} = \mathrm{Vdc}$$

$$\mathrm{Vca} = \mathrm{VCN} - \mathrm{VAN} = -\frac{\mathrm{Vdc}}{2}$$

For 180^0 to 240^0 time period

Only S2 and S3 are close and other three switches are open. Therefore, the following voltages are obtained.

Phase voltage, $\mathrm{VAN} = -\frac{\mathrm{Vdc}}{2}, \mathrm{VBN} = \frac{\mathrm{Vdc}}{2}, \mathrm{VCN} = 0$

From these equations, the line voltages can be derived as below -

$$\mathrm{Vab} = \mathrm{VAN} - \mathrm{VBN} = -\mathrm{Vdc}$$

$$\mathrm{Vbc} = \mathrm{VBN} - \mathrm{VCN} = \mathrm{Vdc}/2$$

$$\mathrm{Vca} = \mathrm{VCN} - \mathrm{VAN} = \mathrm{Vdc}/2$$

For 240^0 to 300^0 time period

Only S2 and S5 are close and other three switches are open. Therefore, the following voltages are obtained.

Phase voltage, $\mathrm{VAN} = -\frac{\mathrm{Vdc}}{2}, \mathrm{VBN} = 0, \mathrm{VCN} = \frac{\mathrm{Vdc}}{2}$

From these equations, the line voltages can be derived as below -

$$\mathrm{Vab} = \mathrm{VAN} - \mathrm{VBN} = -\frac{\mathrm{Vdc}}{2}$$

$$\mathrm{Vbc} = \mathrm{VBN} - \mathrm{VCN} = -\frac{\mathrm{Vdc}}{2}$$

$$\mathrm{Vca} = \mathrm{VCN} - \mathrm{VAN} = \mathrm{Vdc}$$

For 300^0 to 360^0 time period

Only S4 and S5 are close and other three switches are open. Therefore, the following voltages are obtained.

Phase voltage, $\mathrm{VAN} = 0, \mathrm{VBN} = -\frac{\mathrm{Vdc}}{2}, \mathrm{VCN} = \frac{\mathrm{Vdc}}{2}$

From these equations, the line voltages can be derived as below -

$$\mathrm{Vab} = \mathrm{VAN} - \mathrm{VBN} = \frac{\mathrm{Vdc}}{2}$$

$$\mathrm{Vbc} = \mathrm{VBN} - \mathrm{VCN} = -\mathrm{Vdc}$$

$$\mathrm{Vca} = \mathrm{VCN} - \mathrm{VAN} = \frac{\mathrm{Vdc}}{2}$$

2.1.2 Multilevel Inverters

Multilevel Inverters are being extensively used in the renewable energy conversion process for high voltage and high power applications in order to achieve more efficiency than obtained from the Conventional Inverter system. The Multilevel Inverters starting from 3 level to different upper levels, were first Proposed in the year 1975 [41]**.** Multilevel Inverter topologies are of 3 types. The topologies are

- Neutral Point Clamped (NPC)
- Flying Capacitor (FC)
- Modular Multilevel Cascaded (MMC) or H-Bridge Inverter

2.1.2.1 Neutral Point Clamped

The Neutral Point Clamped topology (NPC) gives the best harmonic performance compared with the other basic Multilevel Inverter topologies. The number of diodes required for each phase leg is calculated by (2m-4), where m denotes the level number. Also the active switching devices for each phase leg is calculated by (2m-2). m-level output phase voltage and (2m-1) level output line voltage are obtained from the m-level NPC topology. In NPC topology, the more the converter level increases, the more the auxiliary diodes increases. Therefore, the major design challenge of NPC is considered as the reverse recovery of the large number of clamping diodes. Unlike Modular Multilevel Cascaded (MMC) Inverter, NPC requires a single DC supply. For a three phase m-level Inverter, (6m-12) auxiliary diodes are required. The 3 phase NPC topology shares a common DC bus voltage which has been subdivided by (m-1) capacitors into equal m-levels. Many development of NPC topology have been done in different times. A new NPC PWM 3-phase 3-level Inverter was introduced in 1981 [45] shown in figure 2.7.

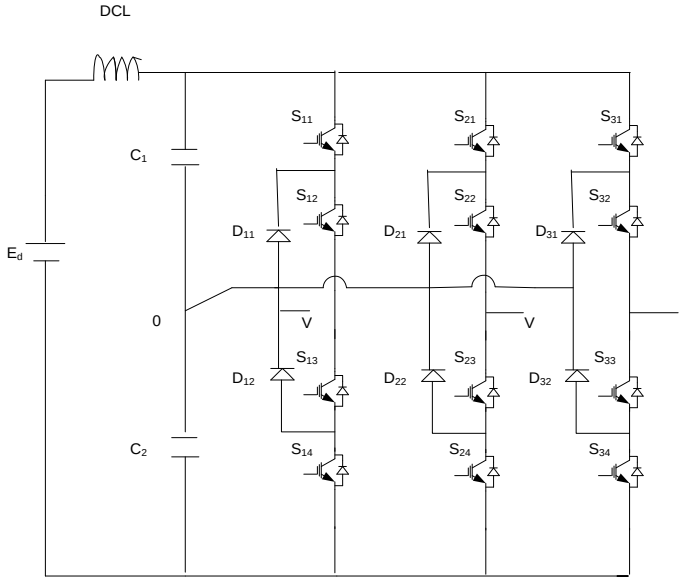

Figure 2.7 Three-phase 3-level NPC Inverter circuit [45]

2.1.2.2 Flying Capacitor

The configuration of the Flying Capacitor (FC) topology is similar to the structure of the Neutral Point Clamped (NPC) topology. The distinction is that the auxiliary capacitors are needed for FC topology, while the auxiliary diodes are required for NPC topology. Active switching devices are calculated by (2m-2) for each phase leg, and the number of capacitors needed for each phase leg is calculated by (2m-4). From the m-level FC topology, the m-level output step voltage and (2m-1) level output line voltage are obtained. FC topology, like NPC topology, shares a typical DC bus voltage that contrasts with the topology of Modular Multilevel Cascaded (MMC). When the amount of converter level is high, the number of necessary capacitors is also high, the main design challenge of FC topology. Thus, the design of a high-level FC Inverter device is impractical. An external control circuit is also needed to recharge the clamping capacitors with the voltage level necessary, which increases the size, weight and expense of the Inverter device. The primary value is that each branch can be evaluated independently. The number of auxiliary capacitors needed for each phase leg will be determined by (m2-3m+2)/2 for 3-phase, if the voltage rating of the capacitors is equal to that of the active switching devices. In [49], a new 3-phase 5-level FC Inverter topology was described shown in figure 2.8.

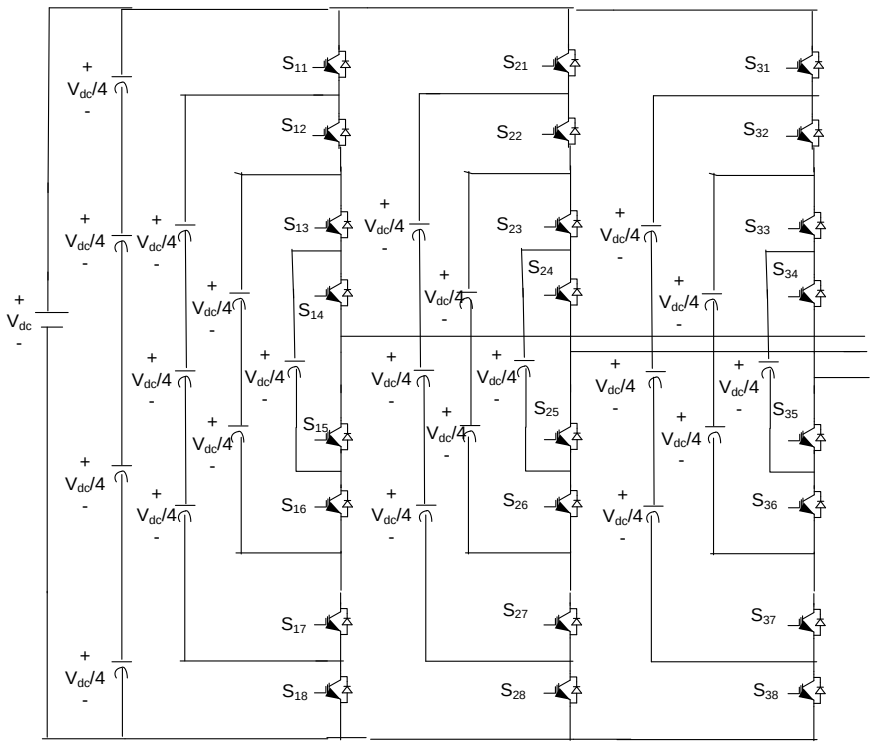

Figure 2.8 Three-phase 5-level FC Inverter circuit [49]

2.1.2.3 Modular Multilevel Cascaded (MMC) Inverter

Among all the above mentioned Multilevel Inverters, the Modular Multilevel Cascaded (MMC) H-Bridge Inverter has drawn a special interest because MMC Inverters require a less number of components and high power quality can be gained from this Inverter. These Inverters are used to extract power from solar system and a high power can be achieved from these Inverters which can be directly connected to the grid without LCL or EMC filter. The more the level increases, the less will be the harmonic content in the output waveform. The output becomes more synthesized with respect to increase of levels or vice-versa which resembles a staircase. The levels can be defined by 3,5,7,9,11,13,15,17,19,21 or more. A MMC Inverter requires 2(m-1) [m=level number] switches, voltage levels can be defined by 2N+1 [where, N= number of cells or dc link voltages]. A m-level MMC Inverter has m-level output phase voltage. The main advantage of MMC Inverter is that with minimum level of voltages maximum number of output voltage level can be obtained. A 3-phase 15-level H-Bridge Modular Multilevel Cascaded Inverter is shown in figure 2.9.

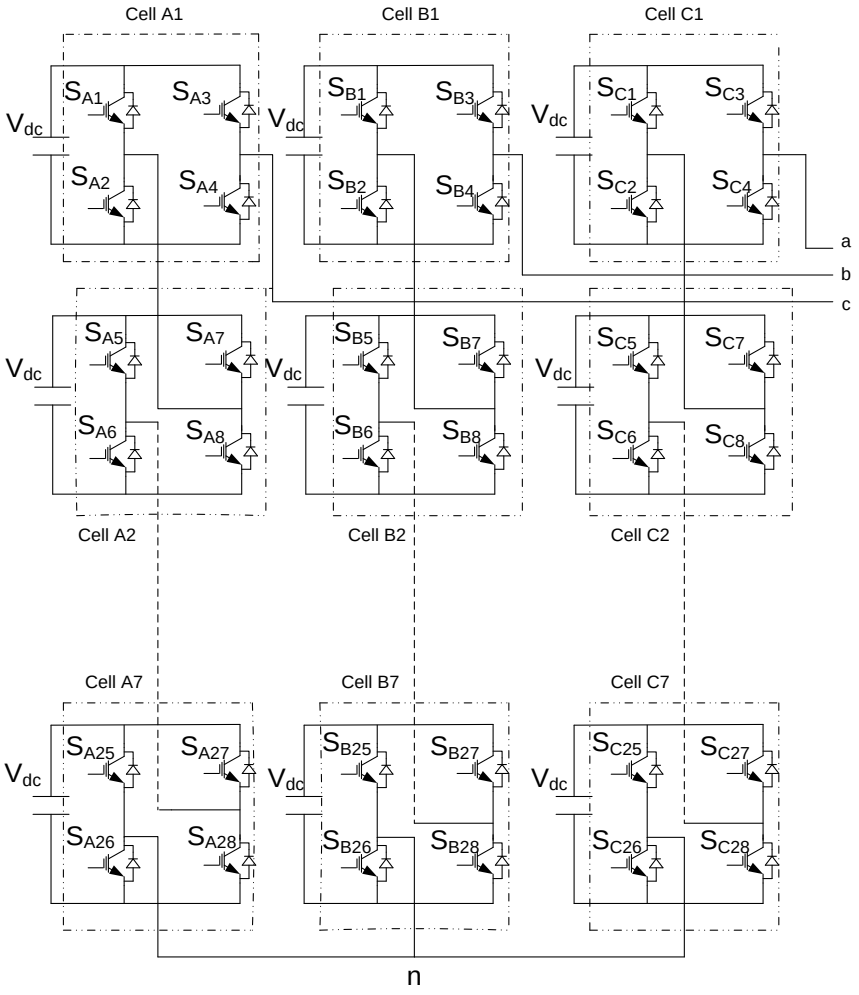

Figure 2.9 Three-phase 15-level H-Bridge Modular Multilevel Cascaded Inverter circuit [55-57]

2.2 Comparison of the 2-level and Multilevel Inverters

Multilevel Inverter starts from 3-level. The output voltage waveform is generated in a 2-level Inverter using PWM with two voltage levels, causing the output voltage and current to be skewed and the THD to be high. On the other hand, the output voltage and current of the 3-level Inverter is even more sinusoidal and the THD is better.

The efficiency of the whole system is dominated by the rectifier losses in light loads for 2-level Inverters.Whereas, the performance at maximum load is higher in 3-level Inverters than in 2-level Inverters. Better rated power consumption means a smaller heat sink and better reliability.

It requires two modules in series in each phase in a three-level Inverter, but only one module per phase is required in a two-level Inverter.

The two-level configuration is noted to be 27 percent cheaper than the three-level configuration, but it is 44 percent higher in a two-level Inverter than in a three-level Inverter in terms of power losses. The higher-level Inverter will have output power of less than 5% THD because it synthesizes the output voltage of the staircase by reducing the harmonic content of the waveform of the output voltage, which is similar to the reference signal of the sinusoidal voltage. Since they are quicker, lighter and cheaper than high voltage switches used in 2-level Inverters, the equipment used in multi-level Inverters are low voltage switches. They endure higher voltages as switches are built in series, so switching losses can be minimized because the switching frequency is smaller than the 2-level Inverter, and the switching speed for low voltage switches is also faster. Multilevel Inverters thus provide better sinusoidal voltage waveform than 2-level Inverters, and using more than two voltage levels, the output voltage can be generated, which allows the THD to be lower. Conduction losses are also smaller due to low forward voltage decline. The dv/dt of the output voltage is lower when using different voltage levels, so the strain in the cables and motor is lower. By switching frequency, conduction losses are not altered, but it depends on the modulation technique. With the Inverter modulation index MI and the load power factor PF, switching losses are independent, but increase linearly with the switching frequency. The conduction losses of the two-level Inverter are smaller compared with the equivalent switching losses for switching frequencies that are widely used. The general comparison between 2-level and Multilevle Inverters are shown in Table 2.3 and 2.4 respectively.

Table 2.3 The general comparison between 2-level/Conventional and Multilevel Inverters

Sl No.	Parameters	2-level	Multilevel
1	Efficiency	Low	High
2	Harmonics	High	Low
3	Output voltage	Low	High
4	Voltage Regulation	Not adjustable	Adjustable

Table 2.4 Comparison between 2-level/Conventional and Multilevel Inverters based on parameter used

	2-level	Diode Clamped MLI	Flying Capacitor MLI	Cascaded H-Bridge MLI
No. of switches per phase	2	2(n-1)	2(n-1)	2(n-1)
No of DC Bus Capacitors	1	(n-1)	(n-1)	(n-1)/2
No of Clamping diodes per phase	0	(n-1)*(n-2)	0	0
No of Flying Capacitors per phase	0	0	(n-1)*(n-2)/2	0

CHAPTER 3

Proposed Loss Calculation Methodology

The Modular Multilevel Cascaded (MMC) Inverter or H-Bridge Inverter is one of the useful Multilevel converters/Inverters that uses the minimum voltage level and generates the maximum output voltage level. Isolated and balanced DC sources are connected to each H-Bridge of the MMC Inverter. A widely accepted high-frequency magnetic link is used to balance DC source voltage together with Maximum Power Point Tracking (MPPT), that also offers electrical insulation between the Photovoltaic system and the grid. Four switching devices are needed for each H-Bridge cell that can yield 3 distinct voltage outputs namely Vdc, 0 and –Vdc. The gate pulses generated by the Third Harmonic Injected PWM (THIPWM) Method and the current flowing through the H-Bridge cell are computed in such a manner as to evaluate the losses associated with it. Gate pulses are necessary for the computation of switching losses only, whereas currents are needed for the computation including both switching losses and conduction losses. There are 84 IGBTs in the 3-phase 15-level Modular Multilevel Cascaded Inverter Circuit, each phase contains 28 IGBTs and is therefore equally distributed in three phases.

3.1 Identification of different losses in the IGBTs

The behavior of IGBTs are observed by the manufacturer at Device Under Test Condition to identify different losses in IGBTs. figure 3.1 demonstrates different types of losses found by the manufacturer when switching device is tested.

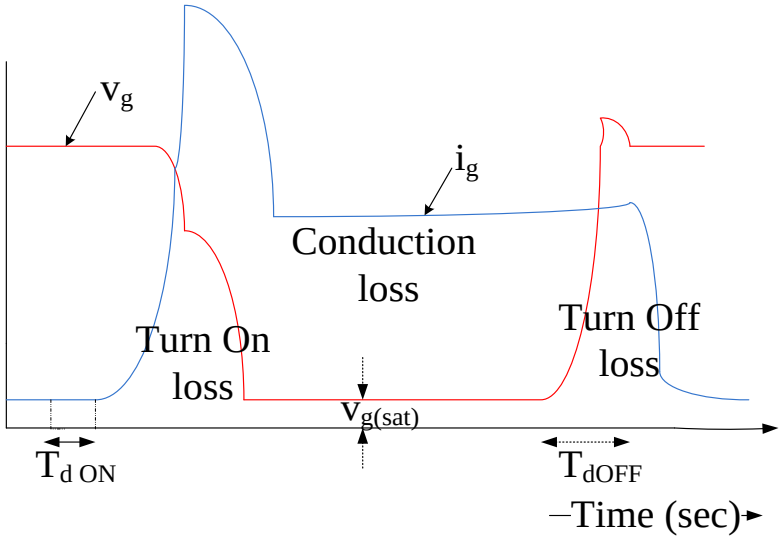

(a)

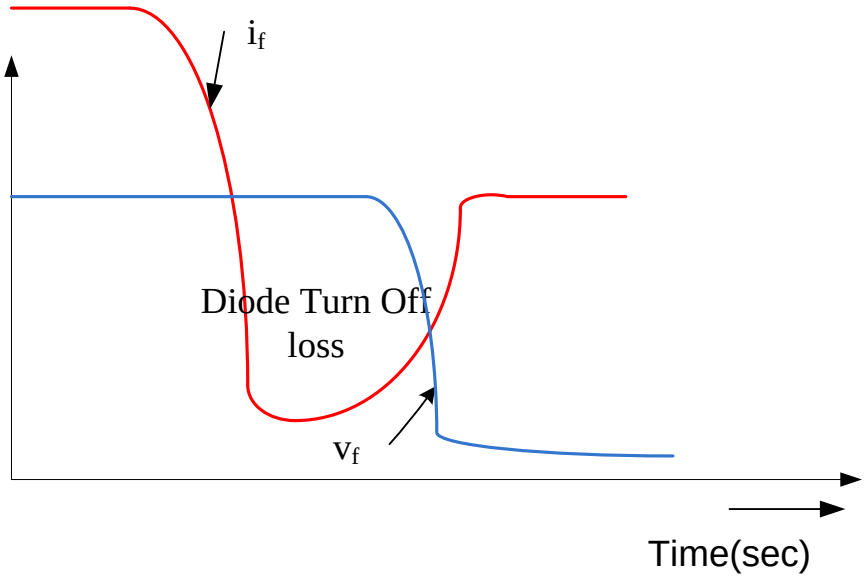

(b)

Figure 3.1 Approximated dynamic behavior of a)Turn-on and Turn-off of IGBT and b) Diode Turn-off at Device Under Test (DUT) condition

There are five types of losses to be assessed for the MMC 3-phase H-bridge Inverter circuit. The losses are as follows,

1. Switching turn-on loss,
2. IGBT switching turn-off loss,
3. IGBT (total) loss of switching,
4. Diode turn-off loss,
5. Loss of IGBT conduction
6. Loss of diode conduction

3.2 Methodology

The calculation process of the losses associated with the Multilevel Inverter has been designed in following four steps

- First, design a circuit to control the positive and negative current of the IGBT.
- Second, a Method has been stated along with a circuit to count the switching losses for both the IGBTs and diodes.
- Third, a Method has been stated along with a circuit to count the conduction losses for both the IGBTs and diodes.
- Fourth, accumulate all the above losses obtained from the IGBTs and diodes to count the total losses associated with the Inverter.

This process has been explained in detail below.

3.3 IGBT input Current Control Circuit

To distinguish the positive and negative current of the IGBT's input current, a circuit has been introduced inside the IGBT. The positive currents are then used for calculating the switching and conduction loss of the IGBT. The negative currents, on the contrary, are used to evaluate the turn-off loss and conduction loss of the diode. The diodes are placed parallel to each IGBT which are

commercially available as a package. The IGBT input current control circuit has been illustrated in figure 3.2 (a) located in each IGBT. The current vs time graph obtained by MATLAB from the above mentioned circuit located in a random IGBT at any instantaneous time has been shown in figure 3.2 (b). The rest individual IGBTs can also give the same current vs time graph but the shape of the graph will not be similar to each other as the amount of current is not same due to different gate pulses.

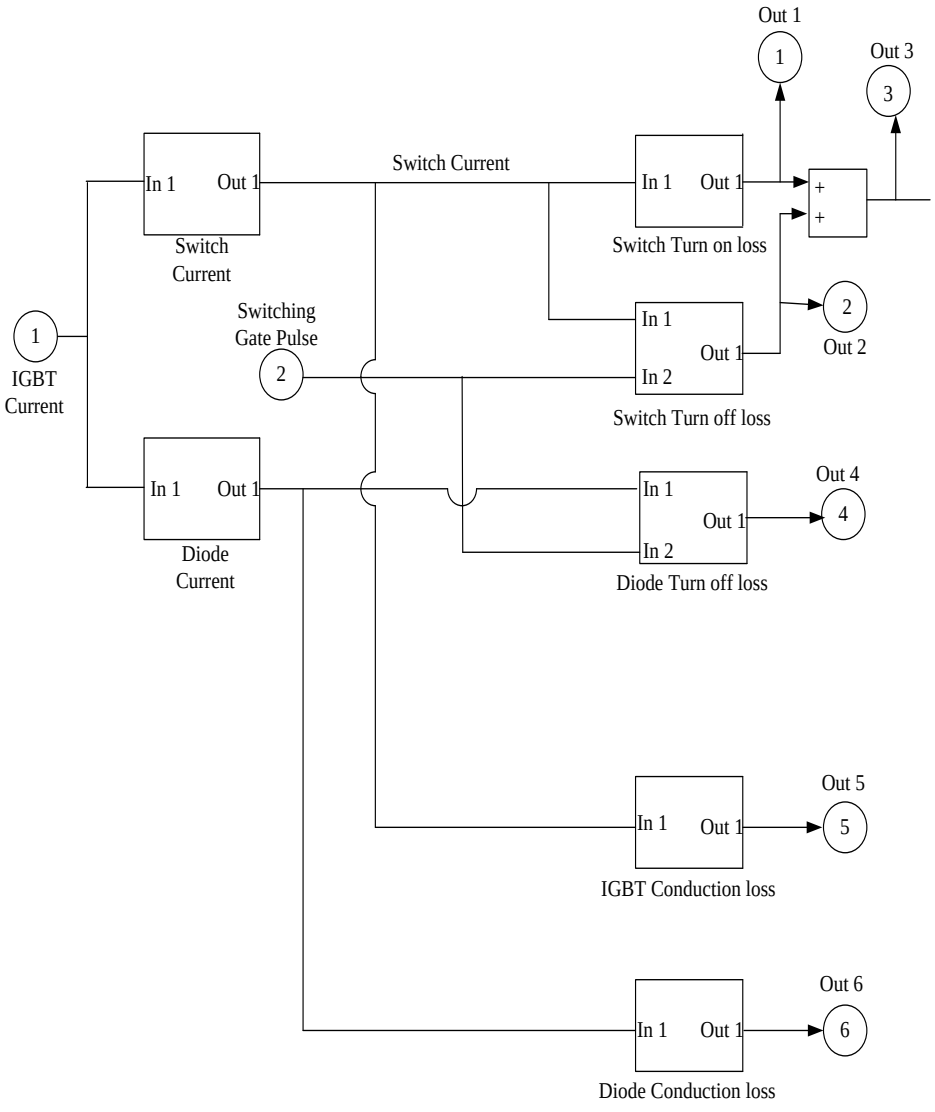

(a)

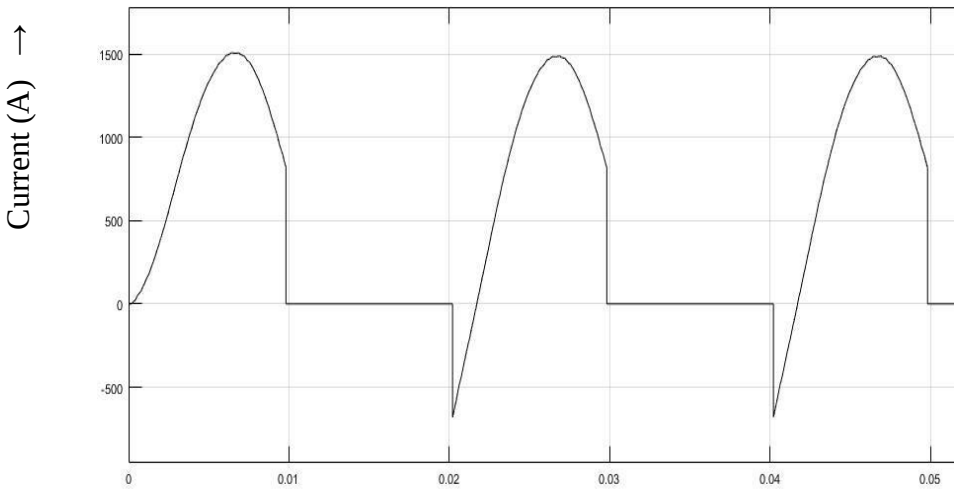

(b)

Figure 3.2 (a) IGBT input current control circuit
(b)Time graph obtained from a random IGBT at any instantaneous time

The above mentioned positive current and negative current from the IGBT input current can be separated and controlled by two separate circuits and the graph of positive and negative current can be illustrated in separate time domains as displayed in figure 3.3(a) (b) and in figure 3.4(a) (b) respectively.

3.3.1 Positive Current Control Circuit

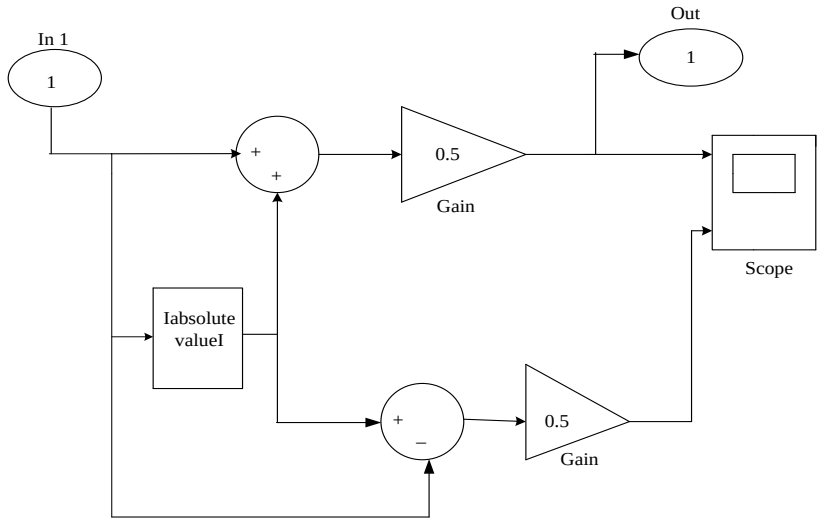

(a)

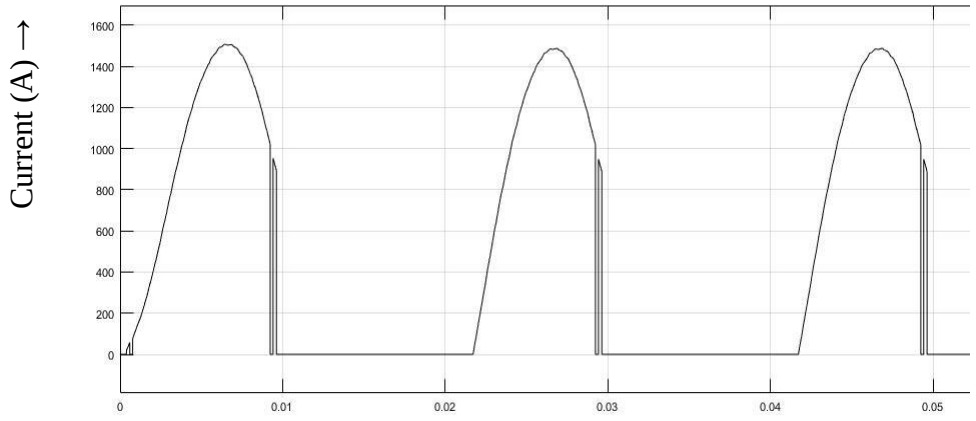

(b)

Figure 3.3 (a) Positive current control circuit (b) Positive current vs time graph obtained by MATLAB

3.3.2 Negative Current Control Circuit

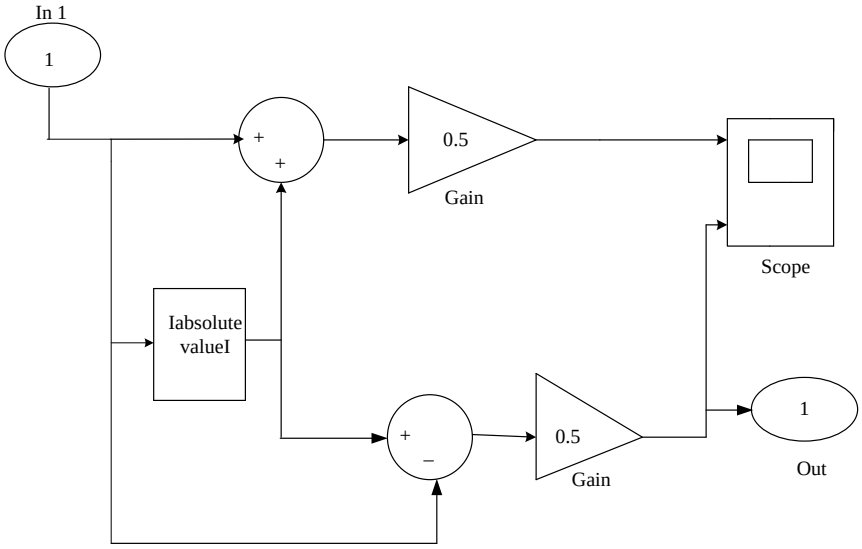

(a)

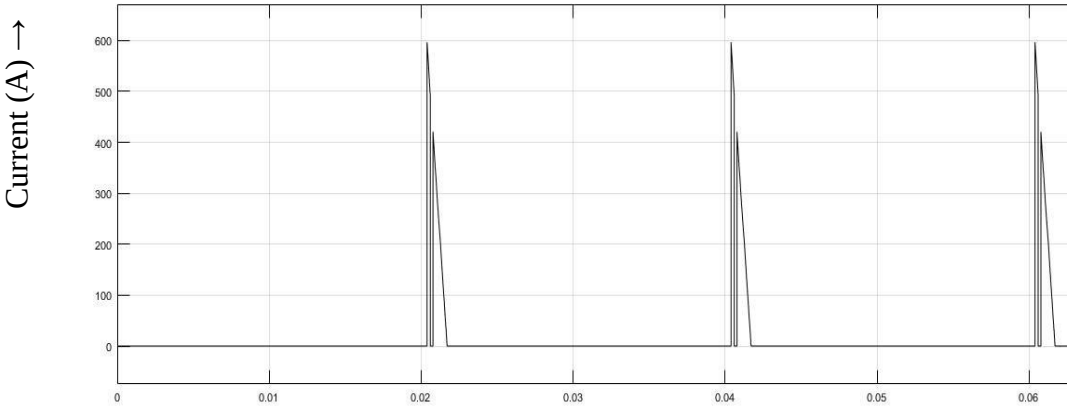

(b)

Figure 3.4 (a) Negative current control circuit (b) Negative current vs time graph obtained by MATLAB

3.4 Switching loss

Theoretically, switching losses can be determined by multiplying the voltage by the definite integral of the current, but practically it is difficult to provide voltage and current time functions during the switching process. The loss for current-switching of the IGBT and the loss of current-recovery of the diode are calculated by measuring the area between current and voltage of the curves supplied by IGBT manufacturing companies in the device under test conditions throughout switching on and switching off time both for IGBT and diode shown in figure 3.1. Hence the above loss curve can be processed to approximate the losses such as $E_{ON\text{-}Time}$ as the turn-on loss of switch, $E_{OFF\text{-}Time}$ as the turn-off loss of switch and E_d as the recovery loss of diode by MATLAB. The turn-on losses of diode are less than 1% compared to the turn-off losses of diode. So, the turn-on losses of diode are neglected. In this thesis, switching losses are approximated by the following 5^{th} order polynomial equation, which can be obtained by the MATLAB curve fitting tool. The energy curves generated by MATLAB have been shown in figure 3.5. Switching losses are of three types namely (1) Turn-on loss of switch; (2) Turn-off loss of switch; and (3) Reverse recovery loss of diode. The circuit for assessing abovementioned switching losses is being shown in figures 3.6, 3.7 and 3.8 respectively.

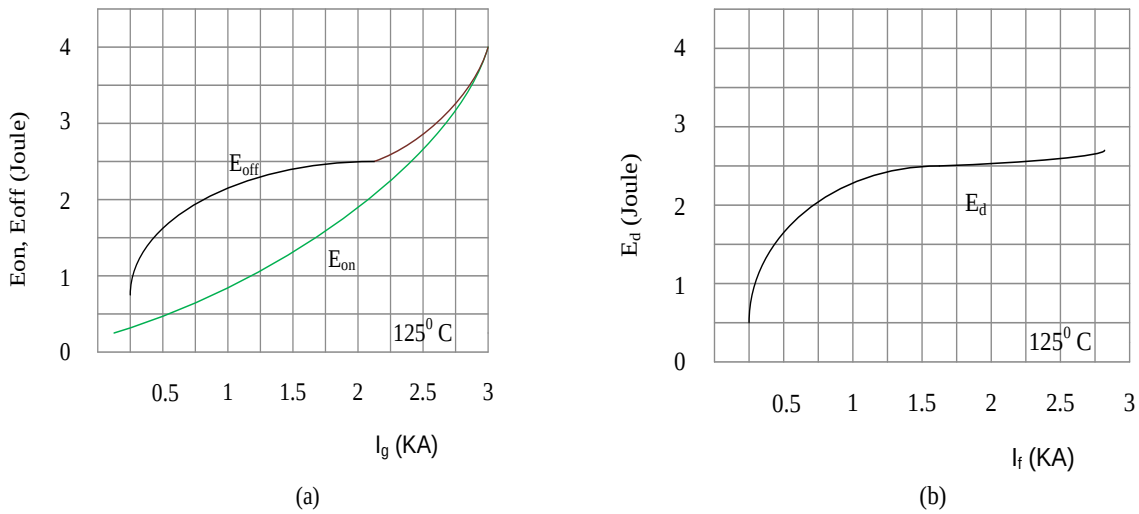

Figure 3.5 (a) Switching energies vs. collector current b) Diode reverse recovery characteristics vs. forward current

The below 5th order polynomial equations, obtained by the MATLAB curve fitting tool to determine the switch turn-on, turn-off and diode reverse recovery losses

$$E_{ON\text{-}Time} = h_1 i_g^5 + h_2 i_g^4 + h_3 i_g^3 + h_4 i_g^2 + h_5 i_g + h_6 \quad (1)$$

$$E_{OFF\text{-}Time} = j_1 i_g^5 + j_2 i_g^4 + j_3 i_g^3 + j_4 i_g^2 + j_5 i_g + j_6 \quad (2)$$

$$E_d = k_1 i_f^5 + k_2 i_f^4 + k_3 i_f^3 + k_4 i_f^2 + k_5 i_f + k_6 \quad (3)$$

The co-efficients of $E_{ON\text{-}Time}$ are,

h1 = -1.95×10^{-23}

h 2 = 3.961×10^{-20}

h 3 = 5.391×10^{-11}

h 4 = 2.552×10^{-08}

h 5 = 0.000738

h 6 = 0.09619

The co-efficients of $E_{OFF\text{-}Time}$ are,

j 1 = -2.831×10^{-17}

j 2 = 5.934×10^{-14}

j 3 = 7.197×10^{-11}

j 4 = -6.343×10^{-7}

j 5 = 0.00203

j 6 = 0.2046

The co-efficients of E_d are,

k 1 = -2.34×10^{-24}

k 2 = 3.211×10^{-20}

k 3 = 5.448×10^{-8}

k 4 = -0.0004056

k 5 = 1.108

k 6 = 127.3

3.4.1 IGBT Switch Turn on loss

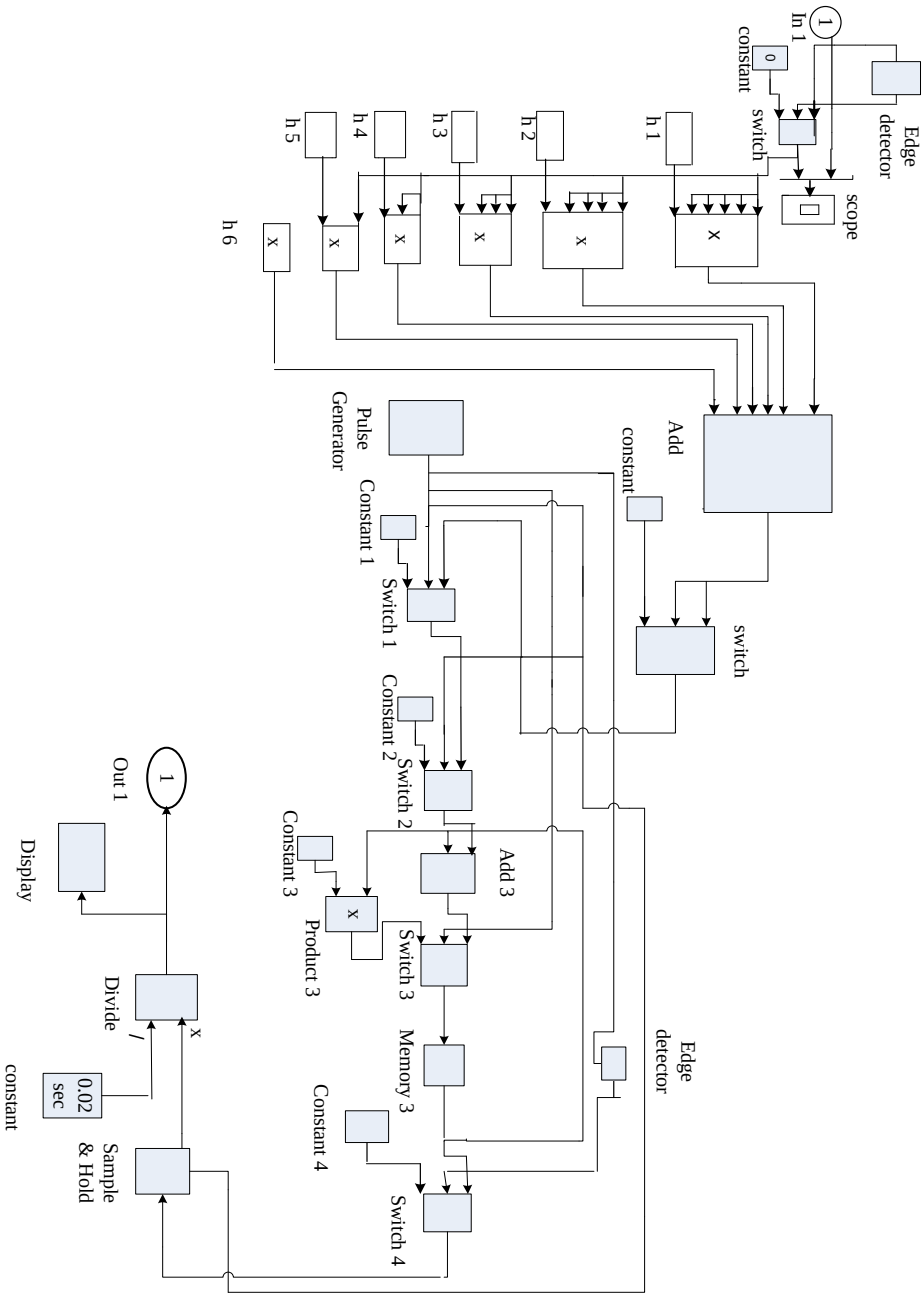

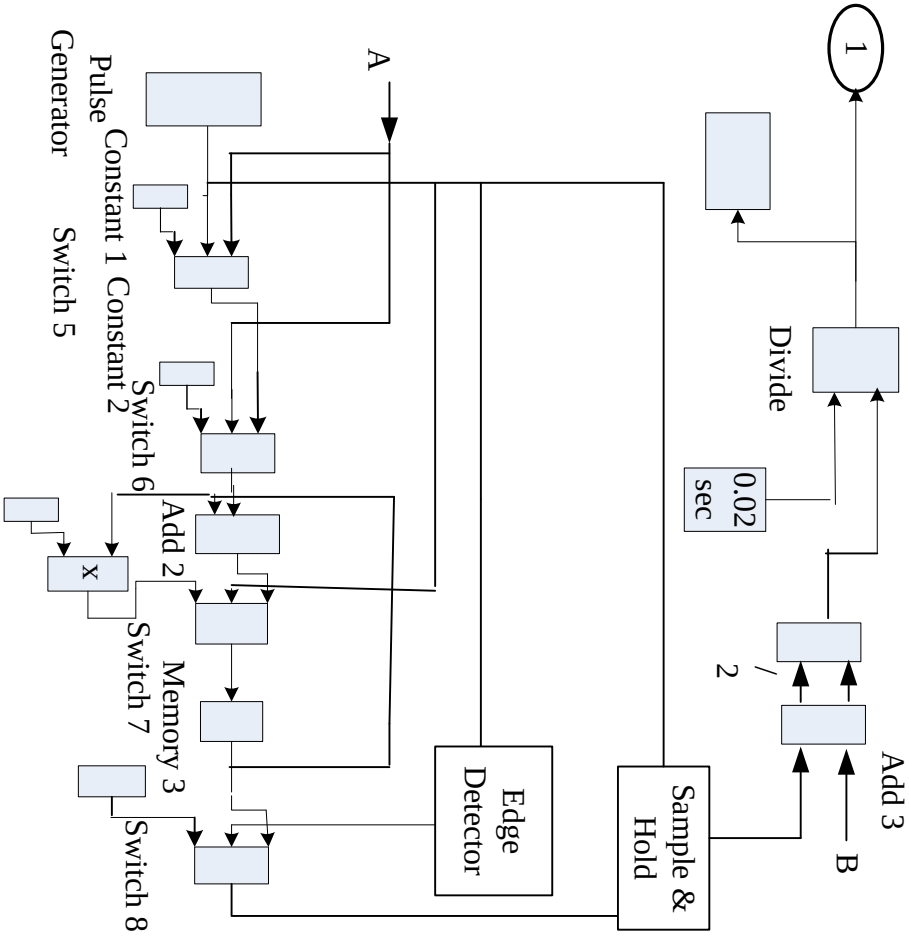

Figure 3.6 Switch Turn-on loss circuit

3.4.1.1 Working Principle

To calculate the IGBT Switch Turn on loss, the positive and rising current are required. For recognizing the rising current, MATLAB tool Edge detector is used. The function of the edge detector is that it compares the present input value to previous value to detect a change. Here when the switch turns on, the edge detector detects the entering current only after getting the gate pulse. Therefore, gate pulse is not required to mention in the design for switch turn on. The rising current is then passed through a switch consists of triple input and single output. The constants of the 5^{th} order polynomial equation for switch turn-on loss are then mentioned in the circuit.

The output of the polynomial equation is then passed through another switch. A pulse generator is used for automatically turning on and off the switch. The input is then passed through two more switches. This is due to the temperature measurement of the IGBT. If IGBTs are getting heated, they can be burnt out. To reduce the heat of the IGBT, the duration of the gate pulses may increase or decrease or the IGBT may be removed. Therefore, to understand the IGBT temperature, a Memory device is used in the design. The function of the Memory device is that it records the starting temperature when the IGBT is in contact. Then it compares the ongoing IGBT temperature with starting temperature as reference and gives a feedback to the reference. By comparing with the reference temperature (starting temperature), an error is measured. That is how the IGBTs are decided to be kept on working or not.

The output of the memory device is then passed through another switch and then passed through the sample and hold device. The function of this device is that it holds the data as energy, the energies are added together and then reset all the data for every alternate 0.02 sec (50% of the time period). These measured data are the losses occur in the system due to switch turn on condition. Loss means energy (in Joules). These losses are then divided by 0.02 sec (half of the time period). After that the output will come in Joule/sec (Watt).

3.4.2 IGBT Switch Turn off loss

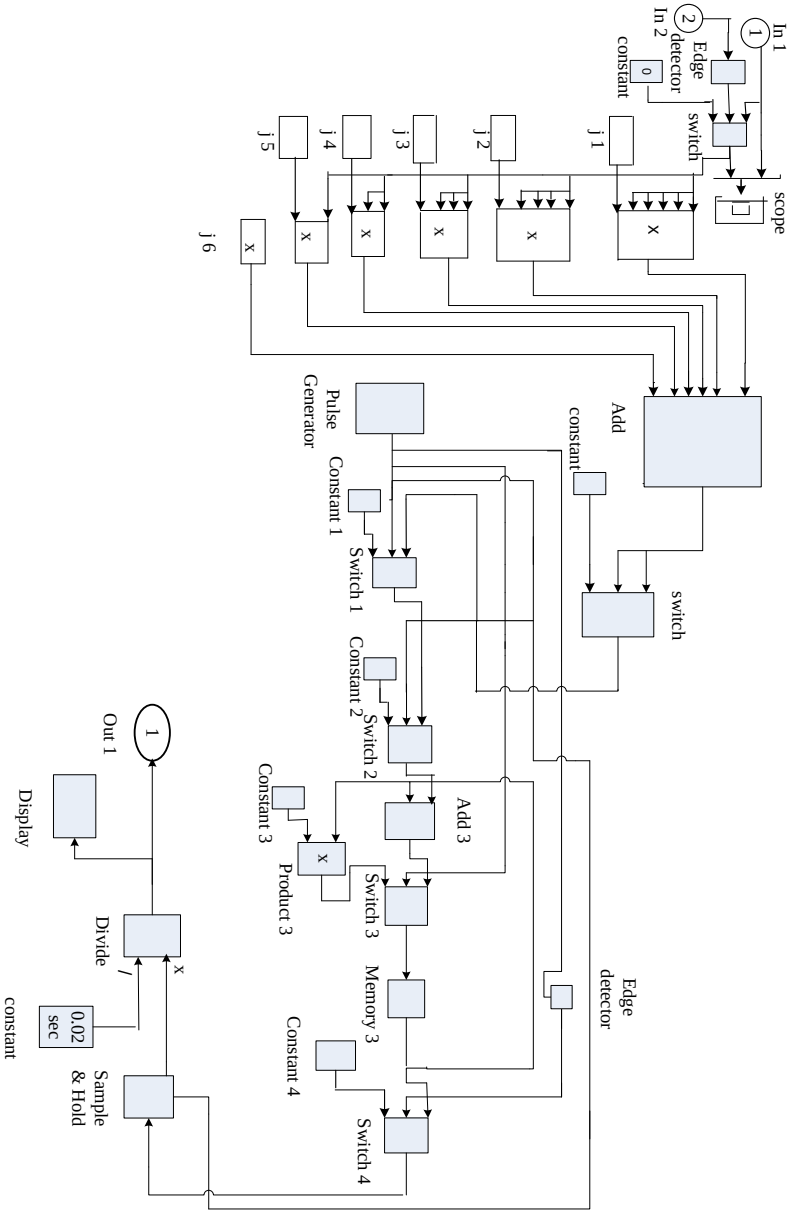

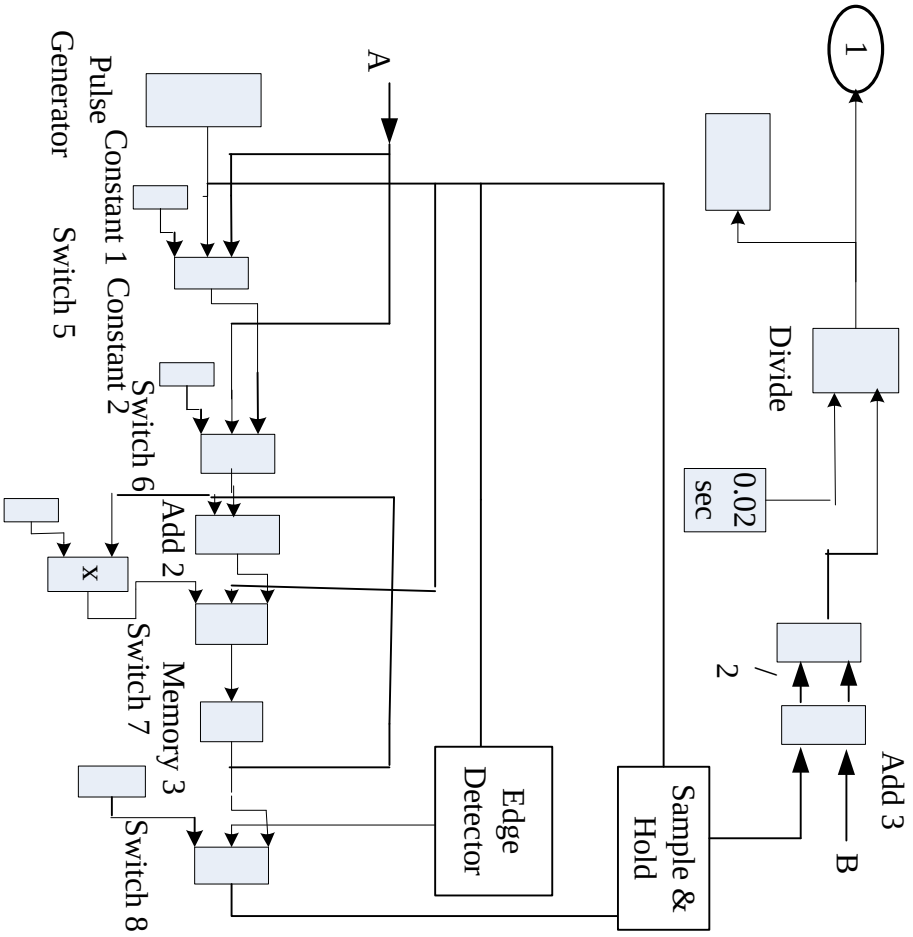

Figure 3.7 Switch Turn-off loss circuit

3.4.2.1 Working Principle

The operating theory of the IGBT switch Turn-off loss circuit design is identical to IGBT switch Turn on loss circuit design. The only difference is Falling Edge detector is used in IGBT Turn off condition because only Falling current is taken into account for this calculation.

3.4.3 Diode Turn off loss

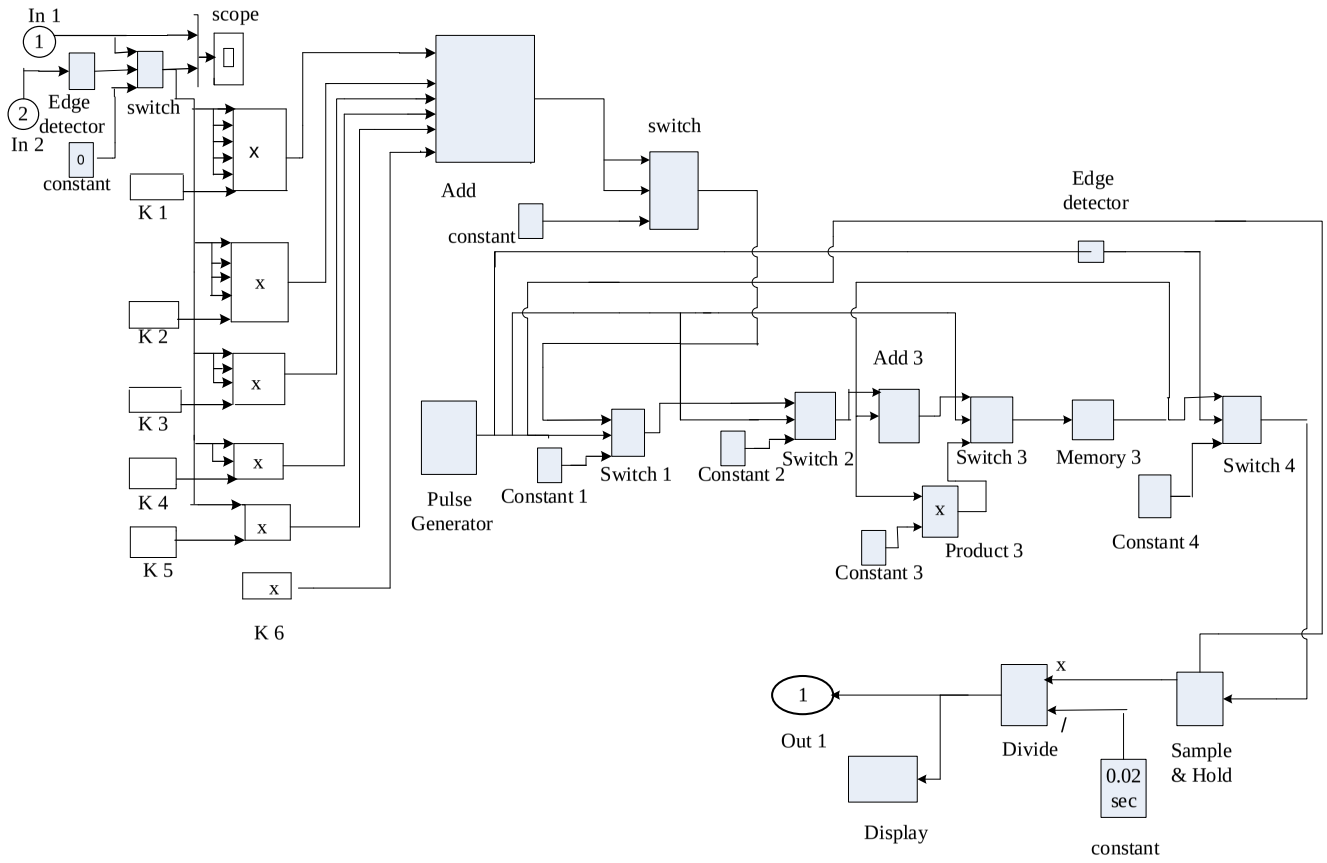
In 1
1
2
In 2
Edge
detector
0
constant
scope
switch
x
K 1
K 2
K 3
K 4
K 5
K 6
Add
constant
switch
Edge
detector
Add 3
Pulse
Generator
Constant 1
Switch 1
Constant 2
Switch 2
Switch 3
Memory 3
Switch 4
Constant 3
Product 3
Constant 4
x
1
Out 1
Divide
Sample
& Hold
0.02
sec
constant
Display

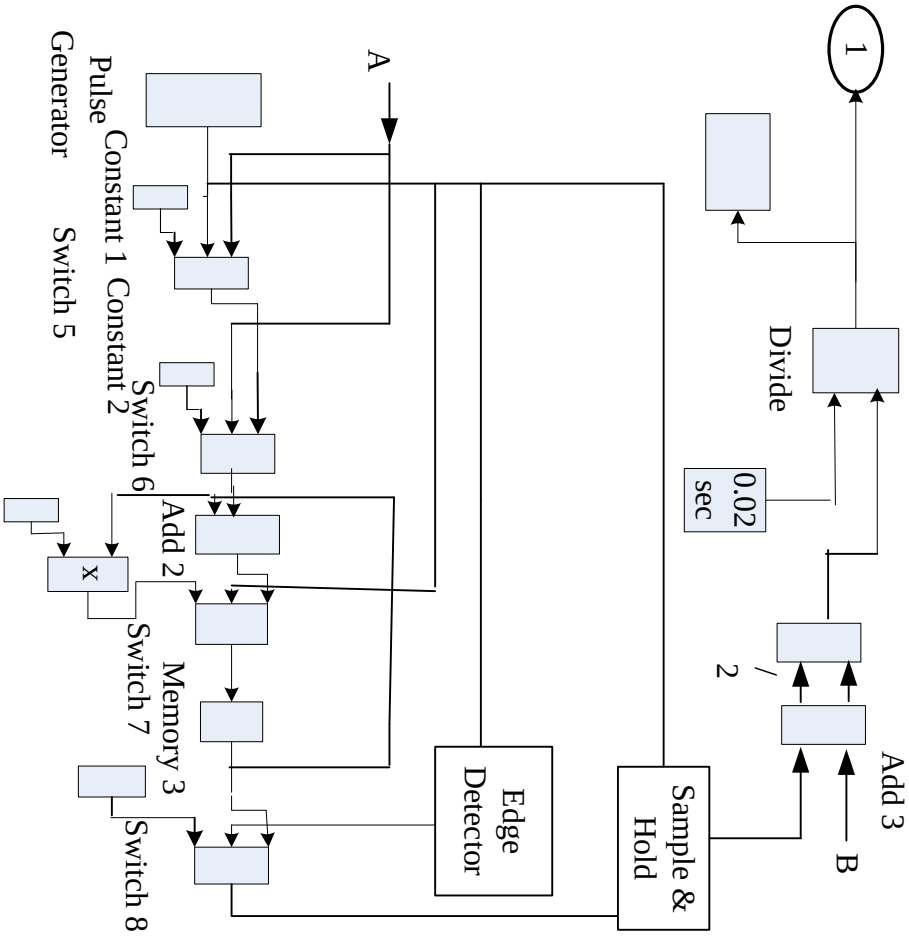

Figure 3.8 Diode Turn-off loss circuit

3.4.3.1 Working Principle

The principle operation of the Diode reverse recovery loss circuit design is similar to IGBT switch Turn on loss circuit design. The only difference is Falling Edge detector is used in Diode reverse recovery condition because only Falling current is taken into account for this calculation.

3.4.4 Total Switching loss

Therefore, the total switching loss for turning ON and OFF the IGBT and reverse recovery of Diode for the fundamental time period T_f (0.02 sec) can be written as follows;

$$P_{IGBT(ON+OFF)} = \frac{1.\ V_{dc(practical)}}{T_f.\ V_{dc(token)}} \sum_{n=1}^{N} [E_{ON\ Time} + E_{OFF\ Time}] \qquad (4)$$

$$P_{Diode(OFF)} = \frac{1.\ V_{dc(practical)}}{T_f.\ V_{dc(token)}} \sum_{n=1}^{N} [E_{d.(}i_f)] \qquad (5)$$

Here $V_{dc(practical)}$ is the voltage provided by the manufacturer's data at which IGBTs are tested in Device under test condition and $V_{dc(token)}$ is the voltage of the MMC Inverter circuit (11016 V) using for this loss calculation Methodology. N denotes the total number of IGBT for n-level Modular Multilevel Cascaded Inverter.

3.5 Conduction loss

The typical current vs voltage on-state characteristic curve of IGBT and the typical current vs voltage forward characteristic curve of diode in different temperatures provided by the IGBT manufacturers. Hence the above curve can be processed to approximate the on-state voltage such as v_g for switch (IGBT) and v_f for diode. In this thesis work the above mentioned process is done by curve fitting tool of MATLAB to obtain 5^{th} order polynomial equation of the on-state voltages. The typical characteristic curves obtained by MATLAB has been illustrated in figure 3.9.

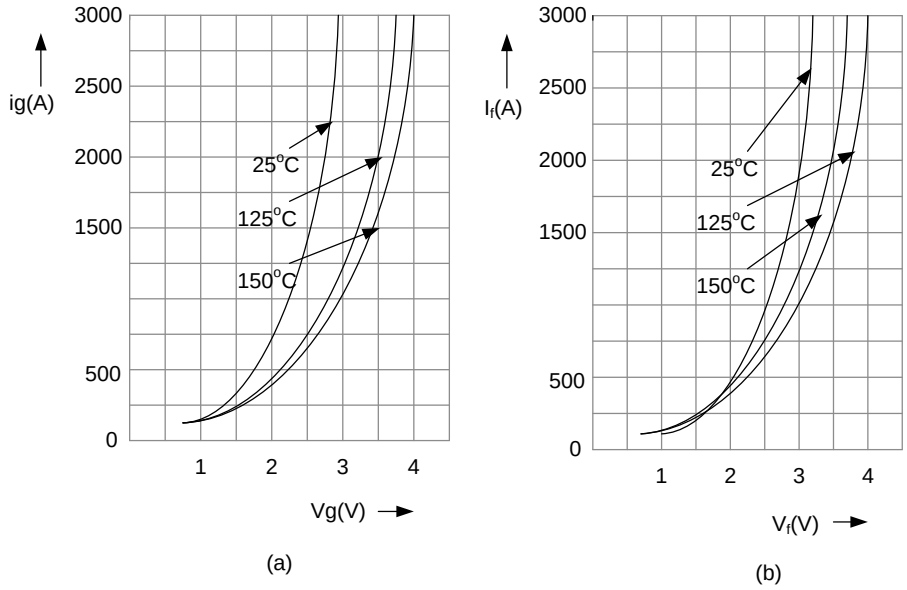

Figure 3.9 (a) Typical IGBT current vs voltage on-state characteristics curve (b) Typical Diode current vs voltage forward characteristics curve

IGBT on-state voltage can be represented by the polynomial equation written below,

$$v_g = C_1 i_g^5 + C_2 i_g^4 + C_3 i_g^3 + C_4 i_g^2 + C_5 i_g + C_6 \qquad (6)$$

Similarly, the on-state voltage of diode can be represented by the below polynomial equation,

$$v_f = F_1 i_f^5 + F_2 i_f^4 + F_3 i_f^3 + F_4 i_f^2 + F_5 i_f + F_6 \qquad (7)$$

The conduction loss is required for calculating both the IGBT and diode. Thus, it is of two types.

- IGBT conduction loss
- Diode conduction loss

3.5.1 Analytical process of IGBT Conduction loss

The Proposed Analytical Methodology is processed with the following systematic continuation. At first, a tangent has been drawn on the typical current-voltage curve at point O (i_{g1}, v_{g1}) as shown in the figure 3.10. Thus, an on-state zero current forward voltage drop v_{g0} as well as a common point of voltage and current ($v_{g1,}$ i_{g1}) for IGBT is obtained.

As a consequence, the following straight line equation has been introduced for the tangent.

$$V_g = v_{g0} + R_g.i_g \quad (8)$$

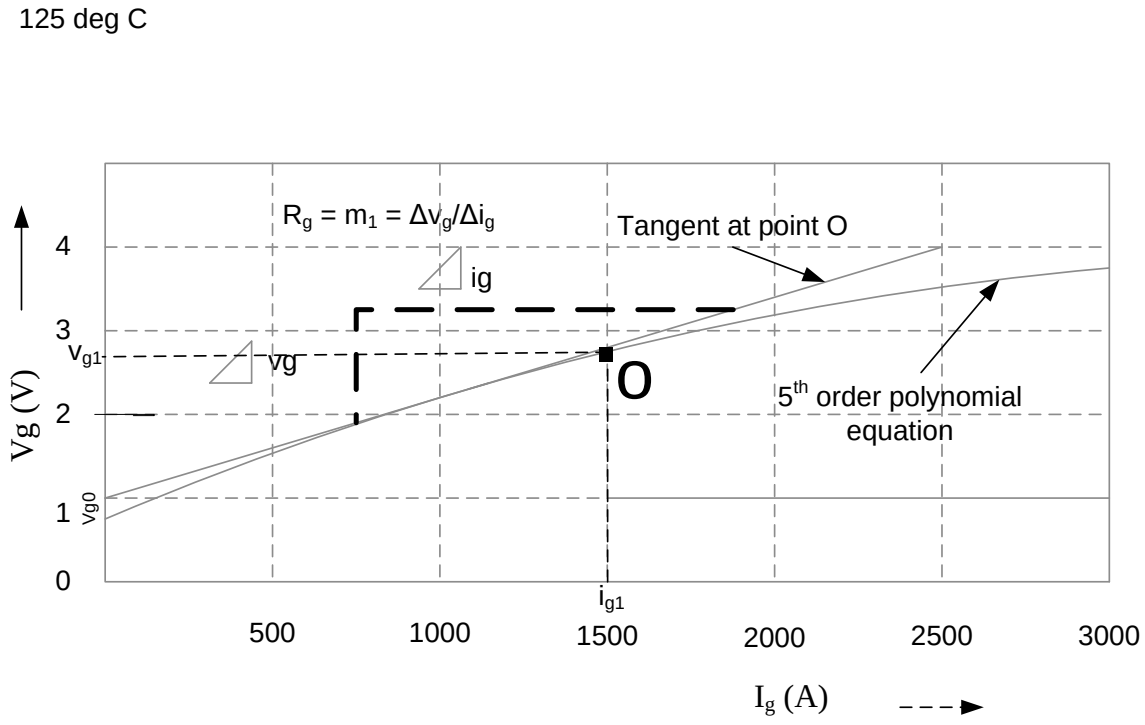

Figure 3.10 Obtaining v_{g0} and R_g for IGBT

From the above curve, the following points have been obtained.

v_{g0} = Forward voltage drop of IGBT on-state zero current collector-emitter

R_g = The on-state resistance of collector-emitter

Therefore, at point O, it can be written,

$$i_g = i_{g1} \text{ and } v_g = v_{g1} \quad (9)$$

Now by differentiating the 5^{th} order polynomial equation of voltage v_g with respect to i_g , the equation of slope m_1 is gotten.

$m_1 = \frac{dv_g}{di_g} = 5c_1 i_g^4 + 4c_2 i_g^3 + 3c_3 i_g^2 + 2c_4 i_g + c_5$ (10)

Using equation (8), (9);

$v_{g1} = v_{g0} + (R_g . i_{g1})$ (11)

Using equ (10) and (11); the zero-current collector-emitter forward voltage equation is gotten for IGBT,

$v_{g0} = v_{g1} - (m_1 . i_{g1})$ (12)

Now getting the above expressions, the instantaneous IGBT conduction losses can be written as following [Similar to the equation (P=VI)],

$P_g(t) = v_g(t).i_g(t)$

$= v_{g0}(t).i_g(t) + R_g.i^2{}_g(t)$ $[v_g = v_{g0} + R_g.i_g]$ (13)

Therefore, the average conduction power loss is found by,

$P_g = \frac{1}{2\pi}\int_0^{2\pi}[P_g(t)]d(\omega t)$ (14)

$= \frac{1}{2\pi}\int_0^{2\pi}[v_{g0}(t).i_g(t) + R_g.i_g^2 \quad (t)]d(\omega t)$ (15)

$P_g = v_{go}.\ I_{g\,(avg)} + R_g.I^2{}_{g\,(rms)}$ (16)

$I_{g\,(avg)}$ and $.I^2{}_{g\,(rms)}$ are the average current and rms current of the IGBT respectively.

For different level of voltages, the amount of currents are different in different time. That is why it is very challenging to measure the instantaneous current of the IGBT. Thus, the Proposed Method is constituted by taking the average and rms current for the conduction loss calculation. The similar Analytical process is also done for diode conduction loss which is described below.

3.5.1.1 The Proposed algorithm designed for IGBT Conduction loss

Figure 3.11 is based on the equation [$P_g = v_{go}.I_{g\,(avg)} + R_g.I^2_{g(rms)}$] of conduction loss obtained from the above mentioned Proposed Method.

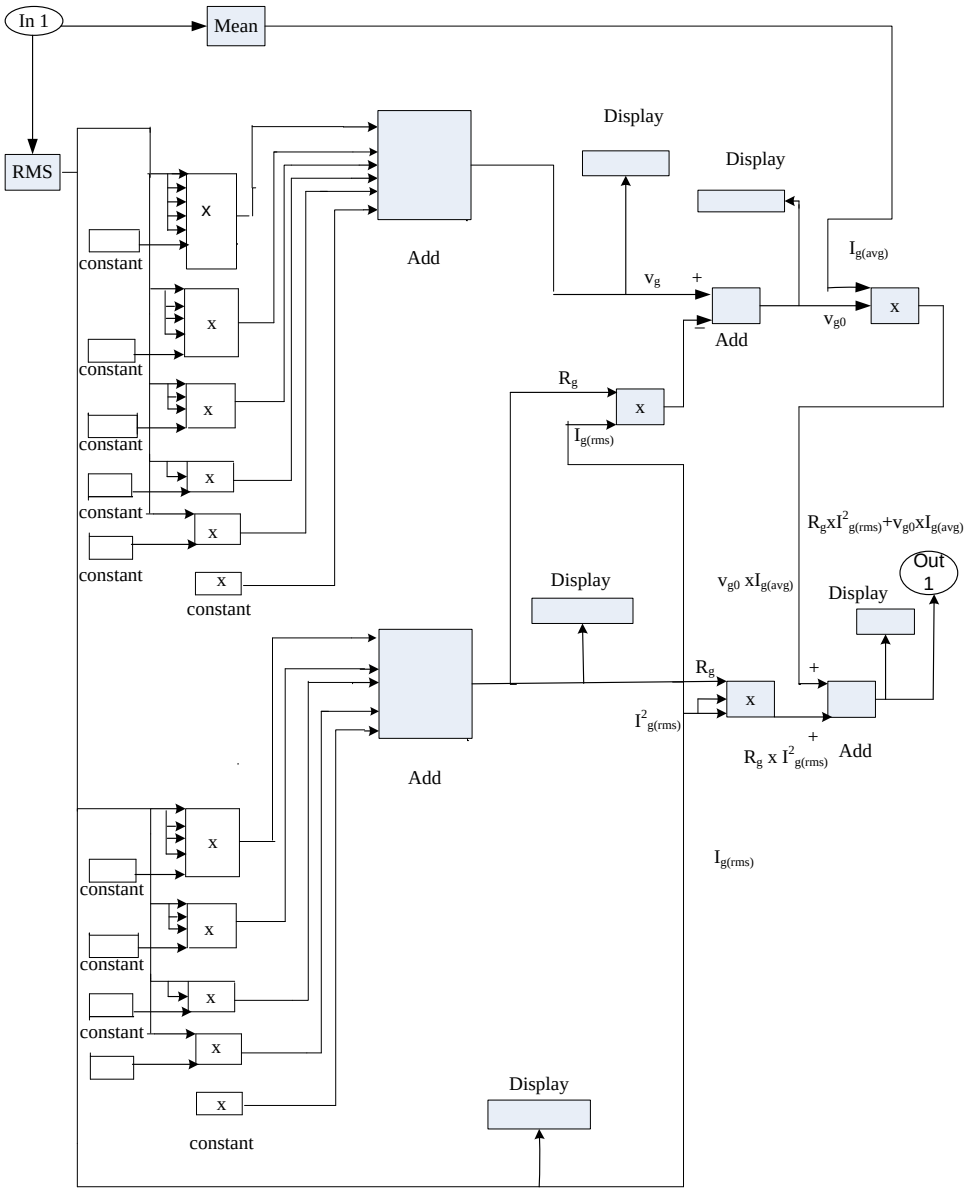

Figure 3.11 IGBT Conduction loss

3.5.2 Analytical process of diode Conduction loss

Similarly for diode, the Proposed Method is processed with the following systematic continuation. At first, a tangent has been drawn on the typical current-voltage curve at point T (i_{f1} , v_{f1}) as shown in the figure. Thus, an on-state zero current forward voltage drop v_{f0} as well as a common point of voltage and current ($v_{f1,}$ i_{f1}) for diode is obtained.

As a consequence, the following straight line equation has been introduced for the tangent.

$$v_f = v_{f0} + R_f.i_f \qquad (17)$$

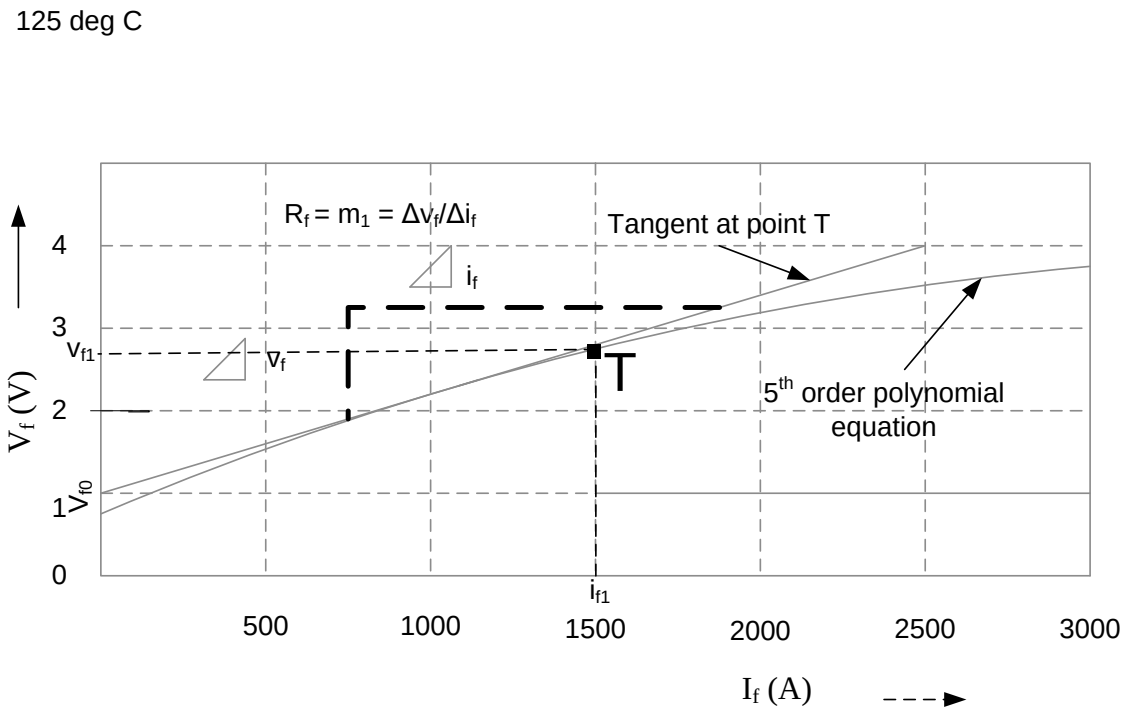

Figure 3.12 Obtaining v_{f0} and R_f for Diode

From the above curve, the following points has been obtained.

v_{f0} = Forward voltage drop of diode on-state zero current

R_f = The on-state resistance of the diode.

Similarly for diode at point T, it can be written as $i_f = i_{f1}$ and $v_f = v_{f1}$ (18)

Now by differentiating the 5^{th} order polynomial equation of voltage v_f with respect to i_f , the equation of slope m_2 is gotten

$$m_2 = \frac{dv_f}{di_f} = 5F_1 i_f^4 + 4F_2 i_f^3 + 3F_3 i_f^2 + 2F_4 i_f + F_5 \quad (19)$$

Using equation (17), (18) and (19); the zero-current collector-emitter forward voltage equation is gotten for diode,

$$v_{f0} = v_{f1} - (m_2 . i_{f1}) \quad (20)$$

Now getting the above expressions, the instantaneous conduction losses of diode can be written as below Identical to the equation (P=VI)],

$$P_d(t) = v_f(t).i_f(t)$$

$$= v_{f0}(t).i_f(t) + R_f.i^2_f(t) \quad [v_f = v_{f0} + R_f.i_f] \quad (21)$$

Therefore, the average diode conduction loss per phase can be written as

$$P_d = v_{fo}.I_{f\,(avg)} + R_f.I^2_{f\,(rms)} \quad (22)$$

Thus, adding both IGBT and diode conduction losses, the per phase total conduction loss with N number of IGBT and diode components is obtained by the following equation,

$$P_{gd} = \sum_{n=1}^{N} [P_g(n) + P_d(n)] \quad (23)$$

3.5.2.1 The Proposed algorithm designed for diode Conduction loss

The Figure 3.13 is based on the equation [$P_d = v_{fo}.I_{f\,(avg)} + R_f.I^2_{f\,(rms)}$] of Diode conduction loss obtained from the Proposed Analytical Methodology.

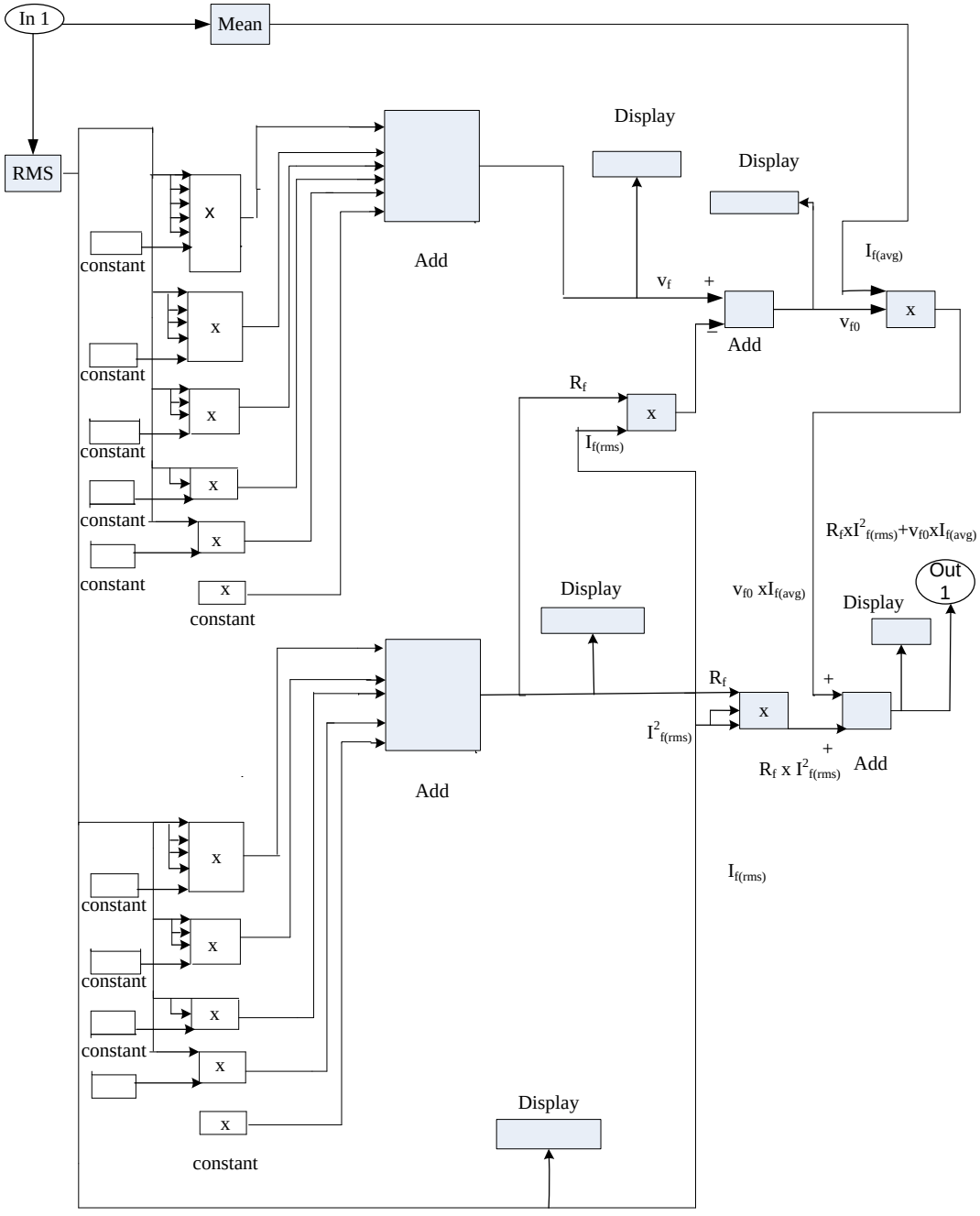

Figure 3.13 Diode Conduction loss

3.6 Loss Calculation

3.6.1 The output obtained from the IGBTs

The IGBT and its corresponding outputs are illustrated in figure 3.14 where outputs are denoted by the number as p_n, q_n, r_n, s_n, t_n u_n [where n =1 to 28].

p_n = switching turn-on loss,
q_n = IGBT switching turn-off loss,
r_n = IGBT switching (total) loss,
s_n = turn off loss of diode,
t_n = Conduction loss of IGBT,
u_n = Conduction loss of diode.

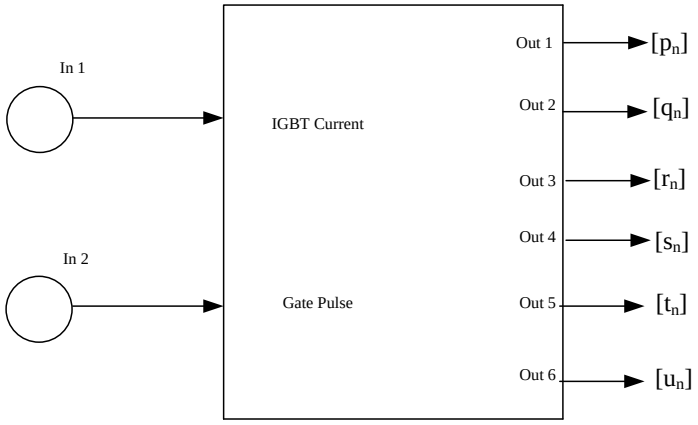

Figure 3.14 IGBT-n of each phase (where n=1 to 28): p_n, q_n, r_n, s_n, t_n, u_n are the outputs showing different types of losses

3.6.2 The Loss data Accumulation

The following individual blocks (Figure 3.15) are called addition blocks which work for collecting the above mentioned output obtained from each IGBT and rearrange the output data as per requirement to measure the losses for the Multilevel Inverter system.

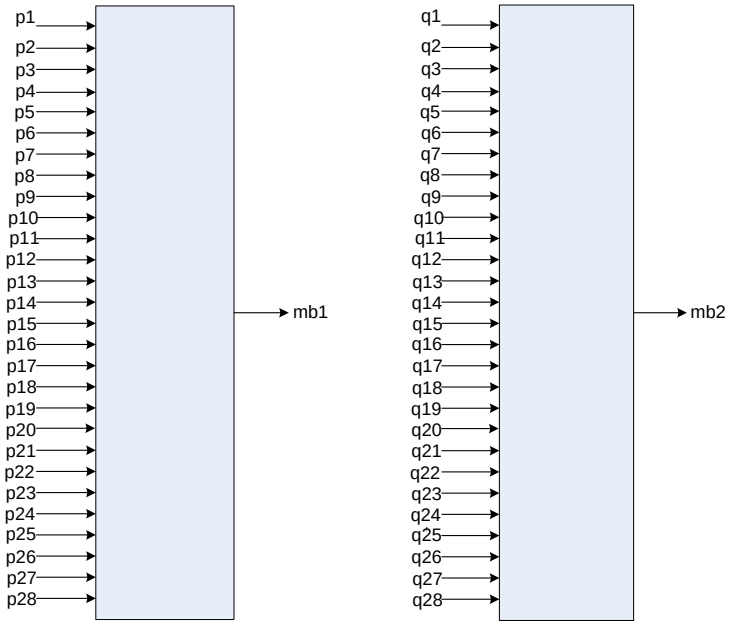

(a) (b)

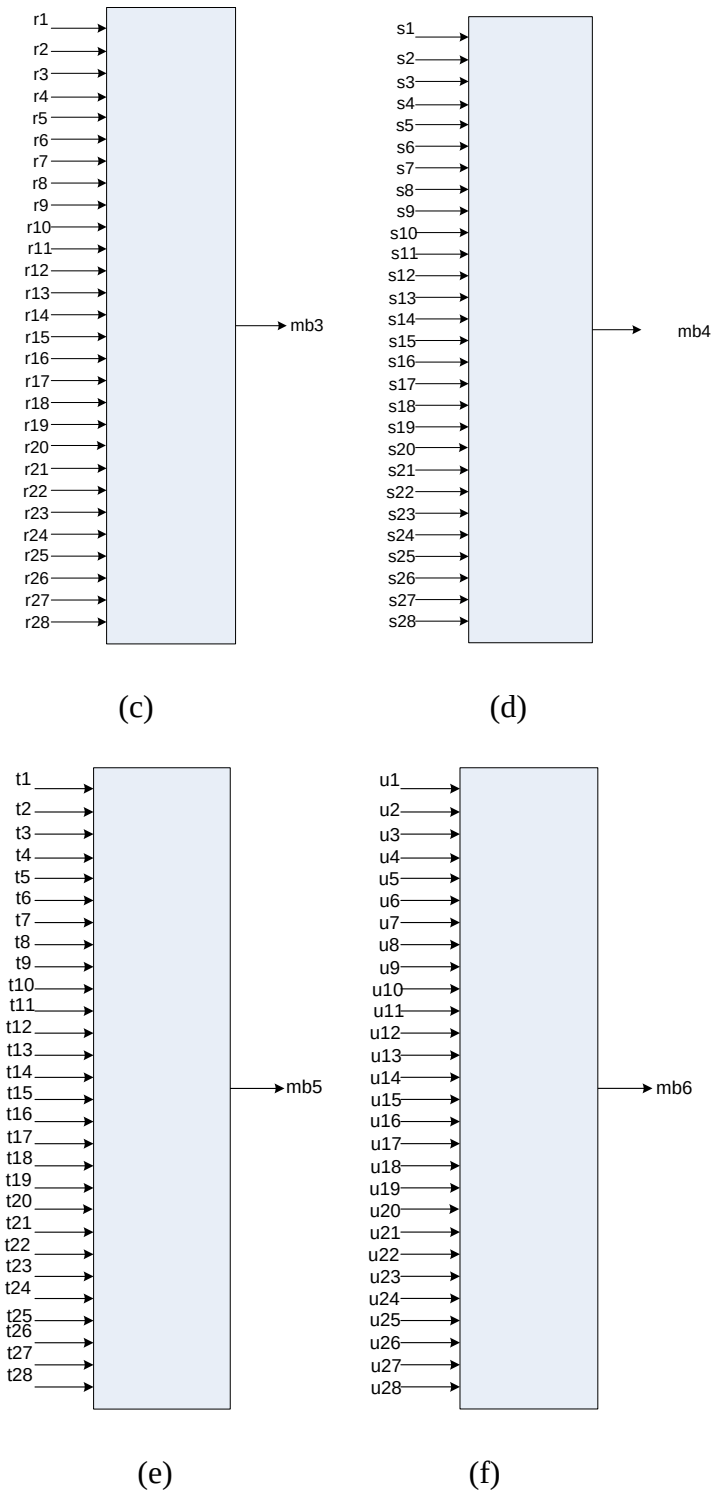

Figure 3.15 (a) mb_1=addition of all switch turn on loss, (b) mb_2=addition of all switch turn off loss, (c) mb_3=addition of total switching loss, (d) mb_4=addition of diode turn off loss, (e) mb_5=addition of all IGBT conduction loss, (f) mb_6=addition of Diode conduction loss; per phase

3.6.3 Total Loss Calculation

Per phase total switching loss, diode turn off loss, IGBT conduction loss and diode conduction loss are taken to calculate the per phase total loss.

Moreover, to calculate the Inverter total loss, at first multiply the total loss (per phase) with 3 and 3-phase total loss will be obtained. Figure 3.16 illustrates the total loss calculated for each phase and 3 phase of the 15-level MMC Inverter using Proposed Method.

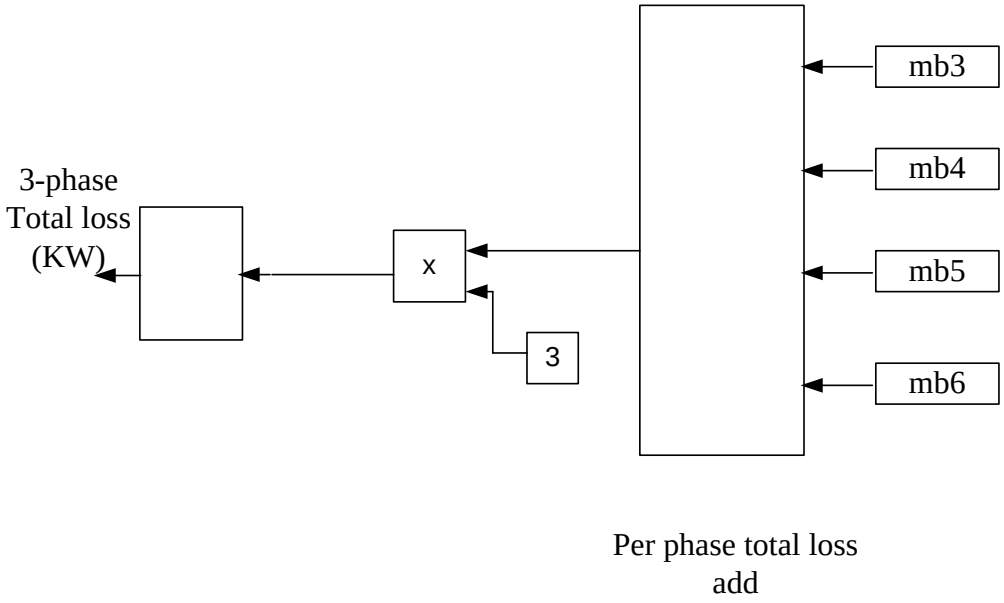

Figure 3.16 Total loss calculated for each phase and 3 phase for the 15-level MMC Inverter using Proposed Method.

CHAPTER 4

PERFORMANCE & RESULTS

The Proposed Analytical Methodology for the loss calculation of the Modular Multilevel Cascaded Inverter with Third Harmonic Injected (THI) PWM has been elaborated in chapter 3. There are various Analytical approaches of measuring conduction loss as well as switching loss of Conventional Inverter, some of are found in the literature [65-69]. However, the Methods developed for the Conventional system cannot be applicable for the multi-level Inverter because it has some specific structures [70].

At Inverter's input side, a high frequency triangular signal known as control signal is generated by signal generator in order to compare with the 3-phase sinusoidal signals known as reference signal. By comparing the signals using comparator, gate pulses are generated to make the switch active.

Sin Pulse Width Modulation is the basic form of PWM where gate pulse is generated by comparing sinusoidal signal with a high frequency control signal. If third harmonic component is imposed to SPWM, the original sin signal wave shape is changed and the wave shape looks like some flatting the top. This composed signal made of sin signal added with third harmonic component is further compared with the high frequency triangular wave to make the gate pulses required for the devices to be active. There are various modulation schemes. An experimental study has been done to make a comparative analysis between SPWM and THIPWM in the paper [56]. Relating to each other, it has been observed that Third Harmonic Injected Phase disposition scheme has lower THD than Sinusoidal Phase disposition scheme. Also it has been observed that applying the other schemes THIPWM has the lower THD than SPWM.

4.1 Loss Factors

To reduce the Inverter's loss, following factors should be considered -

(1) Using proper selection of device concerning with the level number.

(2) The device's working voltage is less than its rated voltage. The device is to be selected according to the high frequency switching and handling high power. Thus a high voltage Inverter must use commercially available devices provided by the reliable manufacturers.
(3) Using Multilevel Inverters instead of Conventional Inverters. Because Multilevel reduces space, cost and maintenance effort as well as increase system efficiency.
(4) Selecting proper modulation scheme.
(5) Selecting the actual level number concerning with loss and available rated device. If level number increases, THD at the output voltage and switching loss decreases. Switching frequency and THD affects the efficiency of the Inverter.
(6) Using proper Pulse Width Modulation (PWM) technique. The current is controlled by the PWM and it is also effective on voltage output and reduction of THD.

4.2 Performance Analysis of Proposed Method for Conduction loss

4.2.1 IGBT Conduction loss (W)

By proceeding the Analytical equation in MATLAB surroundings, loss (W) of conduction is measured by running the circuit varying power factor angle and modulating index. By varying all possible combination of MI and pf angle, all the data has been collected in tabulated form (Table 4.1) and represented in graphical form as figure 4.1. Considering the Multilevel Inverter of 15 level whose loss is calculating. The (output) voltage and current of the Inverter are 11016 V (rms) and 1500A (rms) respectively.

Table 4.1 IGBT Conduction loss data (W) for Single phase

Power Factor Angle (Degree)	Modulation Index									
	0.1	0.2	0.3	0.4	0.5	0.6	0.7	0.8	0.9	1
0	839.7	2098	3877	6169	9023	12527	16627	21435	26498	32938
10	805.3	2065	3853	6123	8955	12448	16490	21268	26287	32665
20	802.2	2050	3811	6046	8823	12242	16184	20848	25730	31940
30	797	2025	3743	5916	8599	11887	15671	20137	24786	30709
40	789.9	1992	3650	5735	8285	11390	14947	19137	23458	28979
50	781	1949	3532	5507	7885	10760	14029	17868	21778	26786
60	770.8	1899	3394	5239	7411	10016	12946	16371	19797	24198
70	759.5	1844	3243	4947	6878	9192	11743	14709	17590	21316
80	751.4	1802	3109	4710	6341	8413	10544	13083	15387	18444
90	1387	3577	6053	10208	10306	17102	18078	26025	28367	36239

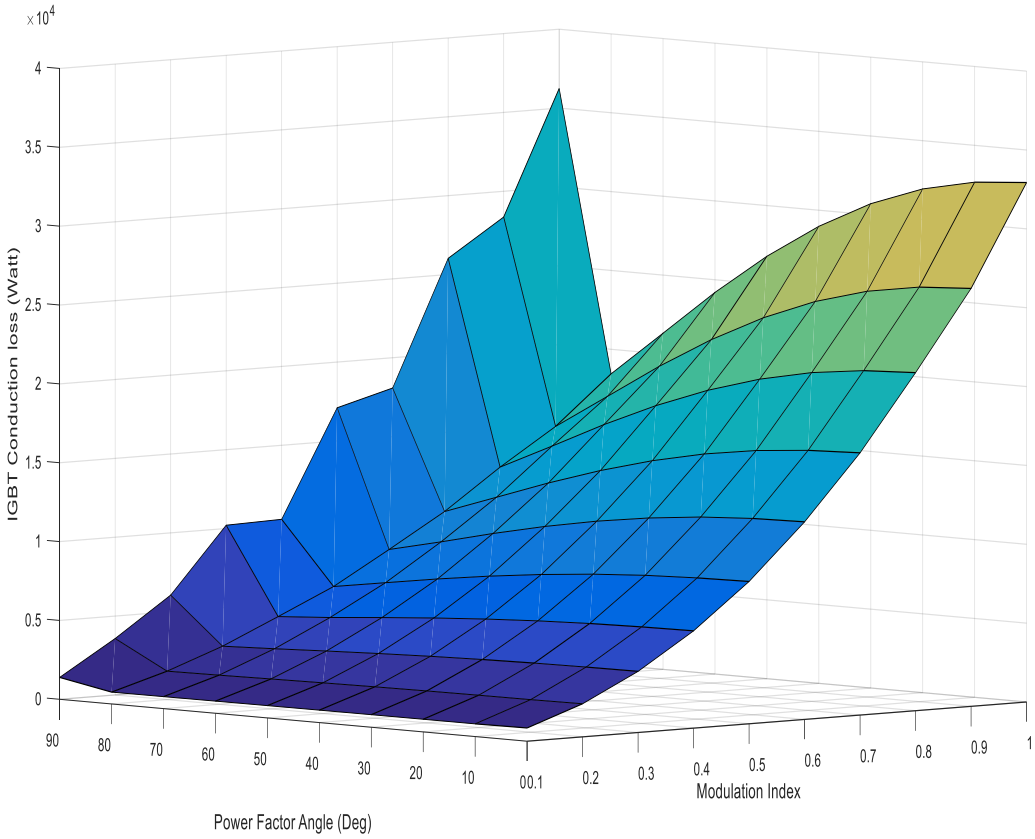

Figure. 4.1 3D figure of IGBT conduction loss (W) for Single phase

The surface plot of switch conduction loss against modulation index and power factor for level-shifted THIPWM (LSTHIPWM) in a three-phase 15 level Multilevel MMC Inverter is shown in the figure 4.1. From the table 4.1, it can be seen that when modulation index increases, loss increases and when power factor decreases, loss decreases.

4.2.2 Diode Conduction loss (W)

Like the IGBT conduction, the process for measuring the loss (W) of conduction is similar for the antiparallel diodes. The data has been organized in Table 4.2 and pictured in Figure 4.2.

Table 4.2 Diode Conduction loss data (W) for Single phase

Power Factor Angle (Deg)	Modulation Index									
	0.1	0.2	0.3	0.4	0.5	0.6	0.7	0.8	0.9	1
0	621.4	1271	1893	2344	2635	2751	2937	2590	1831	699.9
10	614.1	1276	1916	2376	2676	2814	2998	2684	1955	861.7
20	617.2	1289	1943	2433	2773	2958	3179	2930	2287	1312
30	621.9	1310	1990	2528	2933	3190	3488	3346	2840	2055
40	628.2	1338	2057	2661	3160	3518	3930	3952	3637	3115
50	636.2	1374	2144	2832	3453	3950	4517	4761	4700	4519
60	645.6	1417	2249	3040	3815	4485	5255	5775	6033	6273
70	655.8	1465	2370	3279	4237	5111	6132	6978	7615	8350
80	664.6	1511	2492	3529	4679	5767	7067	8265	9302	10568
90	1100	2808	4683	7818	7725	12692	13415	19145	20690	26313

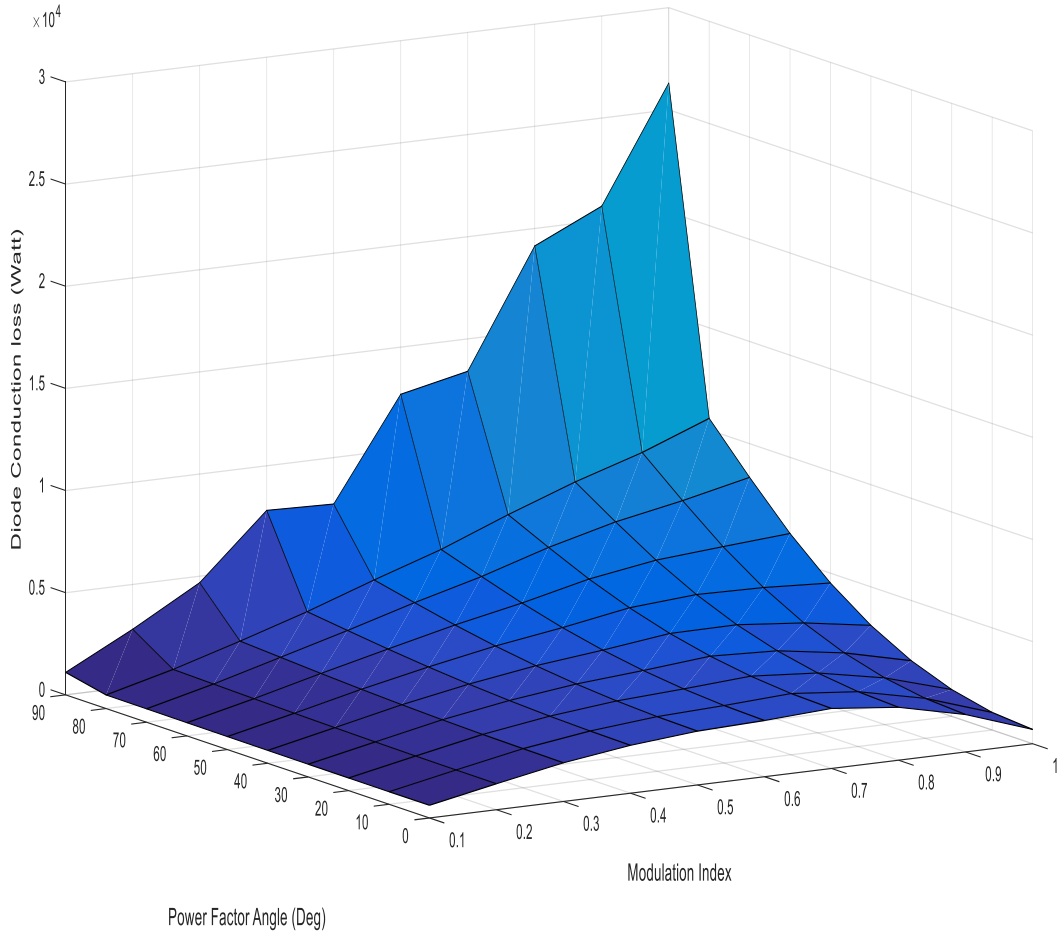

Figure 4.2 3D figure of Diode conduction loss (W) for Single phase

The surface plot of Diode conduction loss against modulation index and power factor for level-shifted THIPWM (LSTHIPWM) in a three-phase 15 level Multilevel MMC Inverter is shown in figure 4.2. From table 4.2, it can be seen that when modulation index increases, loss is consistently increases up to modulation index 0.7. From modulation index 0.8, the change is mostly decreasing. Also diode conduction loss increases when power factor decreases.

4.3 Performance Analysis of Proposed Method for Switching loss

4.3.1 Switch (IGBT) Turn-on loss (W)

By arranging the polynomial equation in MATLAB settings, loss of switching turn on is measured by running the circuit varying pf angle and modulation index. Switching loss is dependent on switching frequency and PWM. Table 4.3 describes the loss (W) of switching in terms of turn on.

Table 4.3 Switch (IGBT) Turn-on loss data (W) for Single phase

Power Factor Angle (Degree)	Modulation Index									
	0.1	0.2	0.3	0.4	0.5	0.6	0.7	0.8	0.9	1
0	1155.9364	813.21	1076.4	946.95	1118.2	1284	1528	1750	1927	2216
10	227.86555	353.69	485.41	613.01	752.38	885	1060	1233	1374	1634
20	234.70876	354.03	469.24	580.67	695.39	810	978	1105	1223	1443
30	233.41712	342.85	447.49	548.07	639.05	737	890	991	1071	1271
40	226.83772	330.59	427.02	514.23	593.56	662	805	882	932	1117
50	225.16027	324.13	412.18	484.93	548.68	597	730	786	808	977
60	223.60496	318.67	400.85	467.72	515.26	541	652	707	703	861
70	227.2651	314.8	391.84	448.13	490.74	486	583	648	620	775
80	222.17565	310.97	383.48	446.28	475.47	451	538	610	573	723
90	321.50683	553.43	733.85	1090.5	835.21	1339	1309	1817	1639	2291

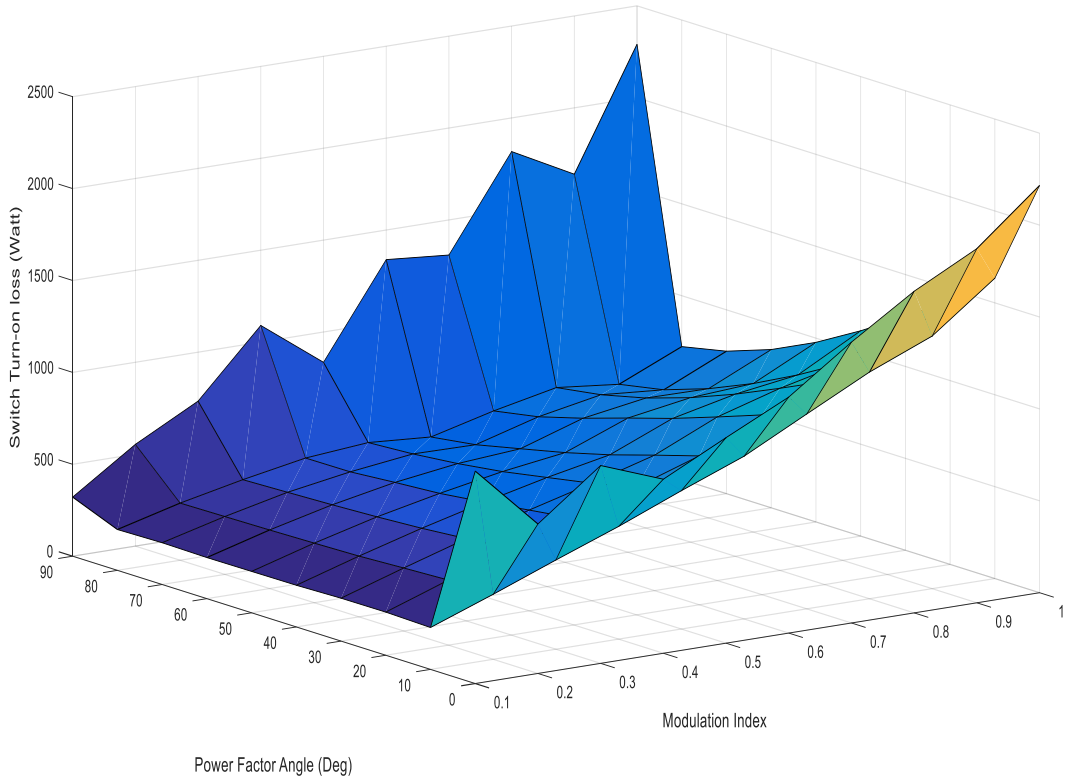

Figure 4.3 3D figure of switch Turn-on loss (W) for Single phase

Switch Turn-on loss depends on switching frequency, switching current and PWM. The figure 4.3 illustrates that IGBT turn on loss is increasing with respect to increase of modulation index. At the higher power factor, the loss is higher.

4.3.2 Switch (IGBT) Turn-off loss (W)

As the procedure discussed for IGBT turn on case, the loss of IGBT turn off has been measured in a same way. Table 4.4 describes the loss (W) of switching in terms of turn off.

Table 4.4 Switch (IGBT) Turn-off loss data (W) for Single phase

Power Factor Angle (Degree)	Modulation Index									
	0.1	0.2	0.3	0.4	0.5	0.6	0.7	0.8	0.9	1
0	870.41	1077.8	1336.8	1558.9	1777.8	1982	2234	2448	2585	2909
10	639.51	948.54	1241.7	1503.9	752.38	2009	2310	2578	2787	3172
20	618.51	937.04	1255	1556.4	695.39	2141	2517	2837	3095	3545
30	615.14	955.3	1286.4	1615	1943.4	2249	2718	3046	3364	3863
40	624.26	971.71	1318.1	1661.5	2002	2357	2843	3213	3553	4153
50	624.13	978.14	1333.9	1705.6	2061.9	2408	2907	3340	3713	4373
60	623.98	972.98	1349.1	1716.9	2099.9	2445	2945	3424	3820	4532
70	613.79	987.4	1358.3	1746.1	2127.7	2437	2935	3484	3902	4625
80	625	996.03	1359.9	1755.5	2141.6	2437	2916	3526	3928	4709
90	803.86	1355.5	1763.3	2382.3	2382.7	3139	3587	4657	5187	6863

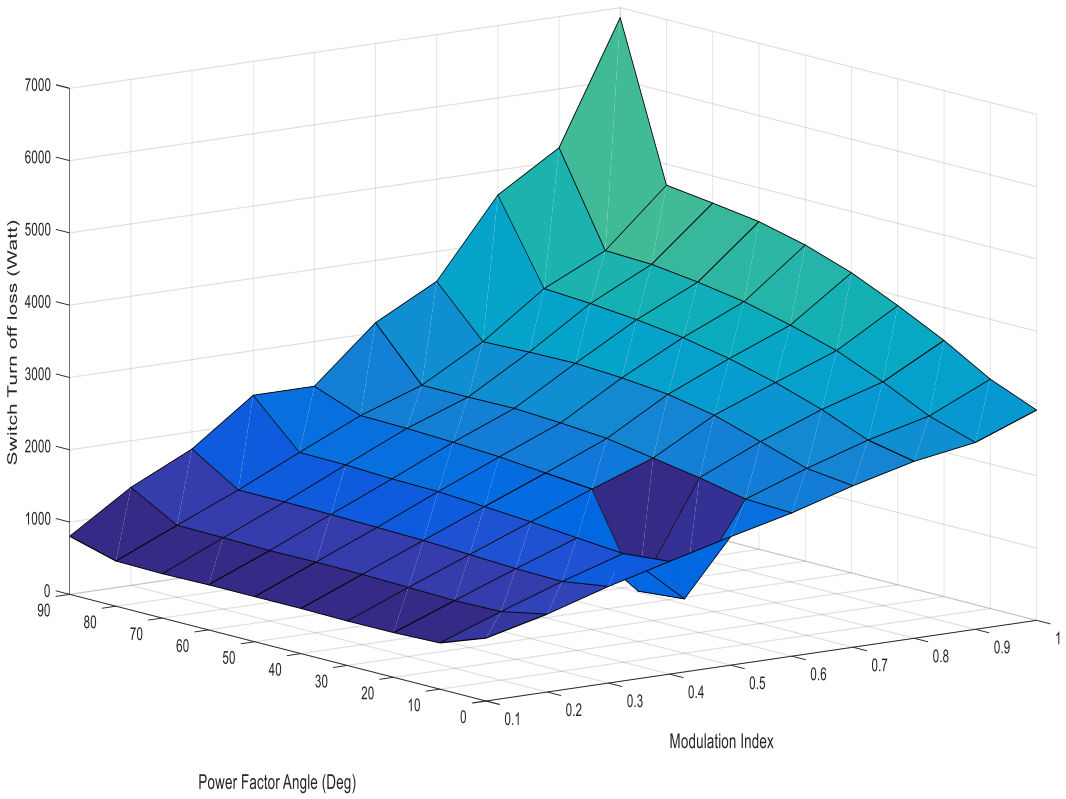

Figure 4.4 3D figure of switch Turn-off loss (W) for Single phase

The figure 4.4 portrayed that switching off loss mostly increasing when power factor is decreasing. The surface plot shows an unnatural change at modulation index 0.5 and power factor angle within 20. As switching loss is dependent on some other factors, thus loss may increase or decrease depends on switching current.

4.3.3 Single phase Switch Turn-on and Switch Turn-off loss (W)

Adding switch turn on and turn off loss, total switching loss has been calculated from MATLAB for taking same condition. Table 4.5 describes the total collectable loss (W) regarding IGBT switching.

Table 4.5 Total Switching (IGBT) loss data (Turn-on and Turn-off) (W) for Single phase

Power Factor Angle (Degree)	Modulation Index									
	0.1	0.2	0.3	0.4	0.5	0.6	0.7	0.8	0.9	1
0	2026	1891	2413	2506	2896	3267	3763	4199	4513	5126
10	867.4	1302	1727	2117	2515	2895	3371	3813	4162	4807
20	853.2	1291	1724	2137	2547	2952	3496	3943	4319	4990
30	848.6	1298	1734	2163	2582	2987	3609	4038	4435	5135
40	851.1	1302	1745	2176	2596	3020	3649	4096	4486	5271
50	849.3	1302	1746	2190	2611	3006	3638	4127	4521	5351
60	847.6	1292	1750	2185	2615	2987	3598	4132	4524	5394
70	841.1	1302	1750	2194	2618	2925	3519	4132	4523	5401
80	847.2	1307	1743	2202	2617	2890	3454	4138	4502	5433
90	1125	1909	2497	3473	3218	4479	4897	6474	6827	9154

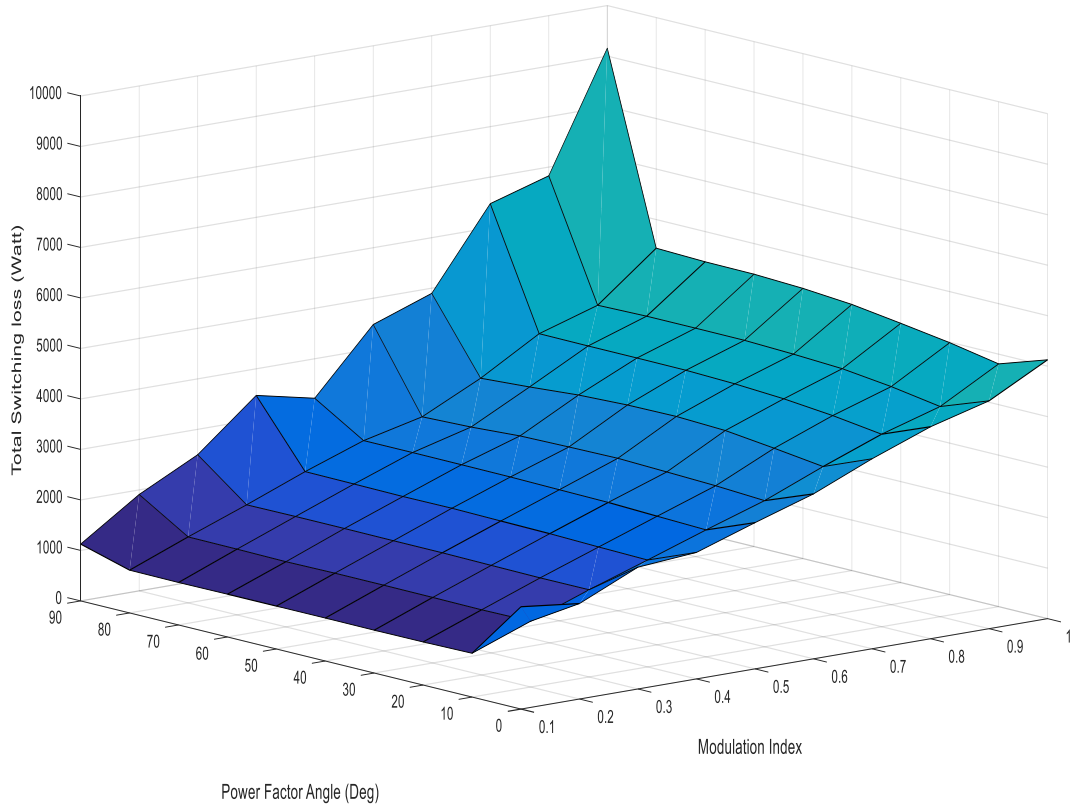

Figure 4.5 3D figure of Total switching (IGBT) loss (W) for Single phase

The figure 4.5 demonstrates that total loss concerning IGBT switching is increasing when power factor is decreasing. Switching loss swing on some influences discussed in section 4.1. To minimize the switching losses, those aspects should be considered.

4.3.4 Diode Reverse recovery loss (W)

Diode Reverse recovery loss is calculated. Diode turn on loss is negligible. Table 4.6 describes the loss (W) data collected from the simulation and figure 4.6 demonstrates the surface plot of Diode Reverse recovery loss.

Table 4.6 Diode Switching loss (Reverse recovery) data (W) for Single phase

Power Factor Angle (Degree)	Modulation Index									
	0.1	0.2	0.3	0.4	0.5	0.6	0.7	0.8	0.9	1
0	217.04	383.5	531.72	673.91	781.09	571.11	560.67	1025.1	1066.4	1194.1
10	311.2	463.6	596.06	701.01	793.45	528.91	522.46	967.71	985.17	1089.1
20	320.01	462.87	574.63	660.41	726.31	458.52	464	854.26	868.41	945.29
30	318.07	448.08	547.86	623.42	665.92	404.88	414.41	775.68	771.38	828.7
40	309.23	432.2	523.99	586.58	623.41	363.85	395.75	707.46	682.26	740.49
50	306.98	424.4	508.02	557.44	583.91	358.07	391.85	650.26	617.73	674.62
60	304.92	418.06	496.99	544.03	559.29	360.09	396.19	613.44	576.16	636.59
70	309.81	413.76	488.37	526.09	543.52	373.13	416.19	592.53	545.78	619.21
80	303.08	408.7	478.43	525.16	534.12	374.81	427.99	575.2	532.69	608.62
90	423.18	646.23	755.95	942.67	700.22	608.79	433.43	997.46	850.66	1048

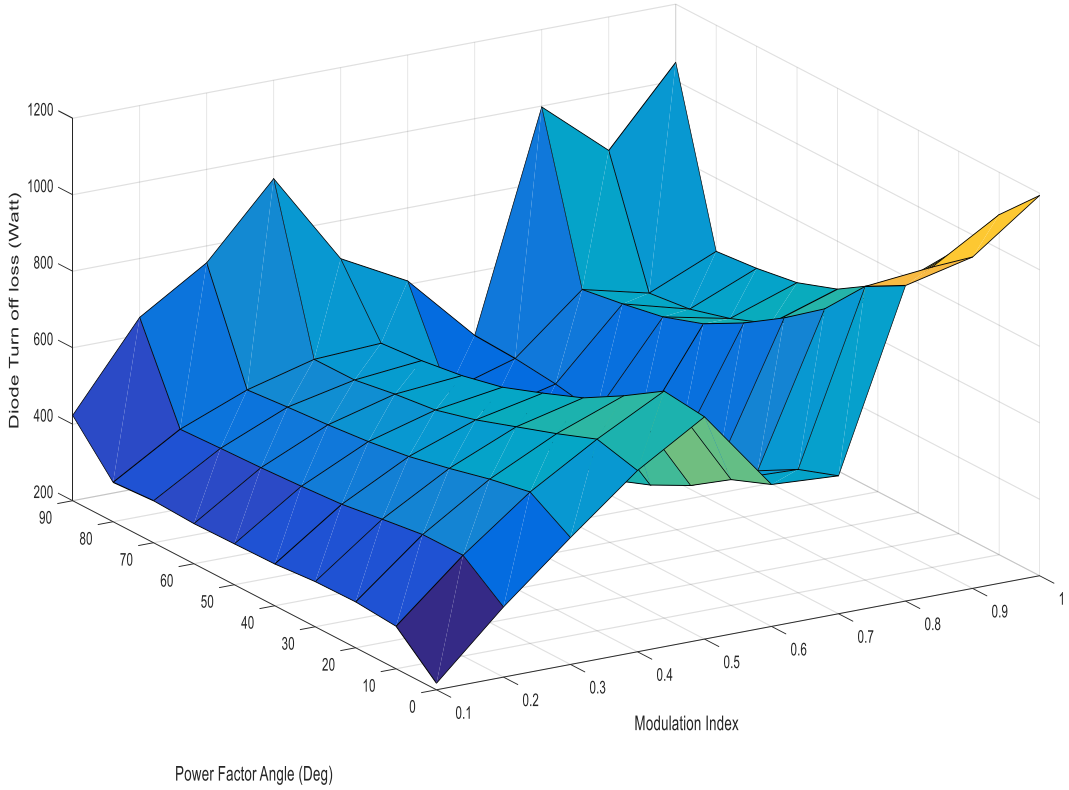

Figure 4.6 3D figure of Diode Reverse recovery loss (W) for Single phase

The figure 4.6 shows the diode Reverse recovery loss diagram with respect to power factor angle and modulation index. Loss varies with different power factors and modulation index. Diode Reverse recovery loss depends on diode current. The surface plot shows minimum loss at the upper modulation indexes and low power factor.

4.3.5 Total Loss (Conduction and switching) (kW) for IGBT (switch) and Diode

The above obtained results are added together by MATLAB blocks for calculating total loss for single phase Inverter. The table 4.7 explains the total loss data (kW) for a single phase Inverter and figure 4.7 shows the total Inverter loss of the Single phase Inverter.

Table 4.7 Single phase Inverter Total loss (kW)

Power Factor Angle (Degree)	Modulation Index									
	0.1	0.2	0.3	0.4	0.5	0.6	0.7	0.8	0.9	1
0	3.705	5.644	8.716	11.69	15.33	19.12	23.89	29.25	33.91	39.96
10	2.598	5.107	8.092	11.32	14.94	18.69	23.38	28.73	33.39	39.42
20	2.593	5.092	8.052	11.28	14.87	18.61	23.32	28.58	33.2	39.19
30	2.586	5.081	8.015	11.23	14.78	18.47	23.18	28.3	32.83	38.73
40	2.578	5.064	7.976	11.16	14.66	18.29	22.92	27.89	32.26	38.1
50	2.574	5.05	7.93	11.09	14.53	18.07	22.58	27.41	31.62	37.33
60	2.569	5.025	7.89	11.01	14.4	17.85	22.19	26.89	30.93	36.5
70	2.566	5.025	7.851	10.95	14.28	17.6	21.81	26.41	30.27	35.69
80	2.566	5.029	7.823	10.97	14.17	17.44	21.49	26.06	29.72	35.05
90	4.036	8.94	13.99	22.44	21.95	34.88	36.82	52.64	56.73	72.75

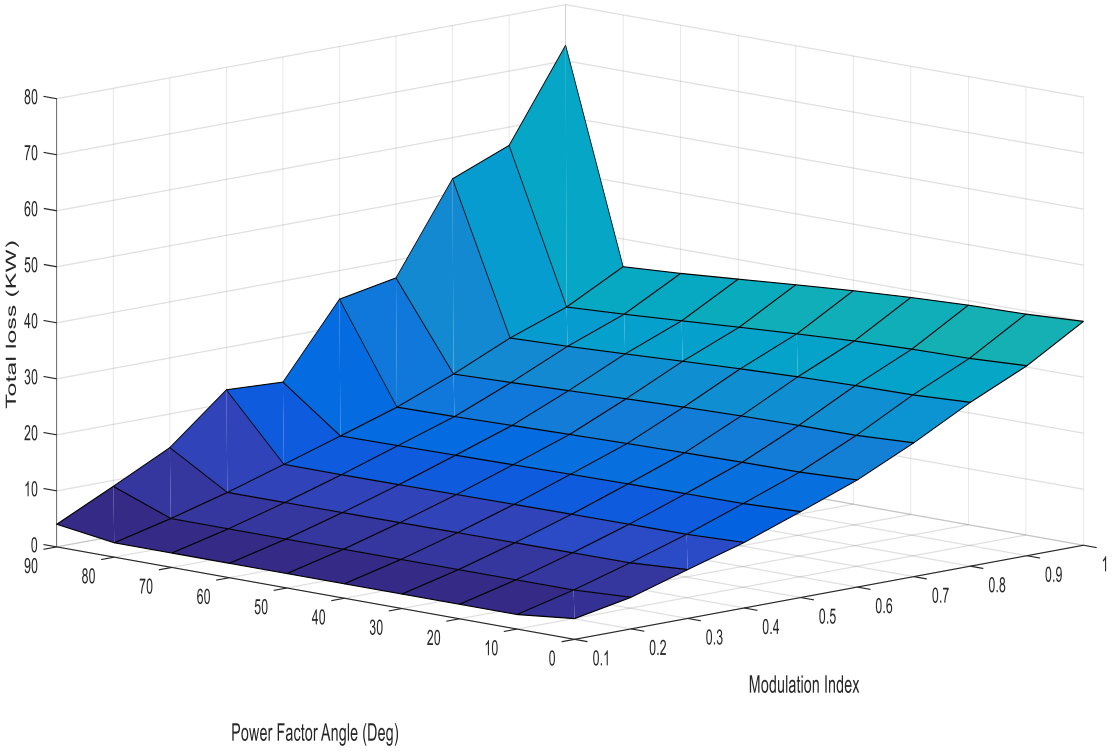

Figure 4.7 3D figure of Inverter total loss (kW) for Single phase

The figure 4.7 shows the surface plot of Inverter's total loss in kW. The loss is consistently increasing with the modulation index. The loss is also smoothly decreasing when power factor decreasing. The loss has an abrupt changes at modulation index 1 and power factor angle 90 in all the cases. This is an unnatural combination which should be avoided.

The total loss (kW) of the 3-phase Inverter have been calculated by multiplying 3 with the Single phase Inverter total loss. Thus, 3-phase Inverter total loss is obtained which is shown in the Table 4.8.

Table 4.8 3-phase Inverter Total loss (Conduction loss and Switching loss) data (kW)

Power Factor Angle (Degree)	Modulation Index									
	0.1	0.2	0.3	0.4	0.5	0.6	0.7	0.8	0.9	1
0	11.11	16.93	26.15	35.08	46	57.35	71.66	87.75	101.7	119.9
10	7.794	15.32	24.28	33.95	44.82	56.06	70.14	86.2	100.2	118.3
20	7.778	15.28	24.16	33.83	44.61	55.83	69.97	85.73	99.61	117.6
30	7.757	15.24	24.05	33.69	44.34	55.41	69.55	84.89	98.5	116.2
40	7.735	15.19	23.93	33.48	43.99	54.87	68.76	83.68	96.79	114.3
50	7.721	15.15	23.79	33.26	43.6	54.22	67.73	82.22	94.85	112
60	7.707	15.08	23.67	33.02	43.2	53.54	66.58	80.67	92.79	109.5
70	7.699	15.07	23.55	32.84	42.83	52.8	65.43	79.24	90.82	107.1
80	7.699	15.09	23.47	32.9	42.51	52.33	64.48	78.18	89.17	105.2
90	12.11	26.82	41.97	67.33	65.85	104.6	110.5	157.9	170.2	218.3

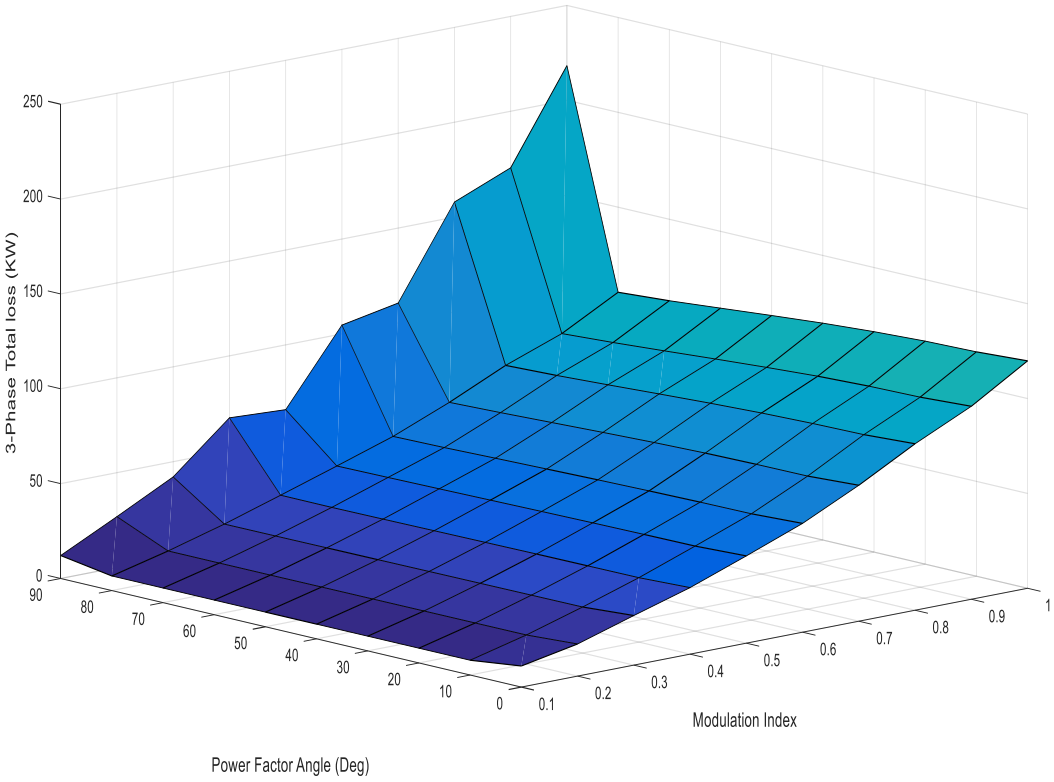

Figure 4.8 3D figure of 3-phase Inverter Total loss (kW)

The surface plot of figure 4.8 illustrates that total switching loss of 3 phase Modular Multilevel Cascaded Inverter of 15-level has a smooth change of losses. The loss is nicely decreasing when power factor decreasing. Loss is also smoothly increasing when modulation index increasing.

4.4 Current graph for Conduction loss:

To understand the average and rms current relationship during IGBT conduction loss, the following curves (Figure 4.9) are plotted at fixed power factor angle 30.

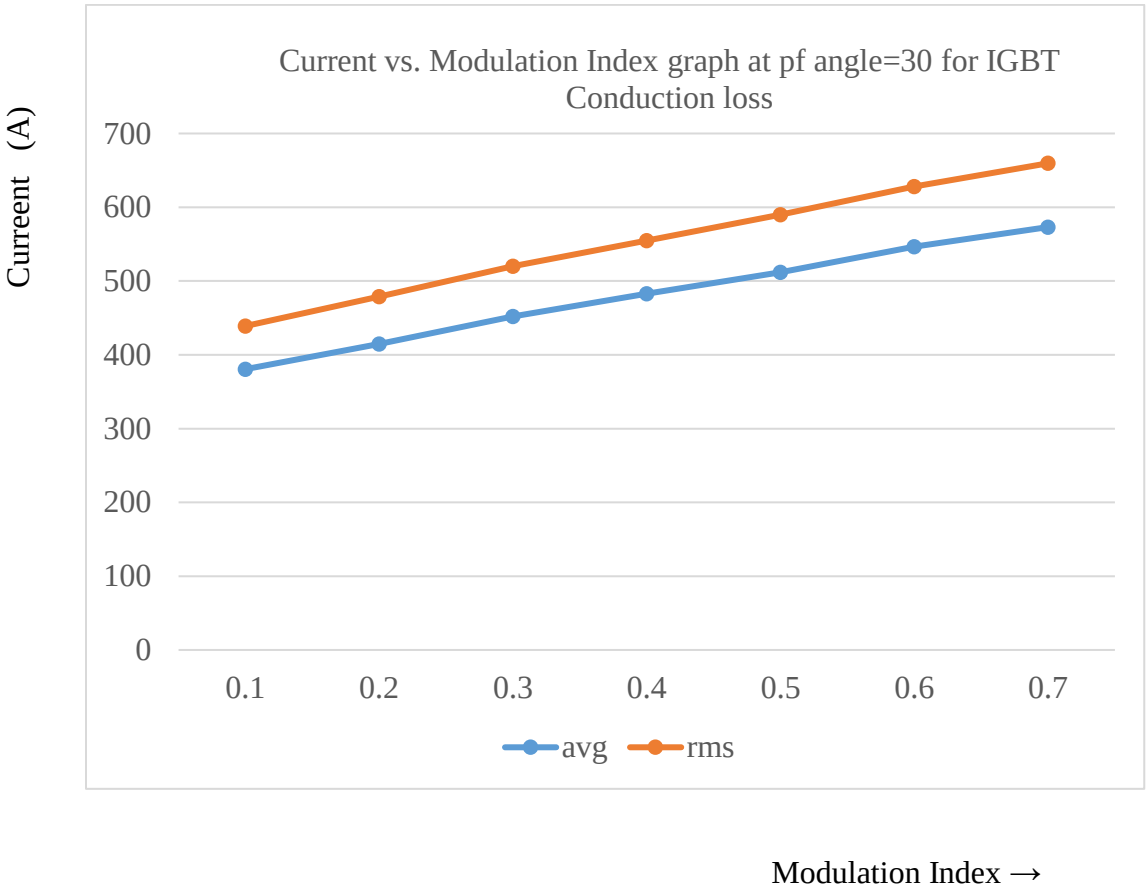

Figure 4.9 Average and rms Current (A) vs Modulation Index graph for IGBT Conduction loss

The figure 4.9 depicted that, rms and average both currents are sharply increasing when modulation index increasing during IGBT conduction loss Because of the higher voltage at upper modulation index, current value is also higher

To understand the average and rms current relationship during diode conduction loss, the following curves (Figure 4.10) are plotted at fixed power factor angle 30.

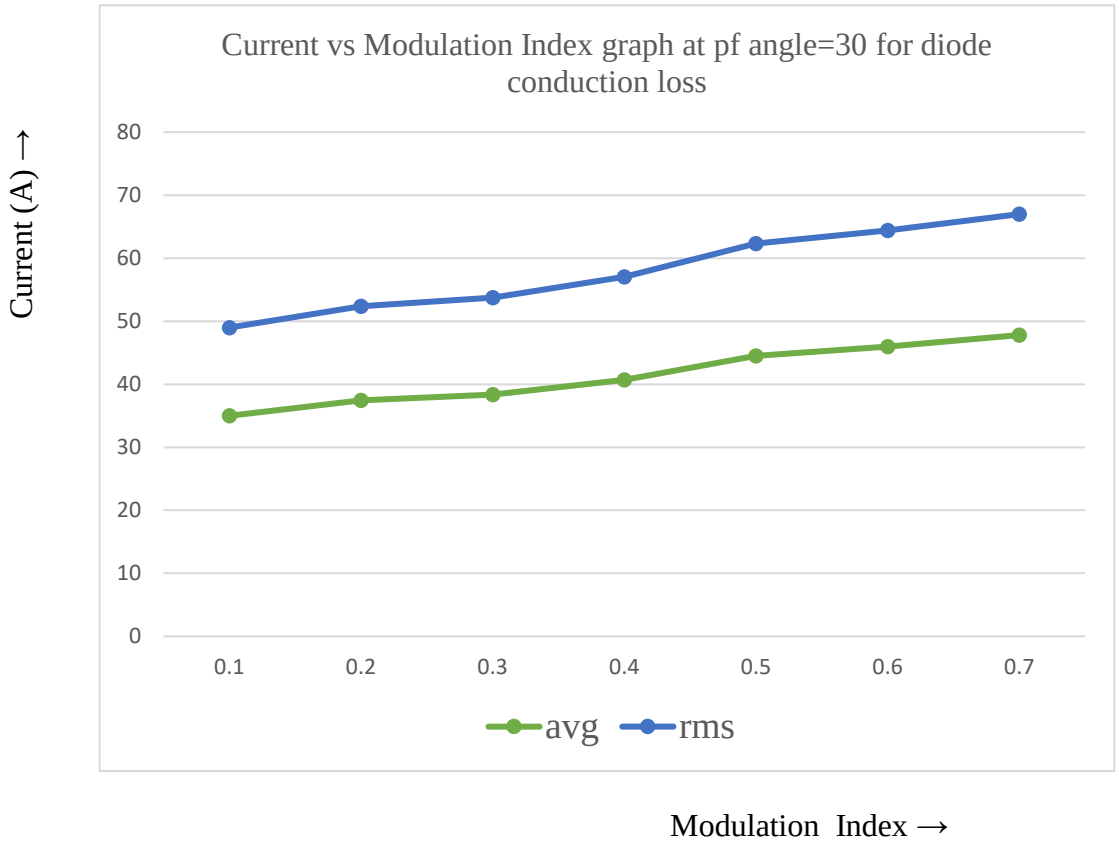

Figure 4.10 Average and rms Current (A) vs Modulation Index graph for diode Conduction loss

The figure 4.10 illustrates that, rms and average both currents are gradually increasing when modulation index increasing during diode conduction loss Because of the higher voltage at upper modulation index, current value is also higher.

Figure 4.11 shows the current (A) vs Power Factor Angle (Deg) graph at the modulation index 0.9 during IGBT Conduction loss.

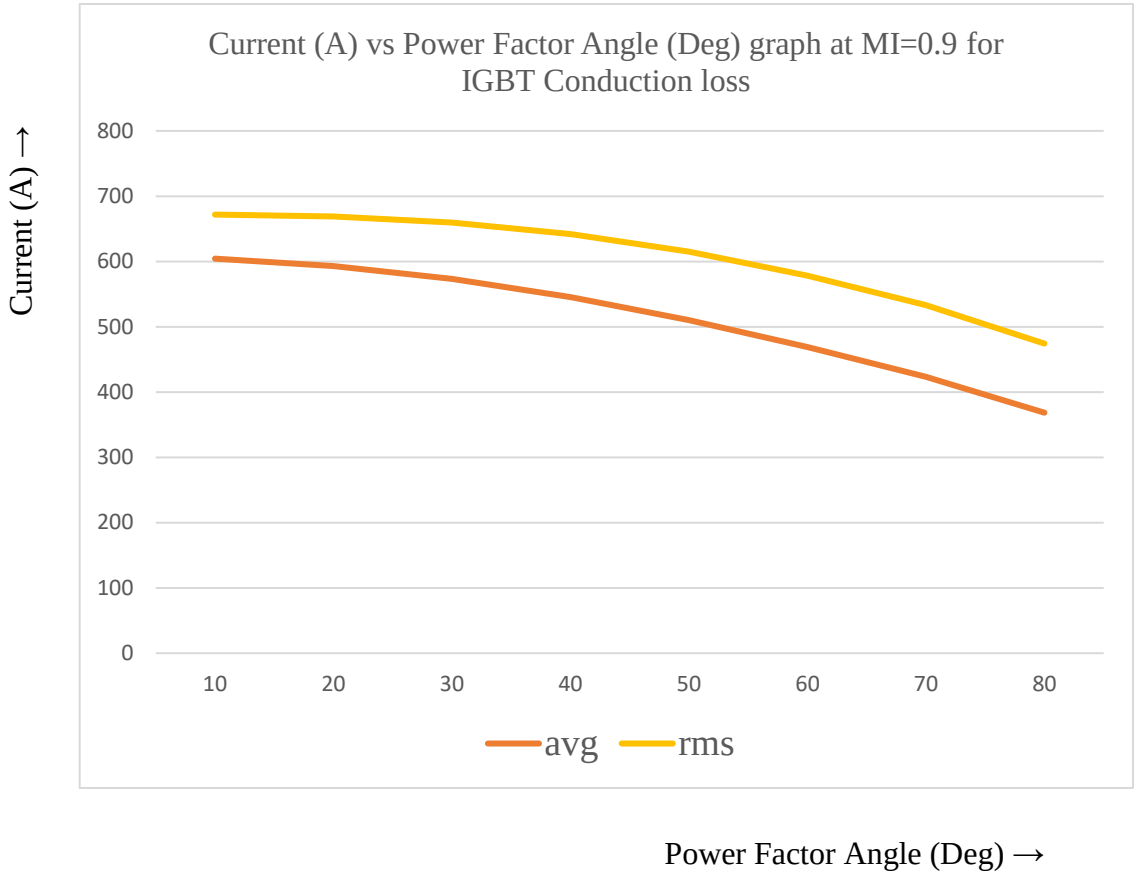

Figure 4.11 Average and rms Current (A) vs Power Factor Angle for IGBT Conduction loss

The figure 4.11 describes that at constant modulation index (0.9), the current gradually decreases with the decrease of the power factor during IGBT Conduction loss.

Figure 4.12 shows Current vs Power Factor Angle graph at Modulation index 0.9 during Diode Conduction.

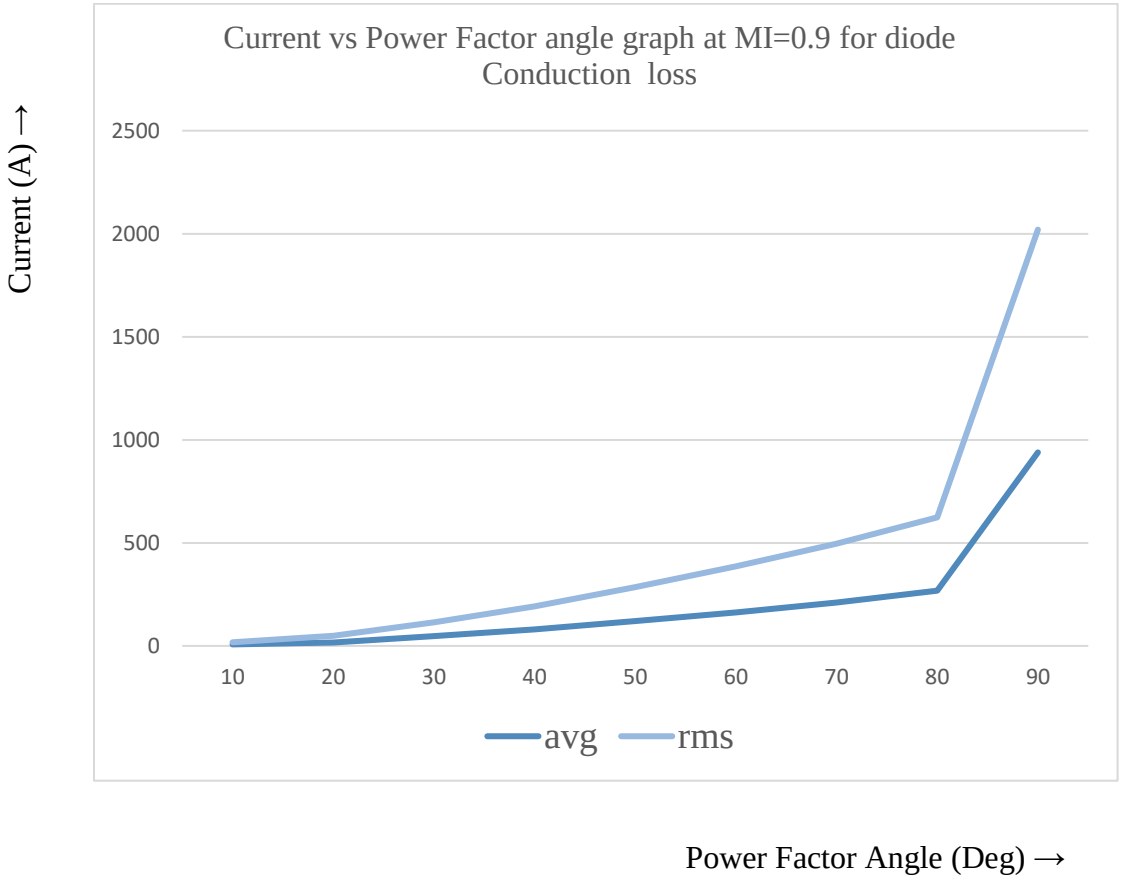

Figure 4.12 Average and rms Current (A) vs Power Factor Angle for diode Conduction loss

The figure 4.12 describes that the current is leisurely increasing with the decrease of power factor during diode conduction. The diode conduction depends on diode current. At modulation index 1 and power factor angle 90, the changes are very high, this combination of switching should be avoided.

Figure 4.13 shows Total loss (kW) vs Power Factor Angle (Deg) at Modulation Index 0.8.

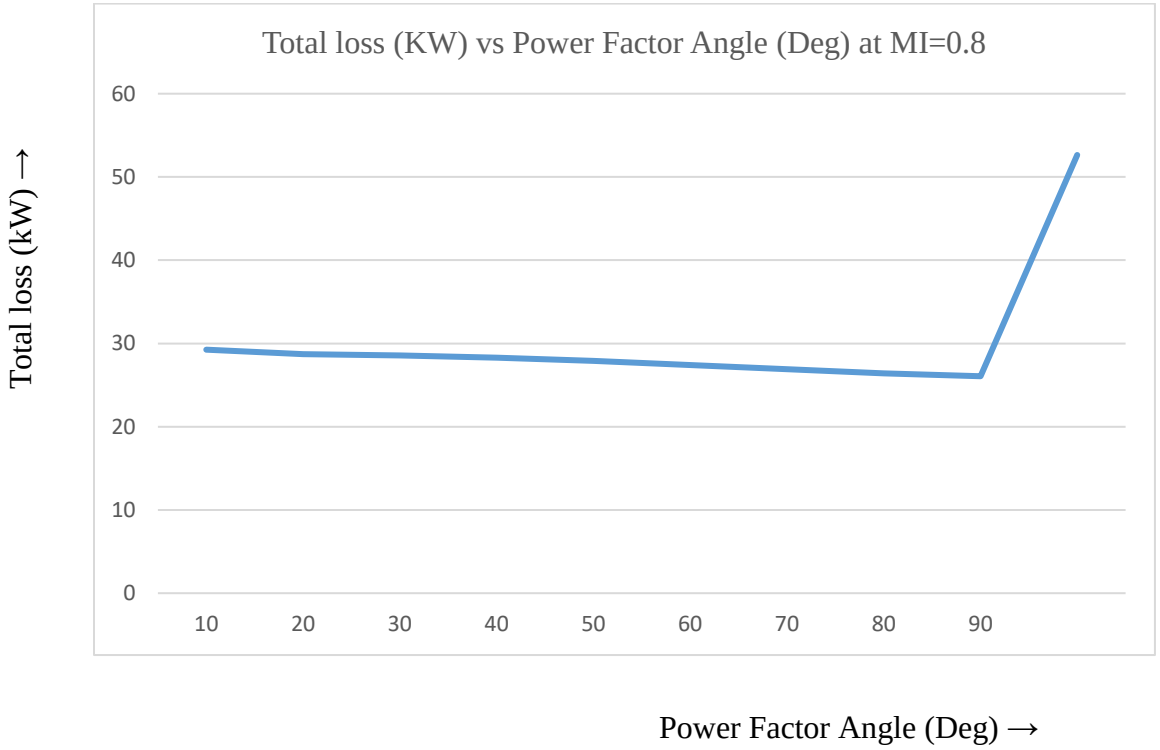

Figure 4.13 Total loss (kW) vs. Power Factor Angle graph

Figure 4.13 illustrates that, total loss of IGBT in single phase is decreasing when power factor decreasing. As the current decreases at low power factor, loss also decreases. The total loss is measured in kW and the total loss vs. power factor graph is plotted at modulation 0.8.

4.5 Achievement

This is my findings that when power factor increases, current increases and loss increases. So , when design a Multilevel Inverter system, it has to be traded off.

4.6 Performance Analysis Comparison of the Proposed Method with the 7-level Modular Multilevel Cascaded (H-Bridge) Inverter

In [72], Losses investigation is done with Sin Pulse Width Modulation (SPWM) controlled single-phase 7-level Cascaded H-bridge Multilevel Converter/Inverter for 11 kV Medium voltage grid connected system. The IGBT FZ250R65KE3 is taken in this work where maximum operating current is 250 A. The loss calculation is done for a fixed Modulation index as well as fixed Resistance (R=24.45 ohm) and fixed Inductance (L=20 mH) in this experiment. The switching loss and conduction loss are calculated for individual switches and cells. 12 switches are required for the 7-level H-Bridge Inverter. The total loss of the Inverter is calculated as 9.03 kW analyzed for the 7-level H-Bridge Inverter using Proposed Method.

4.6.1 Comparison of Loss Performance for Individual Switches

Table 4.9 Loss Performance (W) Analysis of the 7-level H-Bridge Inverter – calculating loss for individual Switches [72]

Losses (W)	Sw 1	Sw 2	Sw3	Sw 4	Sw 5	Sw 6
Switching	1120	160	155	1140	810	810
Conduction	80	20	25	90	40	40

Losses (W)	Sw 7	Sw 8	Sw 9	Sw 10	Sw 11	Sw 12
Switching	810	820	160	1100	1105	160
Conduction	40	30	20	90	85	20

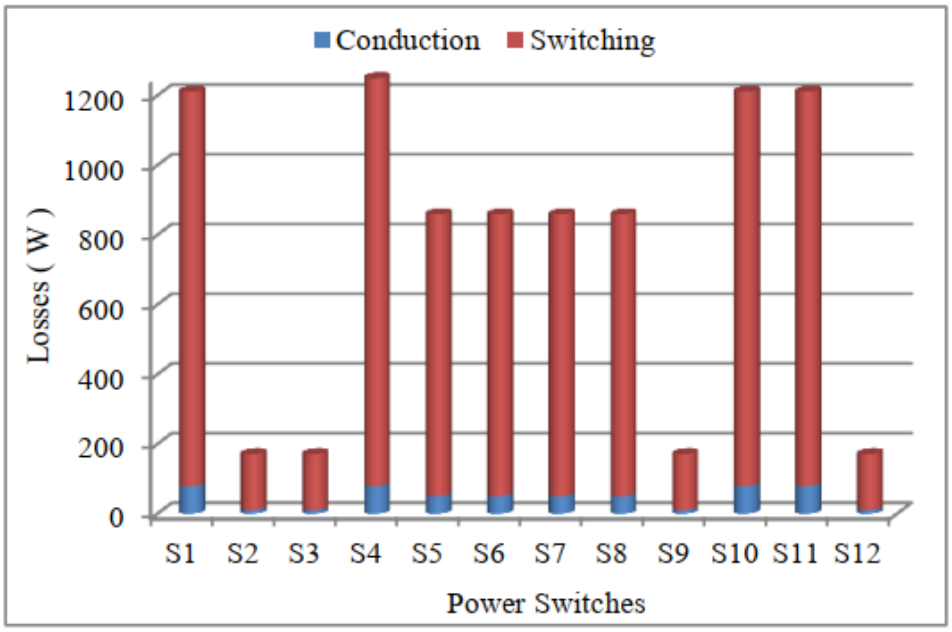

Figure 4.14 Switching losses (W) calculation block-1 [72]

Table 4.10 Loss Performance (W) Analysis of the Proposed Method using 7-level H-Bridge Inverter for individual Switches

Losses (W)	Sw 1	Sw 2	Sw3	Sw 4	Sw 5	Sw 6
Switching	233.16	606.36	346.28	1559.02	224.8	220.46
Conduction	165.83	229.74	153.07	80.6	183.71	183.22

Losses (W)	Sw 7	Sw 8	Sw 9	Sw 10	Sw 11	Sw 12
Switching	578.54	567.45	626.12	227.27	1609.16	340.5
Conduction	132.8	133.4	230.62	165.55	79.54	153.27

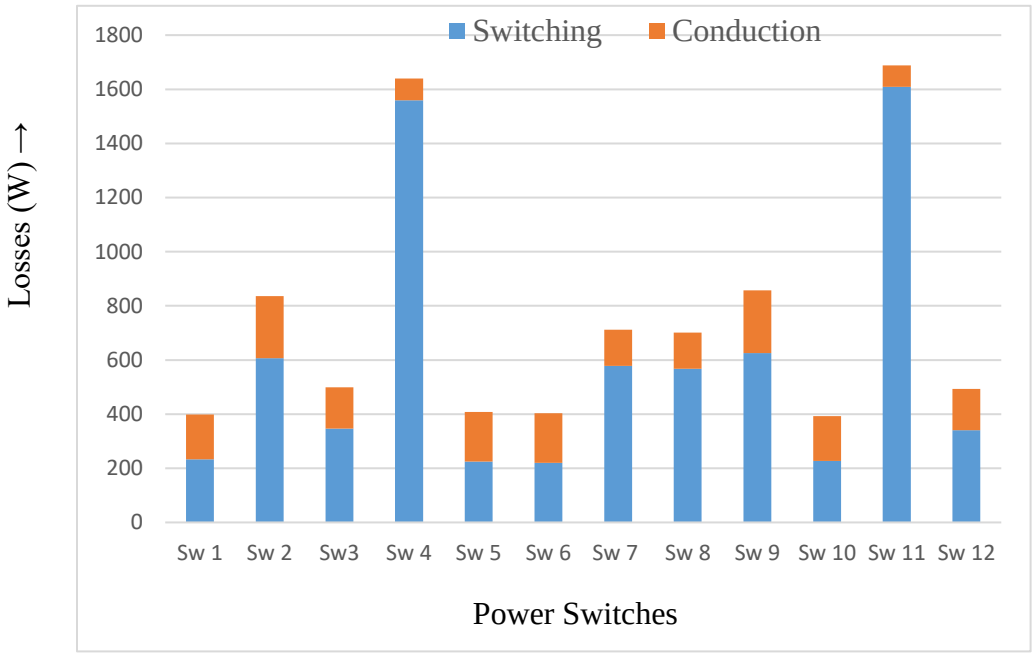

Figure 4.15 Switching loss (W) Calculation using Proposed Method-1

By comparing the Proposed Loss Calculation Method with 7-level MMC circuit [72], the analysis from the Figure 4.14 (Reference) and Figure 4.15 (Proposed) show that each switch experience different losses when compared to other switches in the Inverter. The main reason for this dissimilarities is different current flow through the switches depending on the applied control function. In Figure 4.15, some switches like S1, S5, S6, S10 and S12 produce very low losses around 400 Watts. On the other hand, switches S4, and S11 generate high losses around 1650 Watts. Table 4.09 and Table 4.10 are the losses measured in numeric numbers obtained from the 7-level and the Proposed Method respectively.

4.6.2 Comparison of Loss Performance for Individual Cells

Table 4.11 Performance Analysis of the 7-level H-Bridge Inverter – calculating loss for individual Cells (W) [72]

Losses (W)	Cell 1	Cell 2	Cell 3
Switching	200	300	150
Conduction	2500	3050	2350

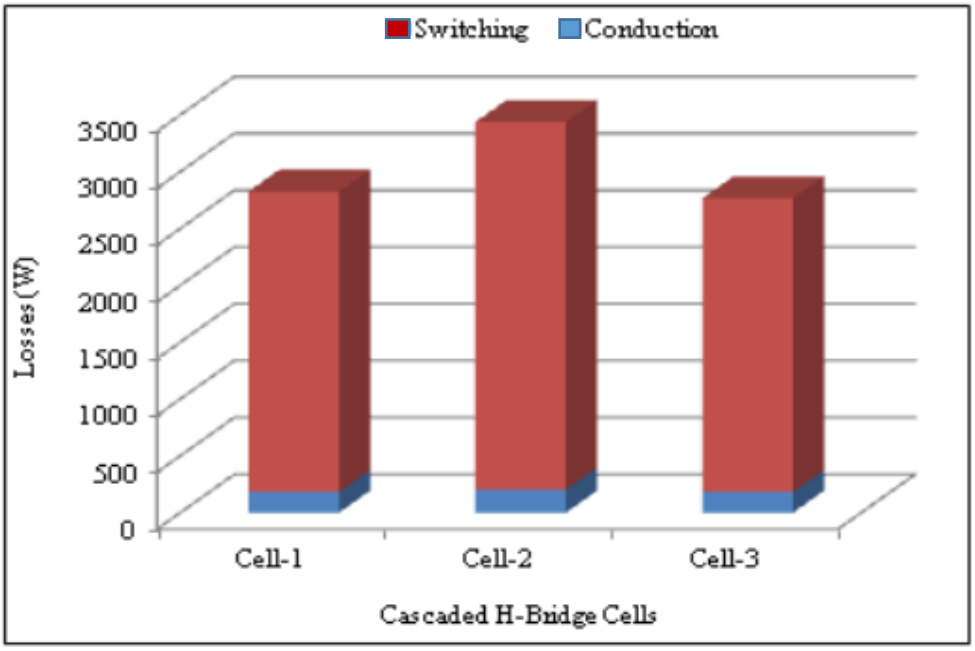

Figure 4.16 Switching losses (W) calculation block -2 [72]

Table 4.12 Performance Analysis of the Proposed Method using 7-level H-Bridge Inverter for individual Cells (W)

Losses (W)	Cell 1	Cell 2	Cell 3
Switching	2744.82	1591.25	2803.05
Conduction	629.24	633.13	628.98

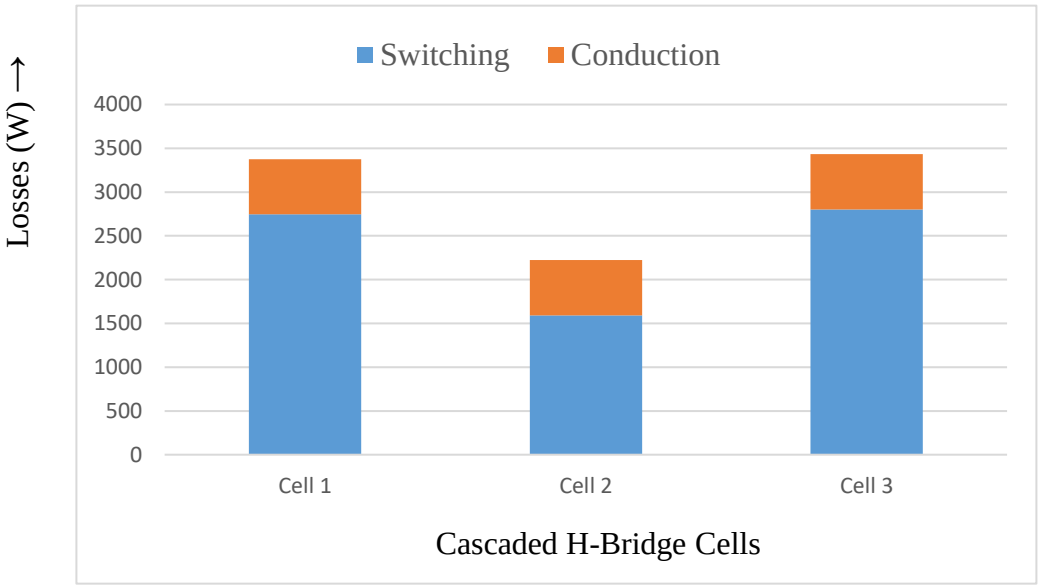

Figure 4.17 Switching Losses (W) Calculation using Proposed Method-2

By comparing the Proposed Mehtod with the 7-level MMC Inverter circuit [72], Figure 4.16 (Reference) and Figure 4.17 (Proposed) show that losses are different in different cells. This is because of current which is different in different cells. In Figure 4.17, cell 1 and cell 3 losses are more compared with the cell 2 loss. Table 4.11 and Table 4.12 are the losses measured in numeric numbers obtained from the 7-level and the Proposed Method respectively.

4.6.3 Comparison of Loss Performance for Total Inverter loss (kW)

Table 4.13 Performance Analysis of the 7-level H-Bridge Inverter - calculating Total Inverter loss (kW) [72]

Total Inverter Loss	9.03 kW
Switching	8462.82
Conduction	540.18

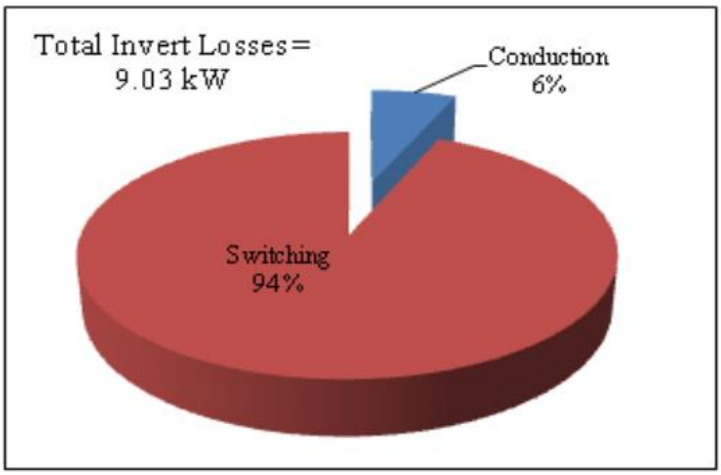

Figure 4.18 Inverter Total power losses (kW) [72]

Table 4.14 Performance Analysis of the Proposed Method for 7-level H-Bridge Inverter calculating Total Inverter loss (kW)

Total Inverter Loss	9.03 kW
Switching	7139.12
Conduction	1891.35

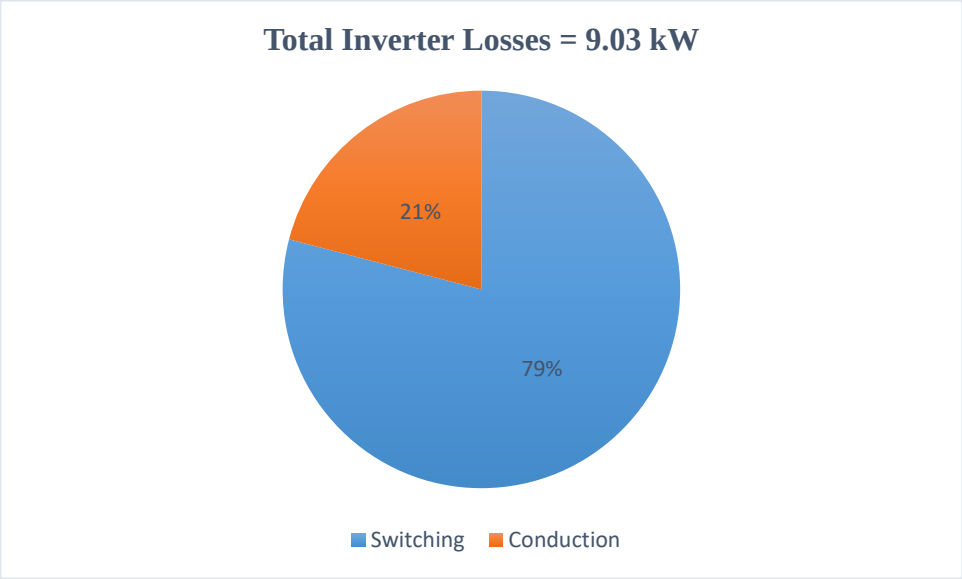

Figure 4.19 Total loss (kW) Calculation for 7-level H-Bridge Inverter using Proposed Method

By comparing the Proposed Loss Calculation Method with 7-level MMC circuit [72], in both cases it is found that the total loss of the Inverter is 9.03 kW. In both cases, majority of the losses come from switching loss as presented in Figure 4.18 (Reference) and Figure 4.19 (Proposed). Table 4.13 and Table 4.14 are the losses measured in numeric numbers obtained from the 7-level and the Proposed Method respectively.

The above figures are obtained from the same specification of the circuit as mentioned in [72] where IGBT maximum operating current is 250 A, output voltage is 11 kV and SPWM technique is used. The loss calculation of the Inverter is done using the Proposed Method shown in figure 4.15, 4.17 and 4.19 respectively. As current varies in different switches and the loss is dependent with the current. Therefore, the losses are different for the individual switches and cells which can not be similar to the reference [72]. However, the total loss estimated as 9.03 kW which is same as the reference paper [72].

4.7 Inverter Output

The Proposed loss calculation Method is applied in a 15 level Modular Multilevel Cascaded Inverter. The Inverter has been simulated by MATLAB and the Proposed loss calculation Method has been incorporated with the Inverter. The wave shape of the gate pulses obtained from the 3-phase 15-level H-bridge MMC Inverter circuit using Third Harmonic Injected Pulse Width Modulation (THPWM), the Inverter output line voltage and THD of the Inverter circuit are shown as following (Figure 4.20, 4.21 and 4.22)

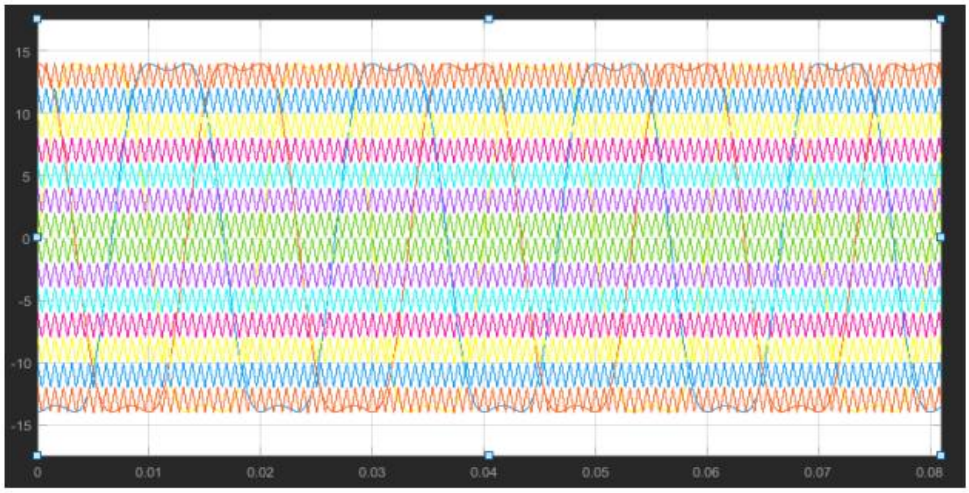

Figure 4.20 MATLAB carrier output to generate gate pulses obtained from the 3-phase 15-level H-bridge MMC Inverter circuit model

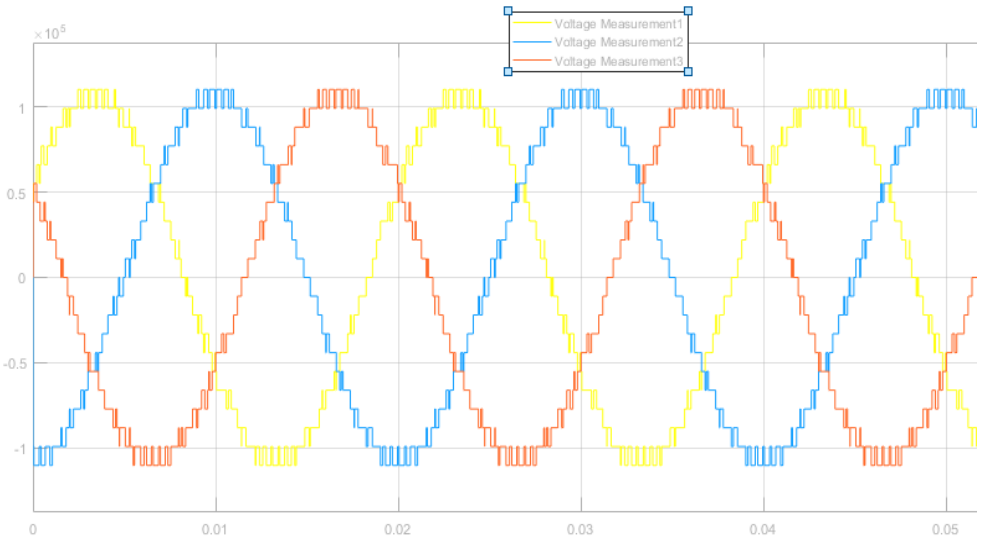

Figure 4.21 The 3-phase output line voltage of the 15-level H-Bridge Inverter circuit model

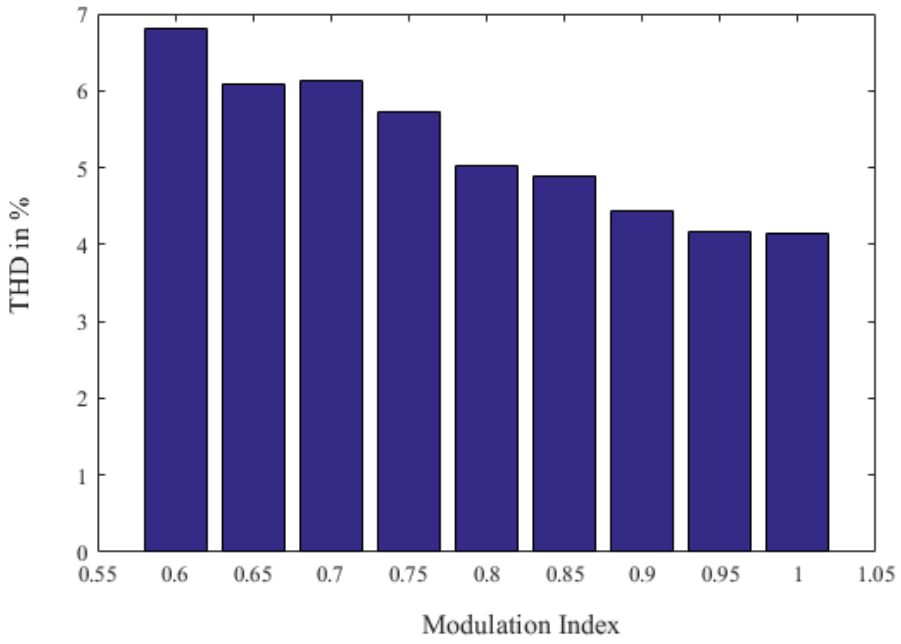

Figure 4.22 Comparison of THD at pf 30 for different Modulation Indexes

Figure 4.20 portraits the waveform after Third Harmonic component has been injected with the Sinusoidal reference signal. Third Harmonic signal is the signal consists of 3 cycles where

Sinusoidal signal has one complete cycle. This composed signal makes an output where peak voltage of the sinusoidal signal has flattened. As explained before, switching loss of the Inverter is dependent on the characteristic waveform of PWM. Therefore, flattening the peak voltage helps reducing the peak current which results reduced THD at the Inverter output. Thus THD of the Inverter's output using Third Harmonic Injected PWM is less compared with the SPWM. Figure 4.21 describes the output line voltage of the 3 phase Inverter showing same frequency as the reference signal. The output looks like a stairway due to Multilevel Inverter. The more the level increases the more has the possibility to get a synthesized wave shape though other factors has also been considered. Figure 4.22 shows the variation of THD of the model circuit. The THD is around 4% at modulation index 1.

CHAPTER 5

5.1 Conclusion

The loss in terms of turn-on, turn-off and conduction for IGBT and diode for Multilevel Inverters has been measured and observed independently. Lastly, the total loss is higher at higher value of modulation index and loss decrease with decrease of power factor but the changes are gradual. The loss result is obtained by the Proposed Analytical Method and current-voltage curve or energy curve of IGBT and diode have been processed in MATLAB with curve fitting tool to get the polynomial taking upper order value for a three phase Modular Multilevel Cascaded Inverter. By the Proposed Method, the switching loss is calculated at the point of switch turn on and turn off. After that all turn on and all turn off within a cycle are added measured in Joule and divided by time period which results power loss measured in Watt. For calculation of conduction loss and switching loss, IGBT's real time value is considered, That is why loss calculation is more precise for both conduction and switching.When switching occurs, the instant current is impossible to measure as IGBTs are driven by high switching frequency having different gate pulses which causes different currents. Therefore, r.m.s and avg. current has been Proposed by the analysis for the loss calculation instead of taking instant current. Finally, all these Proposed equations then driven by MATLAB SIMULINK blocks.

5.2 Future Work

The loss of conduction is dependent with respect to increasing temperature. The loss of switching is dependent with respect to switching frequency, switching current, PWM, level no., THD, device characteristic etc. Therefore to minimize the losses regarding switching- proper loss cause detection and optimum selection of essential features are necessary to be taken. The Proposed loss calculation Method can be implemented on other Multilevel topologies with different PWM by taking appropriate measures. A high power loss means rise of temperature in higher switching frequency. It may have the risk of failure of IGBTs which will cause an uneconomical power conversion. So, in hardware basis better cooling Method as well as equation for cooling Method can be developed for further work.

References

1. A Brief History of Power Electronics and Drives, VOLUME 03, ISSUE 04 (APRIL 2014)
2. Bimal K. Bose, "The Past, Present and Future of Power Electronics," IEEE Industrial Electronics Magazine, June 2009.
3. Pali, B. S., & Vadhera, S. (2016, July). Renewable energy systems for generating electric power: A review. In Power Electronics, Intelligent Control and Energy Systems (ICPEICES), IEEE International Conference on (pp. 1-6). IEEE. (15)
4. N. Mohan, T. Undeland, and W. Robbins, "Power Electronics: Converters, Applications, and Design," 2nd ed., New York: John Wiley & Sons, 1995.
5. N. Mohan, T. M. Undeland, and W. P. Robbins. (2003). Power electronics: converters, applications, and design (3rd ed.).
6. Erickson, R. W. (1997). Fundamentals of Power Electronics. Chapman-Hall. Inc., New York, 517-524.
7. Aghdam, M. H., & Gharehpetian, G. B. (2005, June). Modeling of switching and conduction losses in three-phase SPWM VSC using switching function concept. In Power Tech, 2005 IEEE Russia (pp. 1-6). IEEE.
8. Mahfuz-Ur-Rahman, A. M., Islam, M. R., Fahim, T. A., Islam, M. M., Muttaqi, K. M., & Sutanto, D. (2017, December). Performance analysis of symmetric and asymmetric Multilevel converters. In Humanitarian Technology Conference (R10-HTC), 2017 IEEE Region 10 (pp. 383-386). IEEE.
9. Li, J., Zhao, X., Song, Q., Rao, H., Xu, S., & Chen, M. (2013, May). Loss calculation Method and loss characteristic analysis of MMC based VSC-HVDC system. In Industrial Electronics (ISIE), 2013 IEEE International Symposium on (pp. 1-6). IEEE.
10. Alamri, B., & Darwish, M. (2015, June). Power loss investigation in HVDC for Cascaded H-bridge Multilevel Inverters (CHB-MLI). In PowerTech, 2015 IEEE Eindhoven(pp. 1-7). IEEE.
11. Alamri, B., & Darwish, M. (2014). Precise modelling of switching and conduction losses in Cascaded h-bridge Multilevel Inverters.

12. Stringfellow, J. D., Summers, T. J., & Betz, R. E. (2016, December). Control of the Modular Multilevel converter as a photovoltaic interface under unbalanced irradiance conditions with MPPT of each PV array. In Power Electronics Conference (SPEC), IEEE Annual Southern (pp. 1-6). IEEE.
13. Data Sheet, Doc. No. 5SYA 1437-00 02-2014, 5SNA 1500E250300, HiPak IGBT Module.
14. Aghdam, M. H., & Fathi, S. H. (2005, August). Modeling of Conduction and Switching Losses in Three-Phase Asymmetric Multi-Level Cascaded Inverter. In Proceedings of the 5th WSEAS Int. Conf. on Power Systems and Electromagnetic Compatibility, Greece (pp. 176-181).
15. Judge, P.D. and Green, T.C., 2015, June. Dynamic thermal rating of a Modular Multilevel Converter HVDC link with overload capacity. In 2015 IEEE Eindhoven PowerTech (pp. 1-6). IEEE.
16. Sharma, V. K., Colangelo, A., & Spagna, G. (1995). Photovoltaic technology: basic concepts, sizing of a stand alone photovoltaic system for domestic applications and preliminary economic analysis. Energy conversion and management, 36(3), 161-174.
17. Santos, J. L., Antunes, F., Chehab, A., & Cruz, C. (2006). A maximum power point tracker for PV systems using a high performance boost converter. Solar Energy, 80(7), 772-778.
18. Hua, C., & Shen, C. (1998, May). Study of maximum power tracking techniques and control of DC/DC converters for photovoltaic power system. In PESC 98 Record. 29th Annual IEEE Power Electronics Specialists Conference (Cat. No. 98CH36196) (Vol. 1, pp. 86-93). IEEE.
19. Huang, S., Liao, W., Liu, P., Tang, W., & Huang, S. (2016). Analysis and calculation on switching frequency and switching losses of Modular Multilevel converter with maximum sub-module capacitor voltage deviation. IET Power Electronics, 9(2), 188-197.
20. Alonso, O., Sanchis, P., Gubia, E., & Marroyo, L. (2003, June). Cascaded H-bridge Multilevel converter for grid connected photovoltaic generators with independent maximum power point tracking of each solar array. In IEEE 34th Annual Conference on Power Electronics Specialist, 2003. PESC'03. (Vol. 2, pp. 731-735). IEEE.
21. Feix, G., Dieckerhoff, S., Allmeling, J., & Schonberger, J. (2009, September). Simple Methods to calculate IGBT and diode conduction and switching losses. In Power

Electronics and Applications, 2009. EPE'09. 13th European Conference on (pp. 1-8). IEEE.

22. Ryu, S., Han, D., Ahn, H., & Nokali, M. E. (2007, October). Thermal analysis of PT IGBT by using ANSYS.
23. Sugimoto, H., & Dong, H. (1997, August). A new scheme for maximum photovoltaic power tracking control. In Proceedings of Power Conversion Conference-PCC'97 (Vol. 2, pp. 691-696). IEEE.
24. Tran, P. H. (2011). Matlab/simulink implementation and analysis of three pulse-width-modulation (pwm) techniques.
25. Zeng, R., Xu, L., Yao, L., & Williams, B. W. (2015). Design and operation of a hybrid Modular Multilevel converter. IEEE Trans. Power Electron, 30(3), 1137-1146.
26. Yang, L., Zhao, C., & Yang, X. (2011, October). Loss calculation Method of Modular Multilevel HVDC converters. In Electrical Power and Energy Conference (EPEC), 2011 IEEE(pp. 97-101). IEEE.
27. Hillers, A., & Biela, J. (2014, August). Low-voltage fault ride through of the Modular Multilevel converter in a battery energy storage system connected directly to the medium voltage grid. In Power Electronics and Applications (EPE'14-ECCE Europe), 2014 16th European Conference on (pp. 1-7). IEEE.
28. Adam, G. P., Ahmed, K. H., Finney, S. J., & Williams, B. W. (2011, May). Modular Multilevel converter for medium-voltage applications. In Electric Machines & Drives Conference (IEMDC), 2011 IEEE International (pp. 1013-1018). IEEE.
29. Rodriguez, J., Lai, J. S., & Peng, F. Z. (2002). Multilevel Inverters: a survey of topologies, controls, and applications. IEEE Transactions on industrial electronics, 49(4), 724-738.
30. Rodríguez, J., Bernet, S., Wu, B., Pontt, J. O., & Kouro, S. (2007). Multilevel voltage-source-converter topologies for industrial medium-voltage drives. IEEE Transactions on industrial electronics, 54(6), 2930-2945.
31. Jaboori, M. G., Saied, M. M., & Hanafy, A. A. (1991). A contribution to the simulation and design optimization of photovoltaic systems. IEEE Transactions on energy conversion, 6(3), 401-406.

32. Bose, B. K., Szczesny, P. M., & Steigerwald, R. L. (1985). Microcomputer control of a residential photovoltaic power conditioning system. IEEE Transactions on Industry applications, (5), 1182-1191.
33. Liang, T. J., Kuo, Y. C., & Chen, J. F. (2001). Single-stage photovoltaic energy conversion system. IEE Proceedings-Electric Power Applications, 148(4), 339-344.
34. Ogura, K., Nishida, T., Hiraki, E., Nakaoka, M., & Nagai, S. (2004, June). Time-sharing boost chopper Cascaded dual mode single-phase sinewave Inverter for solar photovoltaic power generation system. In 2004 IEEE 35th Annual Power Electronics Specialists Conference (IEEE Cat. No. 04CH37551) (Vol. 6, pp. 4763-4767). IEEE.
35. Nema, S., Nema, R. K., & Agnihotri, G. (2011). Inverter topologies and control structure in photovoltaic applications: A review. Journal of Renewable and Sustainable Energy, 3(1), 012701.
36. Patrao, I., Figueres, E., González-Espín, F., & Garcerá, G. (2011). Transformerless topologies for grid-connected single-phase photovoltaic Inverters. Renewable and Sustainable Energy Reviews, 15(7), 3423-3431.
37. Agheb, E., Bahmani, M. A., Høidalen, H. K., & Thiringer, T. (2012). Core loss behavior in high frequency high power transformers—II: Arbitrary excitation. Journal of Renewable and Sustainable Energy, 4(3), 033113.
38. Lu, J., Stegen, S., & Butler, D. (2010, June). High frequency and high power density transformers for DC/DC converter used in solar PV system. In The 2nd International Symposium on Power Electronics for Distributed Generation Systems (pp. 481-484). IEEE.
39. Kjaer, S. B., Pedersen, J. K., & Blaabjerg, F. (2005). A review of single-phase grid-connected Inverters for photovoltaic modules. IEEE transactions on industry applications, 41(5), 1292-1306.
40. Lu, D. D. C., & Agelidis, V. G. (2009). Photovoltaic-battery-powered DC bus system for common portable electronic devices. IEEE Transactions on Power Electronics, 24(3), 849-855.
41. Baker, R. H., & Bannister, L. H. (1975). U.S. Patent No. 3,867,643. Washington, DC: U.S. Patent and Trademark Office.

42. Chen, Y., & Smedley, K. M. (2004). A cost-effective single-stage Inverter with maximum power point tracking. IEEE transactions on power electronics, 19(5), 1289-1294.
43. Cho, G. H. (1991). A general circuit topology of Multilevel Inverter. IEEE.
44. Rodriguez, J., Lai, J. S., & Peng, F. Z. (2002). Multilevel Inverters: a survey of topologies, controls, and applications. IEEE Transactions on industrial electronics, 49(4), 724-738.
45. Nabae, A., Takahashi, I., & Akagi, H. (1981). A new neutral-point-clamped PWM Inverter. IEEE Transactions on industry applications, (5), 518-523.
46. Corzine, K., & Familiant, Y. (2002). A new Cascaded Multilevel H-bridge drive. IEEE Transactions on power electronics, 17(1), 125-131.
47. Lai, J. S., & Peng, F. Z. (1996). Multilevel converters-a new breed of power converters. IEEE Transactions on industry applications, 32(3), 509-517.
48. Meynard, T. A., & Foch, H. (1992, June). Multi-level conversion: high voltage choppers and voltage-source Inverters. In PESC'92 Record. 23rd Annual IEEE Power Electronics Specialists Conference (pp. 397-403). IEEE.
49. Xu, L., & Agelidis, V. G. (2002). Flying capacitor Multilevel PWM converter based UPFC. IEE Proceedings-Electric Power Applications, 149(4), 304-310.
50. Xu, L., & Agelidis, V. G. (2006). VSC transmission system using flying capacitor Multilevel converters and hybrid PWM control. IEEE Transactions on Power Delivery, 22(1), 693-702.
51. Wilkinson, R. H., Meynard, T. A., & du Toit Mouton, H. (2006). Natural balance of multicell converters: The general case. IEEE Transactions on Power Electronics, 21(6), 1658-1666.
52. Choi, H., Zhao, W., Ciobotaru, M., & Agelidis, V. G. (2012, June). Large-scale PV system based on the multiphase isolated dc/dc converter. In 2012 3rd IEEE International Symposium on Power Electronics for Distributed Generation Systems (PEDG) (pp. 801-807). IEEE.
53. Kouro, S., Fuentes, C., Perez, M., & Rodriguez, J. (2012, October). Single DC-link Cascaded H-bridge Multilevel multistring photovoltaic energy conversion system with inherent balanced operation. In IECON 2012-38th Annual Conference on IEEE Industrial Electronics Society (pp. 4998-5005). IEEE.

54. Krug, D., Bernet, S., Fazel, S. S., Jalili, K., & Malinowski, M. (2007). Comparison of 2.3-kV medium-voltage Multilevel converters for industrial medium-voltage drives. IEEE Transactions on Industrial Electronics, 54(6), 2979-2992.
55. Alexander, A., & Thathan, M. (2014). Modelling and analysis of Modular Multilevel converter for solar photovoltaic applications to improve power quality. IET renewable power Generation, 9(1), 78-88.
56. Rajasekar, S., & Gupta, R. (2012, March). Solar photovoltaic power conversion using Modular Multilevel converter. In 2012 Students Conference on Engineering and Systems (pp. 1-6). IEEE.
57. Subsingha, W. (2016). A comparative study of sinusoidal PWM and third harmonic injected PWM reference signal on five level diode clamp Inverter. *Energy Procedia*, *89*, 137-148.
58. Rivera, S., Wu, B., Kouro, S., Wang, H., & Zhang, D. (2012, June). Cascaded H-bridge Multilevel converter topology and three-phase balance control for large scale photovoltaic systems. In 2012 3rd IEEE International Symposium on Power Electronics for Distributed Generation Systems (PEDG) (pp. 690-697). IEEE.
59. Colak, I., Bayindir, R., & Kabalci, E. (2010, September). A modified harmonic mitigation analysis using Third Harmonic Injection PWM in a Multilevel Inverter control. In Proceedings of 14th International Power Electronics and Motion Control Conference EPE-PEMC 2010 (pp. T2-215). IEEE.
60. Shuvo, S., Hossain, E., Islam, T., Akib, A., Padmanaban, S., & Khan, M. Z. R. (2019). Design and hardware implementation considerations of modified Multilevel Cascaded h-bridge Inverter for photovoltaic system. Ieee Access, 7, 16504-16524.
61. Sakunde, S. B., & Bavdhane, V. D. Level Shifted Pulse Width Modulation in Three Phase Multilevel Inverter for Power Quality Improvement. International Journal of Science and Research (IJSR) ISSN (Online), 2319-7064.
62. Bose, B. K. (2009). The past, present, and future of power electronics [guest introduction]. IEEE Industrial Electronics Magazine, 3(2), 7-11.
63. Du, Y., & Lu, D. D. C. (2011). Battery-integrated boost converter utilizing distributed MPPT configuration for photovoltaic systems. Solar energy, 85(9), 1992-2002.

64. Hassanpoor, Arman, Staffan Norrga and Alireza Nami. “Loss evaluation for Modular Multilevel converters with different switching strategies.” 2015 9th International Conference on Power Electronics and ECCE Asia (ICPE-ECCE Asia) (2015): 1558-1563.
65. Casanellas, F. (1994). Losses in PWM Inverters using IGBTs. IEE Proceedings-Electric Power Applications, 141(5), 235-239.

66. Dahono, P. A., Sato, Y., & Kataoka, T. (1995). Analysis of conduction losses in Inverters. IEE Proceedings-Electric Power Applications, 142(4), 225-232.
67. Kolar, J. W., Ertl, H., & Zach, F. C. (1991). Influence of the modulation Method on the conduction and switching losses of a PWM converter system. IEEE Transactions on Industry Applications, 27(6), 1063-1075.
68. Mestha, L. K., & Evans, P. D. (1989, July). Analysis of on-state losses in PWM Inverters. In IEE Proceedings B (Electric Power Applications) (Vol. 136, No. 4, pp. 189-195). IET Digital Library.
69. Berringer, K., Marvin, J., & Perruchoud, P. (1995, October). Semiconductor power losses in AC Inverters. In IAS'95. Conference Record of the 1995 IEEE Industry Applications Conference Thirtieth IAS Annual Meeting (Vol. 1, pp. 882-888). IEEE.
70. Kim, T. J., Kang, D. W., Lee, Y. H., & Hyun, D. S. (2001, June). The analysis of conduction and switching losses in multi-level Inverter system. In 2001 IEEE 32nd Annual Power Electronics Specialists Conference (IEEE Cat. No. 01CH37230) (Vol. 3, pp. 1363-1368). IEEE.
71. Zhao, W., Choi, H., Konstantinou, G., Ciobotaru, M., & Agelidis, V. G. (2012, June). Cascaded H-bridge Multilevel converter for large-scale PV grid-integration with isolated DC-DC stage. In *2012 3rd IEEE International Symposium on Power Electronics for Distributed Generation Systems (PEDG)* (pp. 849-856). IEEE.
72. Alamri, B., Alshahrani, S., & Darwish, M. (2015, September). Losses investigation in SPWM-controlled Cascaded H-bridge Multilevel Inverters. In *2015 50th International Universities Power Engineering Conference (UPEC)* (pp. 1-5). IEEE.

73. Moḥ. Rabiula Isalāma, Guo, Y., & Zhu, J. (2014). *Power converters for medium voltage networks*. Springer Berlin Heidelberg.

Publication

[1] http://ajer.org/papers/Vol-8-issue-2/I08025363.pdf (February, 2019- volume 08 – Issue 02) Issue in **American journal of Engineerin**